INVESTIGATION INTO VOLTAGE AND ANGLE STABILITY OF A HYBRID HVAC-HVDC POWER NETWORK

PREPARED BY:

LEONARD CHUKWUMA AZIMOH

SUPERVISOR:

PROF. K.A FOLLY

CO-SUPERVISOR

PROF. SP CHOWDHURY

UNIVERSITY OF CAPE TOWN
IDYUNIVESITHI YASEKAPA • UNIVERSITEIT VAN KAAPSTAD

DEPARTMENT OF ELECTRICAL ENGINEERING
UNIVERSITY OF CAPE TOWN
CAPE TOWN

THIS THESIS IS SUBMITTED TO THE UNIVERSITY OF CAPE TOWN IN FULL FULFILMENT OF THE ACADEMIC REQUIREMENTS FOR THE MASTER OF SCIENCE DEGREE IN ELECTRICAL ENGINEERING

Date: 31 March, 2010

Declaration

I hereby solemnly declare that this document, the content and materials therein are the product of my dissertation and are being submitted as a requirement in fulfillment of my MSc degree in Electrical Engineering department, University of Cape Town. That this work is mine and that it has not been submitted before, for any degree at this University or any other institution for any degree or examination. That any contribution, quotation and information therein have been properly referenced in compliance with the statutory requirement governing intellectual property laws.

Mr. Leonard Chukwuma Azimoh

Signature Signed by candidate 25/05/2010

Signed at the University of Cape Town

Declaration

I hereby solemnly declare that this document, the content and materials therein are the product of my dissertation and are being submitted as a requirement in fulfillment of my MSc degree in Electrical Engineering department, University of Cape Town. That this work is mine and that it has not been submitted before, for any degree at this University or any other institution for any degree or examination. That any contribution, quotation and information therein have been properly referenced in compliance with the statutory requirement governing intellectual property laws.

Mr. Leonard Chukwuma Azimoh

Signature.....

Signed at the University of Cape Town

Acknowledgements

First and foremost, my thanks and praises goes to the almighty God who has watched over me every step of the way, for his favour, grace and divine health, " without you I am nothing" even when I falter you guided my footsteps, I can never thank you enough.

Many thanks to my supervisor Professor K.A Folly for his contributions; both intellectually and financially, your thoroughness, persistence and rejection of any compromise in the pursuit of excellence have sharpened me for the challenges ahead. *"When it comes to doing, it takes some knowing and showing*" Prof you know your stuff.

Special thanks to my co-supervisor Professor Shyama Pada Chowdhury and his indefatigable and amiable wife Professor Sunetra Chowdhury. Prof, without you it won't have been the same, your believe in me rekindled the firing spirit within, you made it happen, your managerial prowess, unyielding spirit in bringing out the best in me is inspiring, it has made me whom I am. My profound appreciations to you Professor Manu A Haddad for giving me the opportunity to work with you and finish my thesis in your highly esteemed University in Cardiff UK, also the contribution of the power group department of Electrical Engineering in the University of Cardiff, Wales, United Kingdom is remarkable, I thank my colleagues in the power group of Electrical Engineering, University of Cape Town for their invaluable and unflinching support; working with you makes the mountain looks like a mole hill, the team spirit and the synergy has made the work less cumbersome. My profound appreciation goes to Professor Trevor Gaunt for being there when it mattered most. To my brothers and sisters I am heavily indebted to your love and understanding over the years, your support, encouragement and most of all, your trust in me is overwhelming. I will never end this piece without acknowledging my family, my wife and sons for the sacrifice and the pain they bore during my absence, brother Daniel whom I left during his first tottering steps on earth, Joy without your support the journey would have been impossible, my profound gratitude to Awele and Olisemekalim I say thank you, your sacrifices during my absence was worthwhile, I love you all more you can imagine.

" I returned, and saw under the sun, that the race is not for the swift, nor the battle to the strong, neither yet bread to the wise, nor yet riches to men of understanding, nor yet favour to men of skill; but time and chance happeneth to them all." – Ecclesiastes 9:11

Synopsis

Despite the fact that the first electricity produced by Thomas Elva Edison in September 1882 was direct current, it had the limitation of being localized. Transmission of power could not go beyond few kilometers due to the low voltage level. Transmission of power over a long distance requires high voltage; otherwise large amount of power will be dissipated as heat (i.e., power loss). With the invention of transformers and induction motors, transmission of power was predominantly done by HVAC transmission due to the inherent ability of the system, to transform energy from low to high voltage and vice versa. Recent development in the power industry has shown that HVAC has its' limitations in transmission of power over a long distance. The HVDC paradigm came about as a result of new discoveries and advancement in the semi-conductor devices. Research has shown that the HVDC transmission systems are able to overcome some of the disadvantages of HVAC, such as its' inability to transmit bulk power over a long distance due to reactive power requirement, difficulties in interconnecting different networks with different frequencies, high power loss during transmission e.t.c., The advantages of HVDC transmission scheme such as bulk power transmission over a long distance, asynchronous connections between networks of different frequencies, under water transmission, cost effectiveness beyond the breakeven point e.t.c. The increasing difficulties in interconnections of weak AC link i.e., systems with low effective short circuit ratio (SCR), as seen in the interconnections of offshore wind farms and on shore onshore grids, the fact that DC cannot be transmitted at low voltages, has spurred engineers to further research on the classical line commuted converter HVDC system. The result is the emergence of the new VSC-HVDC system, which is able to function at lower voltages about 2.5 kV as in Eagle-pass substation, VSC-HVDC USA link with Mexico. Also, it has been found to be able to overcome the problems of low (SCR) when interconnected with a weak HVAC network. The voltage source converter HVDC (VSC-HVDC) is an improvement on HVDC transmission system. Using a voltage source converter (VSC) as opposed to current source converter (CSC) used in the classical HVDC systems for its converter stations. The valves of (VSC) are made of insulated gate bipolar transistors (IGBT) and pulse width modulator (PWM) device, which is used to create the desired wave form in the system. These three transmission schemes, namely, the HVAC, HVDC and VSC-HVDC have their advantages and disadvantages. This study

therefore, investigates the power stability problems of HVDC and VSC-HVDC interactions on their hybrid networks with HVAC link, with the intention of bringing out their weaknesses and strengths. The knowledge of this will assist network planners to be informed on ways of improving the efficiency and quality of power systems network. The simulations for this study was done using DIgSILENT Powerfactory software version 14.0.515. This study encapsulates the three major stability problems affecting power systems network, namely, the voltage stability, transient stability and small signal stability. The voltage stability study was conducted using series of load flows at various levels to plot the VP and QV curves, and the results were used to analyze the systems proximity and sensitivity to voltage collapse, as well as the maximum loading point (MPL) of the network. Furthermore, the voltage angle, and terminal voltage responses during a three-phase short circuit disturbance was also used to analyze the voltage stability of the networks. For the transient stability study, several case studies were investigated and their dynamic performances during three-phase short circuit perturbations were analyzed. The small signal stability investigation was done using modal analysis to determine the small signal stability of the three transmission schemes mentioned above. The transient and small signal stability, which are both subsets of rotor angle stability, were further investigated to show the effect of power systems stabilizer (PSS) and automatic voltage regulator (AVR) on rotor angle stability. The results of the analyses show that the HVDC transmission scheme provides the best alternative for bulk power transmission over a long distance. The VSC-HVDC transmission network is suitable for interconnections where the tie with HVAC networks have a low short circuit ratio (SCR). Other conclusions reached with the investigations are explained in chapter ten.

Table of contents

List of Figures

List of Tables

Chapter 1

Introduction

1.1 Background to the study

The world energy demand increases with increase in industrialization, technological inventions and advancement, and with the burgeoning population in both developed and developing nations of the world. The need to meet the increasing demand has led engineers to harness energy from various sources i.e. Photovoltaic, fossil fuel, Hydro, geothermal, nuclear, wind e.t.c. Very often the sources of energy are located far away from load centers due to comparative cost advantage of production and safety measures, like in the case of citing nuclear plants. To this extent, power from various generation centers are fed into the national grid and transported over a long distance to meet the load demand. Transmission of power over a long distance imposes some strains on the network, also, the load characteristics and switching activities causes some stability problems within the network [1]. The utmost responsibility of power system operators is to supply electric power safely and economically to customers, despite the fact that the measures necessary for safe and stable operation of power networks are at variance with economic justifications, operators are compelled by market forces to meet the demand of the customers in the most economic and efficient manner in order to gain a good market share in the industry (in terms of costumer's patronage). With the commercialization and deregulation of power industry by various government of the world, some customers in power industry gravitate to those companies with the best power integrity. As the power demand in the world is increasing at a fast rate, large centralized power supplies are getting constrained by the minutes. Power from various generation centers are fed into the national grid and transported over a long distance to meet demand, transmission of power over a long distance imposes some strains on the network, also the load characteristics and switching activities causes some stability problems within the network. Market forces, government regulations and environmental requirements are compelling various stakeholders in the industry to improve on power quality transmitted in their networks; because in a competitive industry, some customers will naturally

gravitate to those companies that guarantees the best power quality. Power system stability was first recognize as a source of concern in the early twenties, since then, power engineers has been grappling with this problem till date. Although, many solutions have been proffered to the problem, there are still rooms for improvement. Some papers in power engineering literature [2, 3, and 4] have shown various ways of mitigating the problems of power instability, using different techniques. This work dwells more on the control of HVDC base solutions interconnected with a weak hybrid HVAC system (see [1] page 813 for information on the strength of the network model used in this study) for improving power systems stability. Furthermore, this project takes a glossary look on the parameters of the transmission line. Fundamentally, parameters of a transmission line are series resistance, series inductance, shunt conductance and shunt capacitance, these parameters are distributed within the network and so are their effects. The research investigated the three arms of power stability problems, namely, voltage stability, transient stability and small signal stability. This was achieved using three transmission schemes, namely, HVAC, HVAC-HVDC link, and HVAC-VSC-HVDC link. The HVDC and VSC-HVDC transmission systems were used in this study to study their impact on HVAC system, as a way of improving the power quality supplied to the grid.

For a power system to be rated as having quality, it must meet the following criteria as described in [1]; the power system must have the following criteria:

- Constancy of frequency
- Constancy of voltage
- And an acceptable level of reliability

Therefore, a well designed power network must be able to supply the systems demand and maintain sufficient active and reactive power reserve in order to meet contingencies in demand, it must also be able to maintain a good level of reliability and provide an acceptable level of power quality at a competitive prize.

In power systems, Angle stability, Frequency Stability and Voltage Stability are the major stability issues of power networks, voltage stability problems is mainly due to the systems inability to meet the reactive power demand, whilst the frequency stability problems could be linked to balance in frequency of a system which is dependent on the control of active power, also angle stability otherwise known as rotor angle stability, which is a subset of transient and small signal stability has to do with the study of

electromechanical oscillations of interconnected machines in power systems [5]. This type of instability is normally associated with the generator dynamics.

1.2 Objectives of this research

This project is concerned with investigating the impact of HVDC and VSC-HVDC on the rotor angle and voltage stability of a hybrid HVAC power system network.
The specific objectives are to:

- Investigate the strength and weaknesses of the HVAC, HVDC and VSC-HVDC power transmission systems with regard to power systems stability.
- Investigate the voltage stability, transient stability and small signal improvement of a weak HVAC network by using power systems stabilizer (PSS) and automatic voltage regulator (AVR), also by using HVDC and VSC-HVDC transmission schemes.
- Investigate the impact of HVDC on a hybrid HVAC-HVDC network with respect to power systems stability.
- Investigate the advantage of VSC-HVDC over HVDC with respect to power stability improvement.
- Make appropriate recommendation for planning, control and operation of power systems network, with a view to improving the power quality supplied to the grid.

1.3 Limitations and scope of investigation

This report focuses on power stability studies, encompassing voltage stability, transient stability and small signal stability. The major limitations of this study are as follows:

- Due to the complex nature of HVDC base solutions e.g., classic HVDC and VSC-HVDC systems, modeling and interconnection with HVAC system was difficult.
- During the voltage stability study, computation of the PV and QV curves was achieved using series of load flows at different load levels, this requires a lot of load changes in steps, this is cumbersome and time consuming
- Also the modelling used in the simulation is a simplified version of the actual machine models. These models neglected the stator and network transients. Therefore, a more accurate result will be achieved with a standard machine model.

1.4 Overview of the dissertation

This dissertation consists of ten chapters together with the supplementary chapters.

Chapter one gives a brief introduction of the thesis to the reader, where the background and objective of the dissertation are discussed.

Chapter two describes the literature review on the previous studies that have been done and give a foundation onto which the results and conclusions of the report will be based. Also, the HVAC transmission system was discussed here.

Chapter three presents the HVDC technology, theory of HVDC and appropriate mathematical modelling of HVDC system; control and performance equations are also discussed.

Chapter four presents the VSC-HVDC technology; the advantages, disadvantages and applications of the system were outlined. Also the performance equation and modelling of the system were discussed

Chapter five presents a comprehensive study on power systems stability, classification of power systems are presented, angle stability are discussed, also the equations of motion are discussed also.

Chapter six presents a study on voltage stability, the use of PV and QV curves to analyze voltage stability was discussed in details, also issues relating to voltage collapse and their mitigations were discussed.

Chapter seven presents the simulations and results of this study also discussions and interpretation of results are shown.

Chapter eight Presents a comprehensive study on voltage stability of power systems using three transmission schemes (HVAC, HVAC-HVDC and VSC/HVDC-HVAC networks)

Chapter nine is a continuation of chapter eight; a detailed study of transient stability was done here using the three transmissions schemes in chapter eight. The chapter also, presents the comparison of the results using the three transmission schemes

Chapter ten gives the conclusions and recommendations of this study

Chapter 2

HVAC transmission system

2.1 Literature review

Historically, the first commercial electricity to be transmitted to load by Thomas Alva Edison was the direct current (DC) electric power. Therefore, the first transmission system was dc power system. Thomas Alva Edison's system operated at a very low voltage, for this reason it became a local affair, it is either the generator was located close to the load or vice versa. This situation gave vent to the alternating current (AC) option which then was more feasible for the need of a robust and dynamic electrical technology; unlike the DC it could be transformed from one voltage level to another. It could be transformed from high voltage to low voltage value and vice versa which makes it suitable for transmission and distribution of electricity.

Furthermore, with the invention of AC induction motor by Nikola Tesla, more end users were largely dependent on AC which could be generated at large power plant for HVAC bulk delivery over long distances. For this reason AC originally prevailed over DC as a means of power transmission. However, Edison's DC paradigm resurfaced with the recent discoveries in electronic technologies, the semi conductor devices like the Thyristor valves, Insulated gate bipolar transistor (IGBT), MOSFET, VSC, Mercury arc rectifiers etc. made the design and development of line-commutated current source converter possible. This electronic device enables the conversion of ac to dc at high voltage at the source hence overcoming the initial problem with DC system giving rise to the HVDC system [6, 7]. Both systems have their inherent advantages and disadvantages as will be discussed latter. This project dwells on a hybrid system that will bring about the convergence of the comparative advantages of the two systems and at the same time mitigates on their short falls (with more emphasis on the effect of HVDC base solutions on the hybrid network) for a more stable, reliable and efficient power supply.

2.2 HVAC transmission network

Alternating current (AC) is electricity that changes direction at regular interval. It builds to maximum voltage in one direction and drop to zero and builds up to maximum in

opposite direction and returns to zero. The complete sequence is known as a cycle and the rate at which it repeats itself is known as frequency of the current. In Africa AC power provides energy to home outlet at the frequency 50 Hz or 50 cycles per second [8].

2.2.1 Fundamentals of HVAC Transmission

For the purpose of analyses, because transmission lines are normally interconnected with other elements in the system, simple equivalent circuits are used here to represent the performance of the transmission lines. The assumption is that the line is lossless.

Fundamentally, the parameters of a transmission line are the shunt conductance, the series resistance, series inductance and the shunt capacitance, other parameters like the reactance, admittance, subceptance and impedance e.t.c. also plays a major role on the power transmitted in the transmission line. These parameters are distributed within the network and so are their effects.

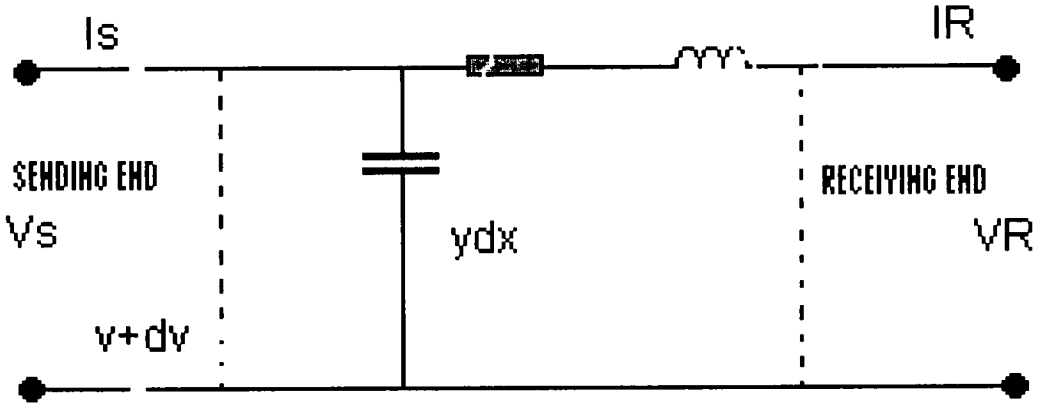

Figure 2.1 Equivalent circuit of HVAC transmission line

The voltage and current relationship for the sending and receiving ends are given as in equations 2.1 and 2.2.

$$V_S = V_R \frac{e^{\gamma l} + e^{-\gamma l}}{2} + Z_C \, I_R \frac{e^{\gamma l} - e^{-\gamma l}}{2} \tag{2.1}$$

$$I_S = I_R Cosh(\gamma l) + \frac{V_R}{Z_C} Sinh(\gamma l) \tag{2.2}$$

Where, V_S is the sending end voltage, V_R is the receiving end voltage, Z_C is the characteristic impedance of the transmission line, γ is propagation constant and l is the length and β = phase constant.

Where

For lossless line, $\theta = \beta l$ and $\gamma = j\beta$ the power transmitted in a power network is simplified as given in equations 2.3 and 2.4.

$$P_S = \frac{E_S E_R}{Z_C \sin\theta} \sin\delta \tag{2.3}$$

$$Q_S = \frac{-E_S(E_R \cos\delta - E_S \cos\theta)}{Z_C \sin\theta} \tag{2.4}$$

Where, P_S represents the active power at the sending end of the transmission network, Q_S represents the reactive power at the sending end of the transmission network, E_S and E_R represents voltages at sending and receiving ends respectively and Z_C is the characteristics impedance of the transmission line. δ is the phase angle displacement between the sending end and receiving end voltages of the transmission line, θ represents the line angle. In a lossless line, when R = 0, maximum power is transferred when δ equals 90^0. Increasing or decreasing these parameters determines the power transmitted along the transmission lines in power networks [1].

2.2.2 Advantages of HVAC and Disadvantages of HVAC

For proper planning of a good network it is essential that the advantages and disadvantages of both systems are highlighted since this will help network planners in the design, operation and control of a reliable network. Advantages of HVAC Transmission system can be found in [9].

Advantages of HVAC

- Ease of transformation of energy from one energy level to another which makes it possible for high voltage transmission and distribution to load.
- Before the break even distance the initial investment is lower for HVAC system than the HVDC alternative. Therefore, HVAC is favourable for short distance transmission since I^2R loss will not be affected much for a shorter distance.

- Various house and office equipment use ac induction motors within their circuits, therefore, it is not feasible to phase out the AC systems.
- HVAC is the base of HVDC without HVAC it will be impossible at the moment to transmit HVDC at low voltage, this is because DC can not be transformed from low voltage to high voltage.

Disadvantages of HVAC

- The disadvantages of HVAC system can found in [9, 10] some of the disadvantages are given below.
  - Cost of implementation is high due to large sum involved in the acquisition of land and right of ways
  - HVAC can not transmit power beyond certain distance, because the loss increases with distance
  - Asynchronous tie with two AC networks is not practicable due to stability problems and difference in frequency.
  - Interference with neighbouring equipment could lead to litigation and unnecessary disturbance from the owners of the equipment.
  - Voltage stability problems
  - Inter-area oscillation
  - Blackouts due to cascading effects
  - Long distance limitations both for under water transmission and over head transmission
  - Because storage capacity of electric power is limited spinning reserve is normally transmitted thereby imposing additional burden on the network.

2.2.3 Reasons for Interconnections of networks

- Possibility to use larger and more economical power plants, by harnessing their comparative cost advantages
- With interconnection of power systems, the flexibility of building new power plants is enhanced, since new plants will readily be connected to the grid.
- Increased reliability in the systems, as a result of the control and operation measure in the grid.
- Power integrity is improved upon in interconnected systems

- Reduction of losses by an optimized system operation (i.e. a well utilized system with high level of efficiency)
- Decentralization of location of power plants this enables utilization of power from renewable energy source this is known as pooling of large power generation stations, since wind farms offshore could be easily connected to the main grid, also power form other sources can do likewise irrespective of their location they can be part of the network.

Chapter 3

HVDC Transmission system

Definition of DC: Direct current (DC) is a continuous flow of electricity in one direction through a conducting medium from a position of higher potential to a lower potential. Like in batteries from +ve pole to –ve pole. DC could be created by generators such as fuel cells, PV cells, by static electricity, lighting and batteries.

Direct Current (DC) from the history of electricity was the first electrical power to be generated and transmitted by Thomas Elva Edison, but could be commercialized because of the reasons stated earlier i.e. inability to transmit under low voltage. The advancement in the semiconductor technology therefore helped in the development of HVDC system. With this technology DC can be transmitted at higher voltages. The first commercial HVDC link was in 1954 linking the Swedish mainland to the Island of Gotland a distance of about 98 km, the link was rated 20MW, 100KV [9, 11] this was achieved using Mercury arc valve. The first Thyristor valve HVDC was commissioned in 1972 at the Eel River project, a 320 MW Back-to-Back DC interconnection, between the power systems of the Canadian provinces of Quebec and New Brunswick [1]. And the longest HVDC submarine cable link was commissioned in1994, known as the Baltic HVDC cable project, linking a distance of 250 km. The first commercial VSC-HVDC (HVDC Light) installation was done in 1997 [12]. Itaipu project, Brazilian-Paraguayan joint venture with the capability of 6,300 MW and 600 KV, and total installed capacity of 12,600 MW. 28% of the power generated is transmitted to Southeastern Brazil, due to the difference in frequencies of the two countries; half of the generation is 50 Hz (Paraguay) and half at 60 Hz (Brazil). The Itaipu power project is the highest HVDC power project implemented till date. The Brazilian-Paraguayan joint venture covers a distance of 785 km [13]. The recent improvement in HVDC technology gave birth to voltage source converter HVDC (VSC-HVDC) otherwise known as HVDC^{PLUS} by Siemens (meaning HVDC power link universal systems) this uses multilevel switching and HVDC light by ABB, this technology uses pulse width modulation, both uses Insulated gate bipolar transistor (IGBT) for power conversion, instead of Thyristors. Voltage source converter (VSC) operates at a very high frequency (1-2 KHz) using pulse width modulation (PWM). This

is the preferred technology for interconnection of Islanded grids to the power system, such as offshore wind farms, the technology utilizes the use of "Black-Start" feature of voltage source converter (VSC) [14].This does not have the need for driving system voltage; VSC-HVDC have the capability to build up a three phase AC voltage via the DC voltage at the cable end, supplied from the converter at the main grid. With this a lot of the problems of the HVDC system were resolved, i.e. interconnection to a weak AC network, commutation failure, also with VSC the converter stations are smaller than that of the classical HVDC system e.t.c.

3.1 The HVDC network

3.1.1 Reasons for HVDC

AC transmission is practically impossible for under water transmission for a distance above 30 Km, this is due to high capacitance of the line requiring intermediate compensation stations.

Asynchronous link between two ac systems where ac ties would not be feasible because of system stability problems or difference in their operating frequencies i.e. 50 Hz, and 60 Hz systems.

Bulk power transmissions over a long distance HVDC system have proven to be the best alternative to HVAC system [1].

3.1.2 Advantages and disadvantages of HVDC system

Advantages of HVDC

HVDC transmission system has a number of advantages when compared with HVAC system as stated in [3, 10, 15, and 16]

- Long distance water crossing. In a long AC cable transmission, the reactive power flow due to the large cable capacitance will limit the maximum transmission distance. With HVDC there is no such limitation, why, for long cable links, HVDC is the only viable technical alternative.
- An optimized HVDC transmission line has lower losses than the optimized HVAC transmission lines for the same power capacity. The power dissipated at the converter station is about 0.6% of the total power transmitted, therefore, the loss from HVDC

comes out lower than the HVAC case practically in all cases, and also HVDC cables have lower losses than the AC cables.

- Asynchronous connection. Sometimes it technically impossible to connect two AC networks due to stability reasons, with HVDC such network can be connected asynchronously and enables independent operations in such a way that stability is not compromised. A HVDC link has been achieved between two AC networks of 50 and 60 Hz frequencies in Japan and South America. In this instance AC option is not possible because of stability issues.
- Controllability. One of the fundamental advantages of a HVDC system its ability to control active power in the link.
- HVDC acts as stability booster and firewall against large blackouts or cascading effects.
- Due to reactive power limitation AC transmission is constrained by distance, for under water transmission AC transmission is not feasible beyond 50 km and for overhead transmission distances above 600 km posses a problem [17].
- When interconnected HVDC can support the operation of the AC interconnection at faults in the system and also control power flow.
- Lower cable cost than AC as it uses ground as one circuit (mono polar links)
- Easy to control flows than AC and no loop flow problem
- The direction of power can be reversed with ease
- No limits in transmission distance. This is valid for both overhead lines and submarine/underground cables.

Disadvantages of HVDC

Some disadvantages of HVDC lines can be found in [1, 9] other disadvantages are described under-leaf:

- Thyristor (converter) stations at each end are expensive compared to AC substations
- Filters required to ensure acceptable waveforms on both the AC and DC sides
- Limited multi terminal DC networks because no acceptable DC circuit breakers
- Requires injection of reactive power
- Converter stations absorbs reactive power

- Generation of Harmonics, the generated harmonics will have adverse effects on the power system; therefore, additional filters are needed to support its operation.

3.1.3 Investment cost

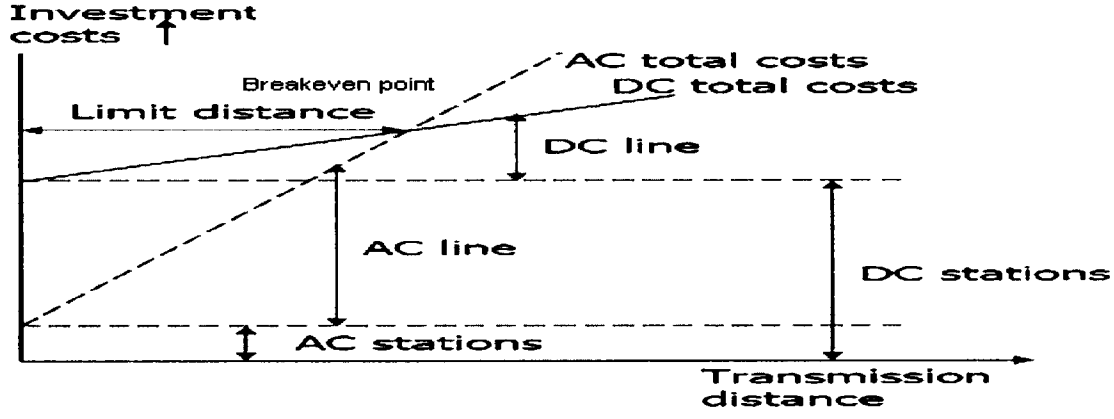

Figure 3.1 Investment cost of AC versus DC transmission systems [18]

From figure 3.1 above it is evident that the initial investment cost for building a HVDC system is higher than that of the HVAC system but when it gets to the break even point (limit distance) where both cost are equal the HVDC system becomes more economically viable than the HVAC system. The break even point is about to 600 Km for over head transmission and about 50 km for under water transmission[1, 17] from this point onwards it becomes more expensive to transmit power using HVAC system. This shows that the HVDC transmission line cost less than HVAC transmission line for the same transmission capacity. Even though, the terminal stations are more expensive in the HVDC case due to the fact that they must perform the conversion from AC to DC and vice versa. On the other hand, the cost of transmission medium (over head lines and cables), land acquisition, right of way costs are lower for HVDC system [10, 18 and 19]. Also, operation and maintenance cost is lower in the DC system, initial loss level is higher in DC (losses due to converter stations) but does not increase with distance. In contrast loss level increases with distance in HVAC systems.

3.1.4 Applications of HVDC Technology

A good number of applications of HVDC can be found in [17, 35] as follows:

- Power flow control in HVAC transmission networks are difficult, HVDC provides suitable control for ac limitations
- Import of power to a congested environment where it's practically impossible to build new lines due to right of way (ROW) requirements. This is due to the fact that, less space is required for the HVDC system compared to the HVAC system
- Delivery of bulk power from large energy source to load over a long distance i.e. connection of remote hydro stations to load centers.

Reasons for Interconnection of networks

- Possibility to use larger and more economical power plants
- Reduction of the necessary reserve capacity in the system
- Increased reliability in the systems
- Decentralization of location of power plants this enables utilization of power from renewable energy source this is known as pooling of large power generation stations, since wind farms offshore could be easily connected to the main grid, also power form other sources can do likewise irrespective of their location they can be part of the network.

3.1.5 Design Consideration

The purpose of implementing network interconnections is to get the best out of the network, keeping in mind the power quality, stability, efficiency and reliability of the system. Also cost benefit of the project is of major concern. Main aim is to meet the need of the customer at the most cost effective and environmentally friendly way. In a liberalized power market the advantages are: pooling of large power generation stations, sharing of spinning reserve and the use of most economic energy resources, taking into account the ecological constraints [20]: nuclear power stations at special locations, hydro energy from remote areas, solar energy from the desert areas and connection of large off-shore wind farms can be connected with HVDC links. HVDC and hybrid AC-DC solutions will play an important role for the system developments, leading to Smart Grid with better controllability of the power flow. In the past, it was easy to meet the rising demand for transmission capacity by building more power plants. Expediency and

obligation to meet customer's demand were the driving force behind system design. Costs were simply pushed to the customers. Hence, power systems with high level of redundancy and integrity were not needed. Today power industries is being deregulated, therefore more efficient ways of operation are emerging, since cost of inefficiency can not be passed over to the customer in a deregulated market. Therefore, the market share of the most efficient producer is expected to rise, because more customers will naturally gravitate to those companies with the best power quality.

3.1.6 HVDC configurations

- Back-to- Back Solution
- HVDC Point-to-point solution
- Hybrid HVDC/HVAC solution
- Multi-terminal links
- Back-to-Back: With this transmission method, two network systems are interconnected at one point, and thus the transmission losses are not significant. Only the bus bar is used as the transmission path. It is desirable for asynchronous tie, it may be designed for bipolar or monopolar links and its' suitable for medium power transmission within short distance
- Point-to-Point: This is used for bulk power transmissions; it has the advantage of fast power flow control and the ability to transmit power up to 800 km and beyond.
- DC systems with more than one terminal is referred to as multi-terminal DC (MTDC), example of this is the Sardinia-Corsica-Italy scheme [1]
- Hybrid HVAC-HVDC network is formed when the AC and DC networks are interconnected together for the purpose of transmission of power within the network.

3.1.7 HVDC Links

- Monopolar links
- Homopolar links
- Bipolar links
- Multi-terminal

Monopolar: This link uses one conductor of negative polarity and uses either ground or water as its return path as shown in figure 3.2. In some cases where the earth resistivity is too high or where there is possible interference with underground and under water structure a metallic return path at low voltage is used. Example: Fennoskan 500 MW, 400KV here sea was used as the return path due to corrosion problem [21].

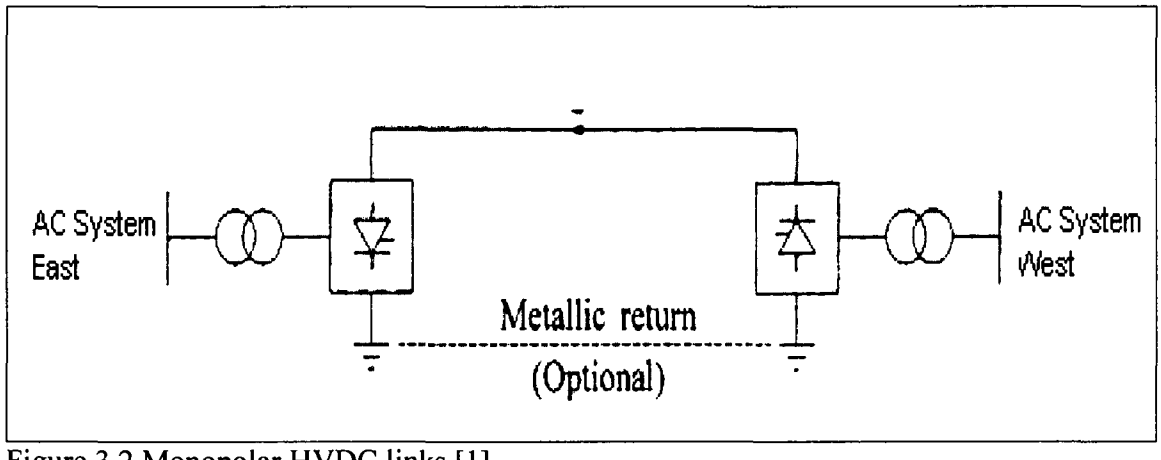

Figure 3.2 Monopolar HVDC links [1]

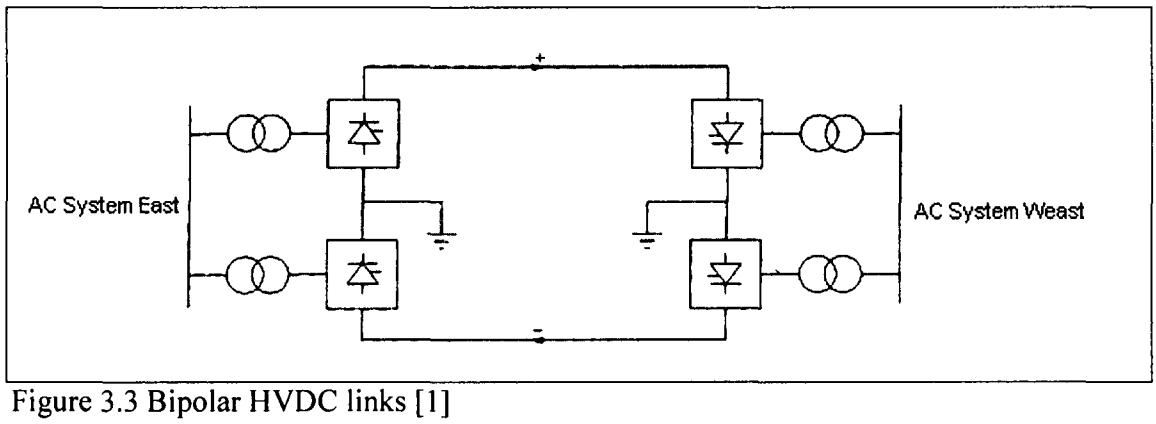

Figure 3.3 Bipolar HVDC links [1]

Bipolar links: This link has two conductors, one positive and the other negative. Each terminal has two converters of the same voltage magnitude. This is connected in series on the DC side, and the junction between the converters is grounded as shown in figure 3.3. It consists of converter transformer, converters, shunt capacitors, DC reactors [22, 17]

Homopolar link: This equally has two or more conductors all having the same polarity, -ve polarity (see figure 3.4) is normally preferred because it causes less radio interference due to corona and the return path is the ground. When there is a fault in one conductor the

entire converter is available to feed the other conductors which normally come with some over load capability and as such can carry more than the normal power. Homopolar links has disadvantage where continuous ground current is not acceptable, ground currents normally affect gas and oil pipe lines that lies within few miles of the systems electrodes. This could cause corrosion of pipeline metals. This is one of the banes of using ground return path [1].

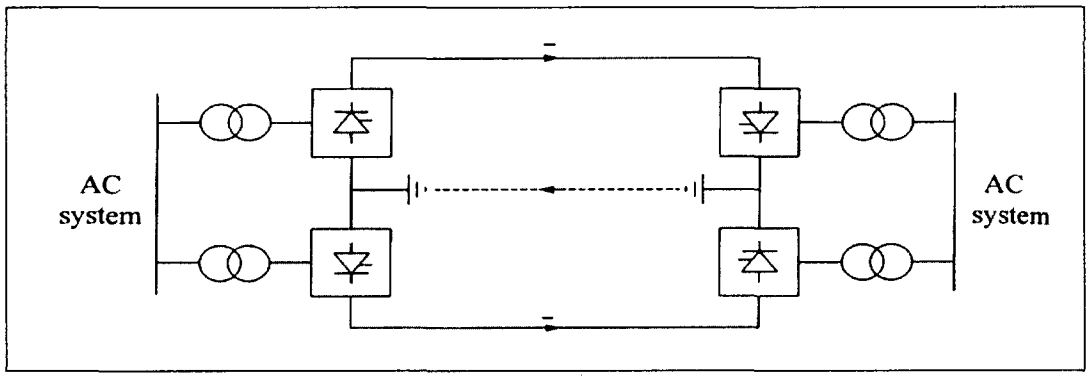

Figure 3.4 Homopolar HVDC link [1]

3.2 Components of HVDC Transmission system

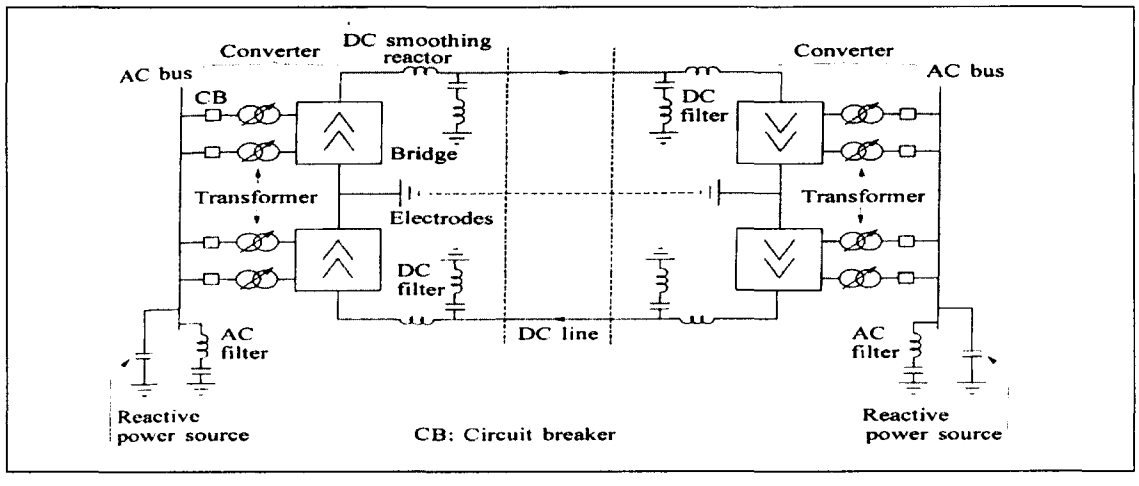

Figure 3.5 HVDC Technologies [1]

3.2.1 Converters

Converters performs ac/dc and dc/ac conversion and consist of valve bridges and transformers with tap changers. The valve bridges consist of high voltage valves

connected in a 6-pulse or 12-pulse arrangement. The converter transformer provides ungrounded three phase voltage source to the valve bridge. Examples of valves are mercury arc valve, thyristor valve, VSC valve e.t.c. with VSC valve converters there is no need to compensate any reactive power consumed by the converter itself and the current harmonics on the AC side are related directly to the PWM frequency. Thus, the amount of filters needed is reduced considerably [23]

3.2.2 Smoothing Reactors

These are large reactors with inductances as high as 1.0 H their functions are as stated in [1] as follows:

- Reduce crest current in the rectifier during dc line faults
- prevents distortion of currents at small loads
- prevents commutation failure at the inverter
- Reduces harmonic current and voltage in the dc line

3.2.3 Harmonic Filters

Filters are used on both the AC and the DC sides of the network to suppress the harmonics generated by converter stations. This harmonics, if not filtered, may cause overheating of the capacitors and nearby generators.

3.2.4 Reactive Power Source

Converter stations absorb reactive power during operation. Under steady state of operation the reactive power absorbed is about 50% of the active power transmitted [1]. This percentage increases under transient conditions and therefore, reactive power sources are normally provided near the converters.

3.2.5 Electrodes

To reduce current densities and surface gradients, large surface conductors are normally used to provide neutral connection to earth. Conductors connected in this manner are referred to as an electrode. However it's advisable to limit current flow through the earth and for this reason metallic return conductors are used for this purpose.

3.2.6 DC Lines

These are overhead lines or cables used for transmission of power.

3.2.7 AC Circuit Breakers

These are used for clearing faults on the transformer side taking dc links out of service. Basically it is used on the ac side of the network. DC faults are cleared by the converter control.

3.2.8 DC Filters

HVDC converters generate harmonics during their operation. These harmonics may cause perturbation of telecommunication equipment. DC filters are used to suppress these harmonics. DC filters are smaller than AC filters as shown in figure 7 above [1].

3.3 Converter theory

The main elements in the converter are the transformers and the valve bridges. The valve bridges are arrays of high voltage switches or valves that sequentially connect the three phase alternating voltage to the DC terminals so that control and conversion of power is obtained. Converter transformer provides interface between the AC and DC system. The valves are electronic switches which conducts current in only one direction, from the anode to the cathode forward direction, when the voltage across the valve is such that the cathode becomes positive with respect to the anode the valve blocks the current. The valve conducts when a positive voltage is applied to the gate; conduction is initiated by applying sustained current pulse of proper polarity to the gate. The current through the valve continues until it drops to zero and a reverse voltage bias appears across the valve, the valve blocks the current in the forward direction until a control pulse is applied to the gate. When the valve is not conducting it should be capable of withstanding forward and reversed bias voltages across the anode and cathodes [1, 24, and 25].

3.3.1 Multi-terminal system

The successes of single and double terminal HVDC systems have led engineers to develop multi-terminal HVDC systems (MTDC). Any HVDC system with more than two terminals is considered to be MTDC. The First application of MTDC was made in Italy in the Sardinia-Corsica scheme, in 1991. Two approaches have evolved in power flow

equation for MTDC, one is sequential solution approach, in this the AC and the DC equations are solved separately at each iteration process [26] and in unified solution approach, AC and DC are combined and solved as one set of equations during each iterative process [27].

There two methods of connection of MTDC, viz., the constant voltage parallel scheme and the constant current series scheme. In the parallel method, the converters are connected in parallel and operated with common voltage. This could either be radial or mesh network as shown in figure 3.6 and 3.7. Whilst in the series method the converters are connected in series with common series current flowing through the terminals as shown in figure 3.8. Sometimes, there could be hybrid of the both methods.

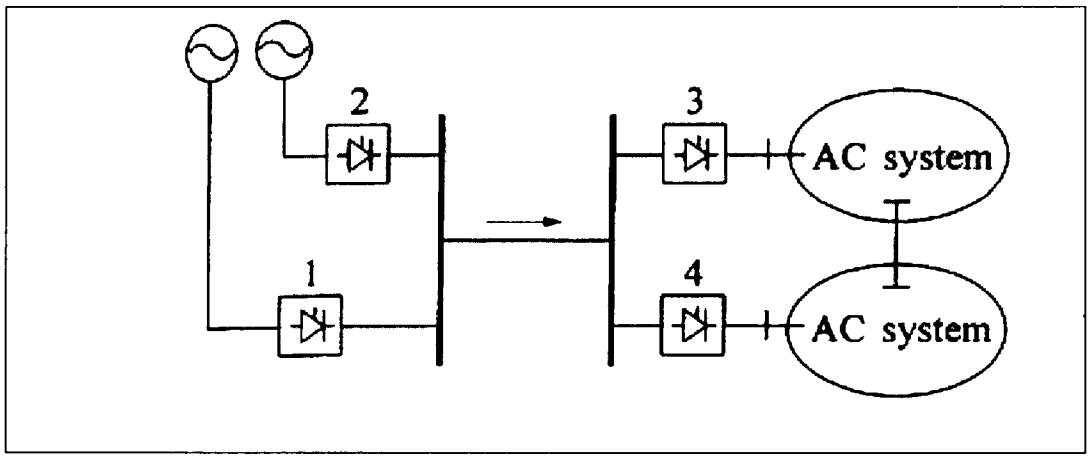

Figure 3.6 Parallel MTDC with radial network [1]

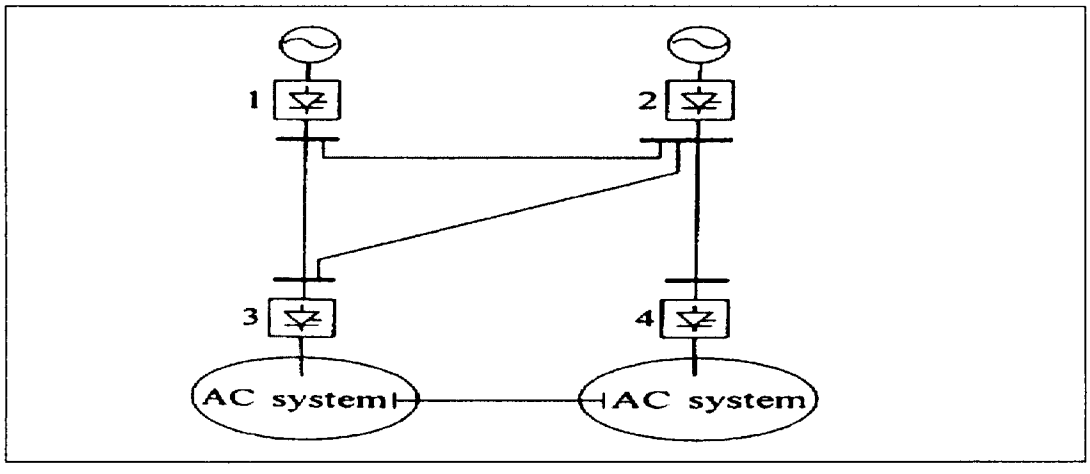

Figure 3.7 Parallel MTDC with and mesh network [1].

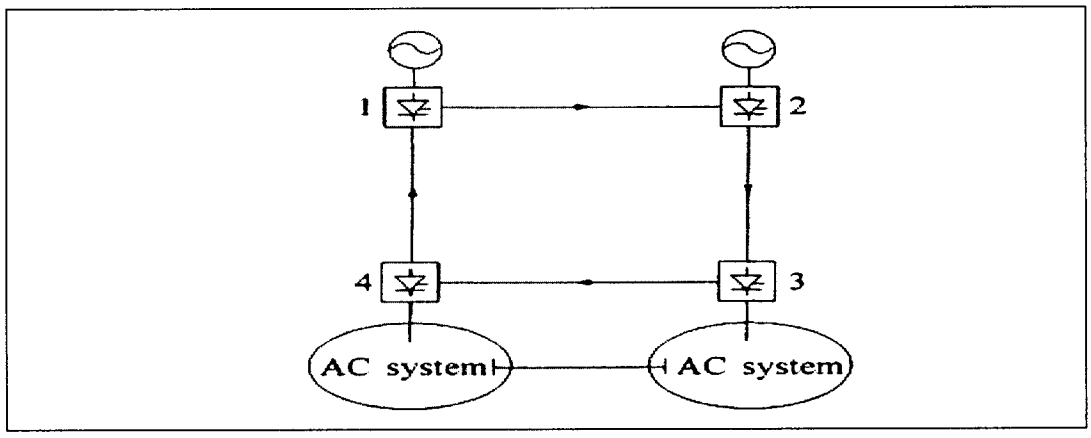

Figure 3.8 Shows series connected MTDC method [1]

The parallel scheme is most practically accepted method, because it has few operational problems, compared to series method it has fewer losses, it is easier to control and its' scalable [1].

3.4 HVDC Technology

HVDC technology involves the conversion of AC to DC at the transmitting end (rectifier) and the conversion of DC to AC at the receiving end (Inverter). There are three ways of achieving these conversions as discussed in [28].

3.4.1 Natural commutated converters

This is achieved by the thyristor technology. Thyristor is a controllable semi-conductor that can carry very high current up to 4000A and at the same time able to block voltages up to 10kV. Connecting the thyristors in series builds up a thyristor valve which is able to operate at a very high voltage. The thyristor valve operates at net frequency of 50 Hz or 60 Hz and by means of control angle it is possible to change the voltage level of the bridge. This ability is the way by which transmitted power is controlled rapidly and efficiently

3.4.2 Capacitor commutated converters

This is an improvement on thyristor based commutation; this is achieved by connecting a commutation capacitor in series between the converter transformer and the thyristor valves. The commutation capacitor improves the commutation failure when connected to weak networks.

3.4.3 Forced commuted converters

This type of converters introduces a spectrum of advantages; e.g. feed of passive networks (without generation), independent control of active and reactive power, and power quality. The valves of these converters are built with semi-conductors with the ability to turn on and also to turn off. They are known as voltage source converters (VSC). Two types of semi-conductors are normally used in the VSC, viz., the GTO (gate-off-thyristor) or the IGBT (Insulated gate bipolar transistor). The VSC commutates with high frequency and not net frequency. The operation of the converter is achieved by pulse width modulation (PWM). With PWM it is possible to create any phase angle and/ or amplitude (up to a certain limit) by changing the PWM pattern, which can be done almost instantaneously. This makes the PWM voltage source converter an ideal component in transmission network. From transmission network view point it acts as a motor or generator without mass that can control active and reactive power almost instantaneously

3.5 Converter theory and performance equation of HVDC

Three phase, full wave bridge circuit also known as Graetz bridge is used as the bench model for HVDC converters because, it provides better utilization of converter transformers and lower voltages across the valve when not conducting. This is known as peak inverse voltage and it is used to rate the valves. The AC side of the valve has on load tap changer for voltage control. Also it is normally star connected with grounded neutral, whilst the valve side is either star or delta connected with ungrounded neutral as shown in figure 3.9 as described in [1].

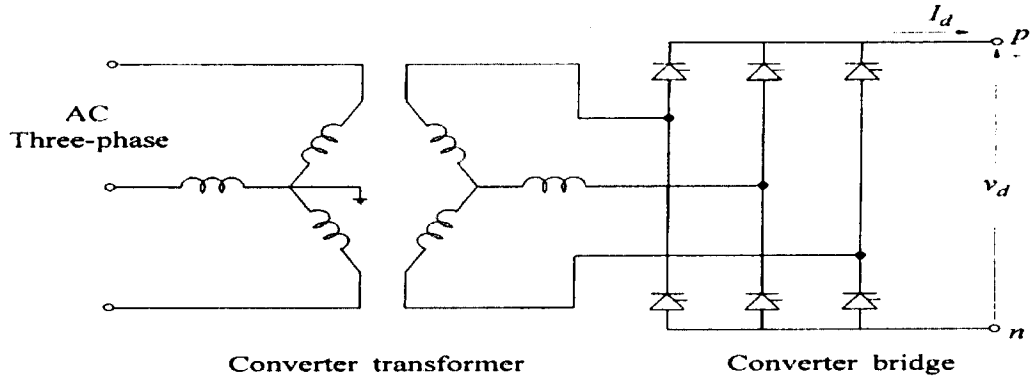

Figure 3.9 Three-phase, full-wave Graetz Bridge [1]

3.5.1 Description of three-phase, full wave Bridge circuit

Assumptions made [1]

- The AC side is made of constant source of voltage and frequency in series with a lossless inductance
- The direct current is constant and ripple free
- When not conducting the valve is said to have infinite resistance and zero resistance when conducting (an ideal switch)

The line-to-neutral voltage of three-phase bridge circuit are given below

$$e_a = E_m \cos(\omega t + 60^0) \quad (3.1)$$

$$e_b = E_m \cos(\omega t - 60^0) \quad (3.2)$$

$$e_c = E_m \cos(\omega t - 180^0) \quad (3.3)$$

Line-to-Line voltages

$$e_{ac} = e_a - e_c = \sqrt{3} E_m \cos(\omega t + 30^0) \quad (3.4)$$

$$e_{ba} = e_b - e_a = \sqrt{3} E_m \cos(\omega t - 90^0) \quad (3.5)$$

$$e_{cb} = e_c - e_b = \sqrt{3} E_m \cos(\omega t + 150^0) \quad (3.6)$$

3.5.2 Analysis with no ignition delay

In figure 3.10 the Cathodes of valves 1, 3 and 5 are connected together at the top. Valve 1 conducts when the phase to neutral voltage of phase (a) is more positive than the voltages of other phases. At this stage the valves of the three cathodes is at equal potential with the anode of valve 1, valve 1 conducts and valves 3 and 5 will not conduct because their cathodes is at higher potential than their anodes. At the bottom, the anodes of valves 2, 4 and 6 are connected together. Valve 2 conducts when phase c voltage is more negative than the two remaining phases.

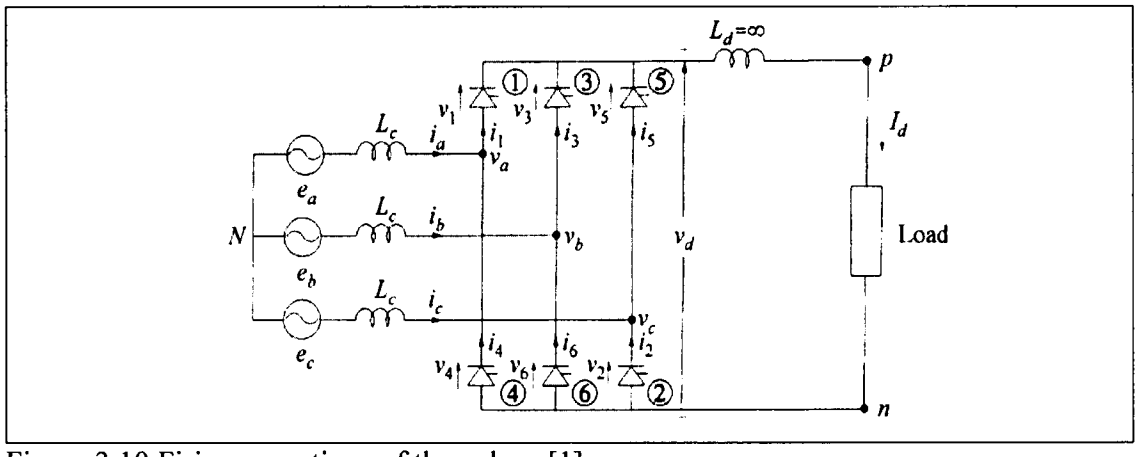

Figure 3.10 Firing operations of the valves [1]

Valve 1: This conducts when ωt is between -120^0 and 0^0, since e_a is greater than e_b or e_c

Valve 2: Conducts when ωt is between -60^0 and 60^0, since e_c is more negative than e_a or e_b at this instance.

Valve 3: Just after $\omega t = 0^0$, e_b becomes more positive than e_a and valve 3 conducts, valve 1 extinguished because its cathode becomes more positive than the anode (higher potential).

Valve 4: Conducts when $\omega t = 60^0$, e_a is more negative than e_c, causing valve 4 to ignite and valve 2 to extinguish.

Valve 5: Valve 5 conducts when $\omega t = 120^0$, e_c becomes more positive than e_b at this moment valve 3 is extinguished.

Valve 6: At $\omega t = 180^0$ conduction switches from valve 4 to 6 at the bottom, and at $\omega t = 240^0$ conduction switches from valve 5 to valve 1 at the top as shown in figure 3.10. Thus completing one cycle of conduction and the process continues as long as the system is operational. For a 6 pulse valve it takes six such periods to complete a full cycle of operation [1].

$$V_{do} = \frac{3\sqrt{6}}{\pi} E_{LN} = 2.34 E_{LN} \tag{3.7}$$

$$V_{do} = \frac{3\sqrt{2}}{\pi} E_{LL} = 1.35 E_{LL} \tag{3.8}$$

$$V_{do} = \frac{3\sqrt{3}}{\pi} E_m = 1.65 E_m \tag{3.9}$$

Equations 3.7 and 3.8 represents root mean square (RMS) values for line-to-neutral and line-to-line voltages, whilst equation 3.9 represents the peak value. E_{LL} and E_{LN} are the RMS values for line-to-line and line-to-neutral voltages. E_m is the peak value of line-to-neutral voltage. V_{do} is the ideal no load voltage [1].

3.5.3 Analysis with delay ignition

Gate and grid control are normally used to delay the ignition of the valves, α represents the delay angle. With delay, valve 3 conducts when $\omega t = \alpha$ rather than $\omega t = 0$, valve 4 ignites when $\omega t = \alpha + 60^0$, valve 5 ignites when $\omega t = \alpha + 120^0$ e.t.c. Valves will not ignite if $\alpha > 180^0$ [1]

Average direct voltage V_d when the delay angle is equal to α is:

$$V_d = V_{do} \cos\alpha \tag{3.10}$$

3.5.4 Analysis with commutation overlap

The time taken to transfer current from one phase to another is called commutation time or overlap time. Due to the presence of inductance L_c in the system this transfer is not automatic. The angle associated with this is known as overlap angle μ during operation μ is less than 60^0 full load values are within 15^0 to 25^0, with $0^0 < \mu < 60^0$. During commutation, the three valves conduct simultaneously, between commutations, only two valves conducts. A new commutation begins every 60^0, and last for angular period of μ [1].The current, voltage and resistance during overlap are given as follows:

$$I_d = \frac{\sqrt{3}E_m}{2\omega L_c}(\cos\alpha - \cos\delta) \tag{3.11}$$

$$V_d = V_{do}\cos\alpha - R_c I_d \tag{3.12}$$

$$R_c = \frac{3}{\pi}\omega L_c = \frac{3}{\pi} X_c \tag{3.13}$$

$\cos\alpha = -\cos\beta$ and $\cos\delta = -\cos\gamma$

X_c and R_c are the commutation reactance and resistance, R_c accounts for voltage drop due to overlap, it is not a real resistance therefore, it does not consume power. At the end of commutation $\omega t = \delta$ [1].

Where,

α = ignition delay angle

δ = extinction delay angle

μ = overlap angle

3.6 Converter operation

With no overlap

$$V_d = V_{do} \cos\alpha \tag{3.14}$$

With overlap

$$V_d = \frac{V_{do}}{2}(\cos\alpha + \cos\delta) \tag{3.15}$$

The transitional value of ignition delay angle, beyond which inversion takes place, is given as follows:

$$\cos\alpha_t + \cos\delta = 0 \tag{3.16}$$

$$\alpha_t = \pi - \delta_t = \pi - \alpha_t - \mu = \frac{\pi - \mu}{2} \tag{3.17}$$

Therefore, the effect of the overlap is to reduce the transitional value of the ignition angle from 90^0 to $90^0 - \frac{\mu}{2}$

Where,

δ_t = transitional value of the delay angle, beyond which inversion takes place

α_t = the transitional value of extinction angle, beyond which inversion takes place

The change over of conduction from one out going valve to another incoming valve must be complete before the commutating voltage becomes negative, in order for the commutation to be successful. This means that commutation from valve1 to valve 3 is possible only when e_b is more positive than e_a. The current changeover from valve 1 to valve 3 must be complete before e_a becomes more positive than e_b with sufficient

margin to allow for valve de-ionization. The values α, μ, β and δ are related as follows:

$\delta = \alpha + \mu$ = extinction delay angle

$\beta = \pi - \alpha$ = ignition advance angle

$\gamma = \pi - \delta$ = extinction advance angle

$\mu = \delta - \alpha = \beta - \gamma$ = overlap

During faults the overlap decreases with firing angle reaching about 90^0 the ac harmonic will increase for a given line current [29]. When the overlap increases the harmonic component decreases at full load overlap is about 20^0 and firing angle about 15^0.

3.5.1 Abnormal operations

- **Arc-Back**

This is referred to as conduction in the reverse direction which occurs when there is an inverse voltage across a valve. Arc back occurs more during rectification than inversion. Causes of arc-back are as follows: over current, high rate of change of current after at the end of conduction, high peak inverse voltage etc. To overcome, a bypass valve is connected across the valve group as shown in figure 3.11. Arc-back is common with mercury valves. Thyristor valves are free from this anomaly [1].

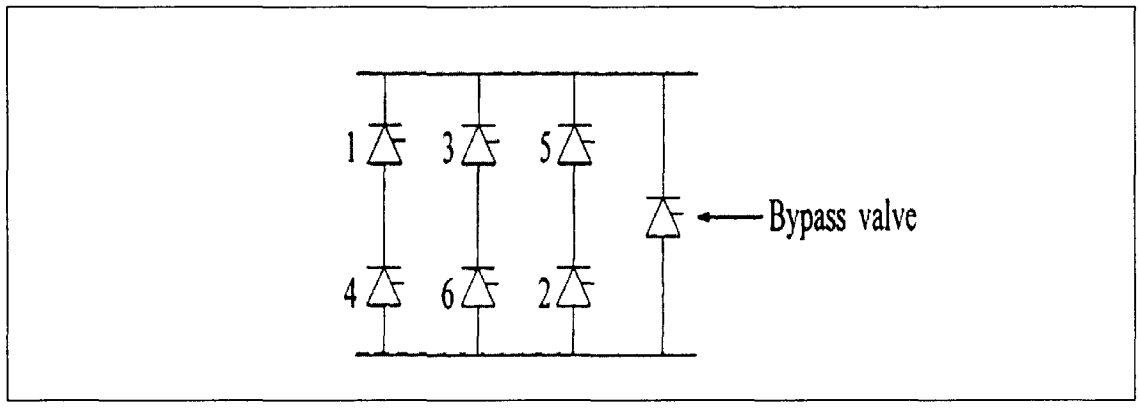

Figure 3.11 Bypass operations [1]

3.5.2 Commutation failure

Failure to complete commutation before the commutating voltage reverses with sufficient margin for de-ionization is known as commutation failure. This phenomenon is

associated with inverter and it normally occurs during perturbations, like high direct currents or low ac voltage. Commutation failures occur in rectifiers only when the firing circuit fails. [1]

3.5.3 HVDC control systems

$$I_d = \frac{V_{dor}\cos\alpha - V_{doi}\cos\gamma}{R_{cr} + R_L - R_{ci}} \tag{3.18}$$

$$P_{dr} = V_{dr} I_d \tag{3.19}$$

$$P_{di} = V_{di} I_d = P_{dr} - R_L I^2{}_d \tag{3.20}$$

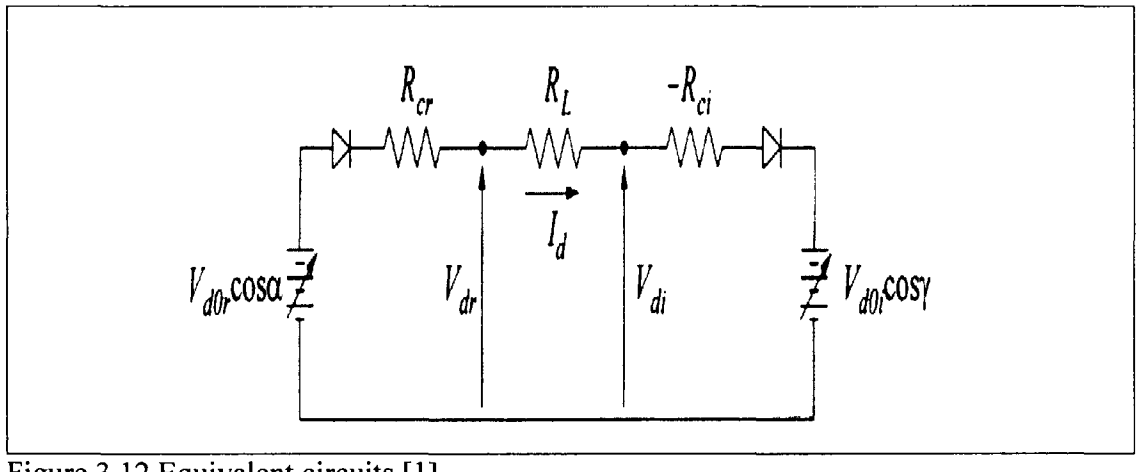

Figure 3.12 Equivalent circuits [1]

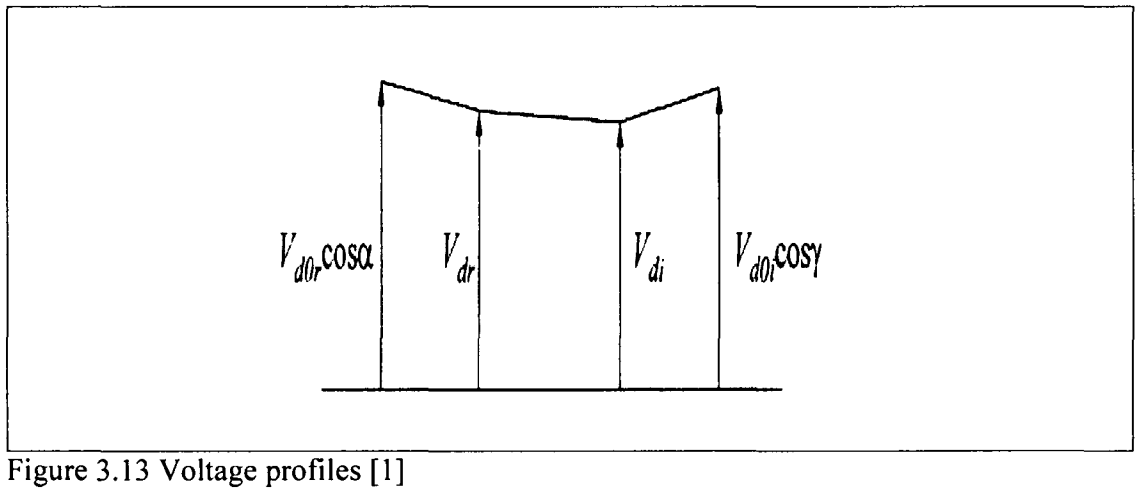

Figure 3.13 Voltage profiles [1]

The Control of the direct current I_d, direct voltage V_d and power P_d (as shown in figure 3.12) at any point in the line are achieved by varying the internal voltages $V_{dor}\cos\alpha$ and

$V_{doi}\cos\gamma$ through grid/gate control of valve ignition angle, ac voltage is controlled by tap changing of the converter transformer.

In the HVDC control the Grid/Gate control is a rapid action, the time range is within 1-to-10 ms. whilst tap changing action for the restoration of converter angle parameters to their normal range is slow, the time range is within 5-to-6 seconds.

Control is important for maintaining the power factors at the sending and receiving ends as high as possible, to keep the direct voltage close to rated value and also, for the prevention of commutation failure in the case of mercury-arc valve. Small change in V_{doi} and V_{dor} shown in figure 3.13 causes a large change in I_d (25% change in rectifier or inverter voltage will result in 100% change in I_d) [1, 30].Therefore rapid control of HVDC is essential; otherwise high currents resulting from these changes could damage the valve. Direct voltage along the line in the transmission line should be close to rated value to minimize the direct current and line losses.

To achieve high power factor α and γ are kept as low as possible, $\alpha_{\min}$ for the rectifier is about 5^0. The normal range of operation of a rectifier is within the range 15^0 to 20^0. Minimum extinction angle is maintained at the inverter to avoid commutation failure. Sufficient room is allowed for de-ionization before the commutating voltage reverses at $\alpha = 180^0$ or $\gamma = 0^0$, the extinction angle γ is equal to $\beta - \mu$ with the overlap μ depending on I_d and the commutating voltage. Because of the possibility of changes in DC and AC even after commutation had begun. Sufficient commutation margin above γ limit must be maintained, in a 50 Hz systems acceptable value for $\gamma = 15^0$ and $\gamma = 18^0$ for 60Hz systems [30].

3.5.4 Rectifier/Inverter characteristics

During operation the rectifier operates at constant current (CC) condition whilst, the Inverter operates under constant extinction angle (CEA). By changing α the rectifier maintains constant current, once $\alpha_{\min}$ is reached no further voltage increase is possible. The rectifier operates at constant ignition angle (CIA) as shown by the two segments in figure 3.14 AB represents CC and FA represents CIA.

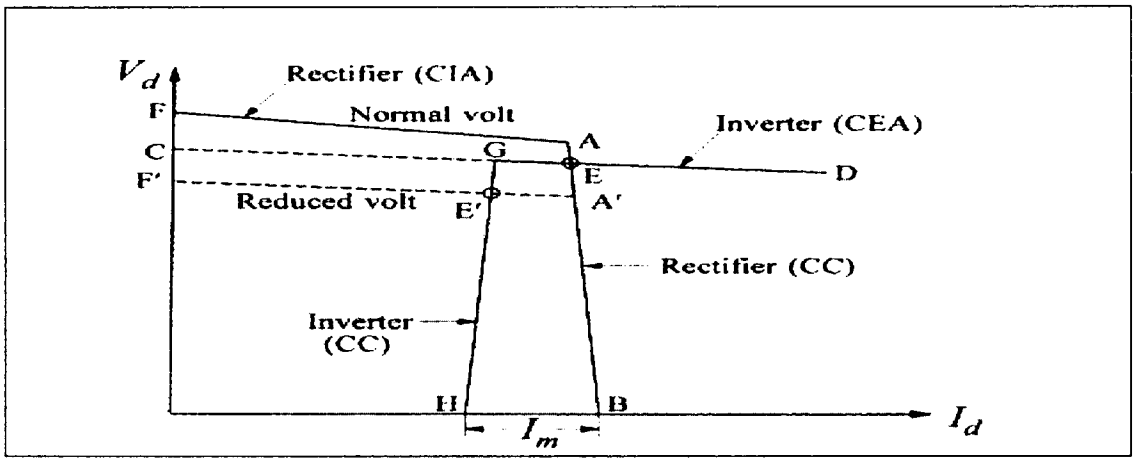

Figure 3.14 Rectifier/Converter characteristics [1]

FAB represents the normal operating characteristics of the rectifier. At reduced voltage the operation shifts to F'A'B. CEA characteristics of the inverter intersects the rectifier characteristics at E but it does not intersect at reduced voltage F'A'B. Thus a large reduction in the voltage will cause current and power to be reduced to zero depending on the reactor used. That is why inverters are normally provided with current controllers set at lower voltage than the rectifier. The inverter characteristic is given by DGH. The difference between the rectifier current order and inverter current order is known as current margin I_m. In practice this is normally set at 10-to-15% [1].

Under normal operating condition given by the intersection at E the rectifier controls the direct current and the inverter the direct voltage. At reduced rectifier voltage (possibly due to perturbation) given by the intersection E' the rectifier takes over the voltage control while the inverter takes the current control.

3.5.5 Tap Changer control

Whenever α and γ exceed their maximum range within few seconds the tap changer control is used to keep them within the acceptable range.

3.5.6 Voltage dependent Current order limit (VDCOL)

This is used to correct problems associated with operation under low voltage conditions. It reduces the maximum allowable direct current when the voltage drops below a predetermined value. This ensure stable operation, because when voltage drops by more than 30%, the reactive power demand of the remote converter increases with the attendant consequences on the system [1]. With the action of VDCOL there are no risks of commutation failure and voltage instability at reduced voltage.

3.5.7 HVDC power flow reversal

HVDC is capable power flow in either direction. Its control features allows for bidirectional power flow and power reversal is achieved through a prescribed series of ramps. This can be very fast with or without blocking of firing valves. The reversal of power may include the followings - reduction of current to 0.1 to 0.5 p.u via a step or ramp and decrease/increase of voltage via ramp or exponential function followed by a current ramp to reach the required level. Power reversal could be achieved within 20 to 30 ms [1]

3.5.8 Strength of HVDC/HVAC Interactions

The interaction of ac/dc depends largely on the strength of ac system relative to the capacity of the dc link. AC system can be considered to be weak from two perspectives; when AC impedance is high and when AC system mechanical inertia is low. HVDC control also plays important role in determining the good interaction between the hybrid network systems irrespective of the strength of the network.

For the comparison of ac strength relative to dc strength short circuit ratio (SCR) is used

$$SCR = \frac{short-circuit-MVA-of-ac-system}{dc-converterMW-rating} \tag{3.21}$$

Short circuit MVA is given by

$$SC-MVA = \frac{E^2_{ac}}{Z_{th}} \tag{3.22}$$

Where E^2_{ac} the commutation bus voltage at rated dc power and Z_{th} is the thevenin equivalent impedance of AC system. To include the effects of AC side equipment (filters, shunt capacitors, synchronous condensers e.t.c) associated with the dc link effective short circuit (ESCR) ratio is used. The system strength is considered [1] as follows;

High if ESCR is more than 5

Medium if ESCR is between 3 and 5

Low, if ESCR is less than 3

With improvement in AC/DC control the system strength is now classified as follows:

High if ESCR is more than 3

Medium if ESCR is between 2 and 3

Low, if ESCR is less than 2

In addition to SCR the phase angle of the thevenin equivalent impedance or damping angle has an impact in AC/DC interaction typical values of damping angle is between 75^0 and 85^0[1].

Effects of low ESCR

- High dynamic over-voltage
- Voltage instability
- Harmonic resonance
- Voltage flicker

3.5.10 HVDC response to a fault in a weak ac system

- Inverter extinction angle increases to maintain volt-second commutation margin
- The AC voltage is reduced , thereby aggravating the situation
- Power control increases dc to restore power
- Inverter consumes more VARs at reduced voltage

3.5.11 Solutions to problems of weak systems

Synchronous condensers or Static Var compensators are used to mitigate the problems associated with the use of weak ac systems. Also HVDC controls play a vital role in this respect. HVDC under this condition switches from power control to current control utilizing voltage dependent current order limit (VDCOL) to reduce the DC current for low AC voltage. On the other hand, Synchronous condenser basically reduces the system's effective impedance, thus shifting the parallel resonance frequency to higher frequencies at which damping is better.

3.5.12 Effective Inertia constant

$$H_{dc} = \frac{Total - rotational - inertia - of - ac - system, - MW'S}{MW - rating - of - dc - link} \qquad (3.23)$$

The ability of ac system to maintain the required frequency and voltage depends on the rotational inertia of the AC system; (here the total rotational inertia of ac system represents the aggregate sum of the rotational inertia of all the generators in the system). For good performance, the AC system should have a minimum inertia relative to the size of the dc links. A measure of the relative rotational inertia is the effective DC inertia constant. For satisfactory operation 2.0 to 3.0 seconds is required [1].

3.6 Modeling of HVDC system

In order to model a HVDC system, clear understanding of the following equations and parameters are of paramount importance [1].

$$V_{do} = \frac{3\sqrt{2}}{\pi} BTE_{ac} \tag{3.24}$$

$$V_d = V_{do}\cos\alpha - \frac{3}{\pi} X_c I_d B \tag{3.25}$$

Or

$$V_d = V_{do}\cos\gamma - \frac{3}{\pi} X_c I_d B \tag{3.26}$$

$$\Phi = \cos^{-1}\left(\frac{V_d}{V_{do}}\right) \tag{3.27}$$

$$P = V_d I_d = P_{ac} \tag{3.28}$$

$$Q = P\tan\Phi \tag{3.29}$$

Where

E_{ac} = RMS line-to-line voltage on HT bus

Note that E_{ac} was here instead of E_{LL} to show reference to the high tension bus, both stands for RMS Line to Line voltage values

T = transformer turns ratio

B = number of bridges in series

P = active power

Q = reactive power

$X_c = \omega L_c$ = commutating reactance per bridge/phase

V_d = direct voltage

I_d = direct current

Chapter 4

The VSC-HVDC system

The development of VSC-HVDC was informed by the need to overcome the inherent disabilities of the HVDC system as stated earlier in this thesis. It uses more advanced semiconductor technology such as the insulated gate bipolar transistor (IGBT) instead of the normal thyristor valves for conversion of power. The first installation of VSC HVDC was a 3MW test line by ABB in 1997 [31, 36].This technology is commercially available today in the market as $HVDC^{PLUS}$ or HVDC light [32]. In this thesis it will be referred to as VSC-HVDC. Today up to about 330 MW underground transmissions are in commercial operation or in the process of construction [33, 36]. The major strength of this novel technology is its ability to control the active and reactive power independently. This makes it more viable for connection of offshore wind farm to the onshore grid than the line commuted converter HVDC (LCC HVDC) system. Despite the achievements of VSC HVDC it is limited by the converter MVA ratings, it has not been known to transmit power beyond 300 MW. Also it has high switching cost.

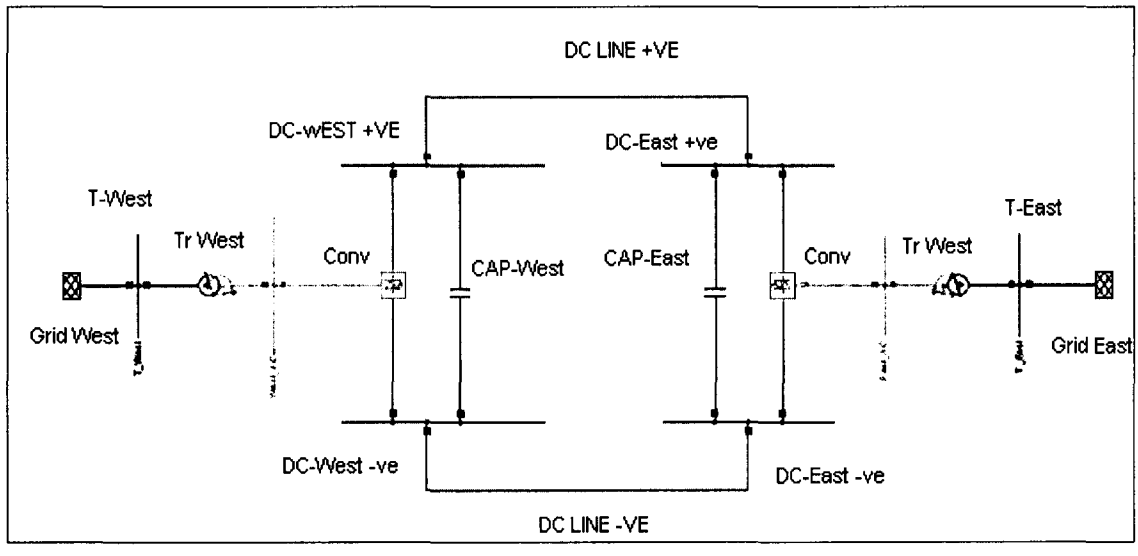

Figure4.1 Shows Schematic diagram of VSC-HVDC System [34]

4.1 Components of VSC-HVDC

As shown in figure 4.1 above the VSC-HVDC system consists of Converters, DC Capacitors and cables, Converter Transformers, phase reactors e.t.c. as stated in [35]

4.1.1 Converters

VSC-HVDC converter stations utilizes the use of Insulated gate bipolar transistors (IGBT) and Pulse width Modulation (PWM) is used to create the desired wave form, phase angle and magnitude of the fundamental frequency component. The conversion process is done by two converter stations, one acting as a rectifier and the other as an Inverter. The two converters are connected using DC cables through a bipolar link. Some times back-to-back arrangements are used for these connections.

4.1.2. Phase reactors

This is used for controlling both the active and reactive power flow by regulating the current through them. They are also used to reduce the frequency harmonics (of the AC currents) caused by the switching action of the voltage source converters.

4.1.3. DC Capacitors

DC capacitors are provided on both sides of the converter stations to act as an energy buffers and keep the power balanced during transients and also to reduce the voltage ripple on the DC side.

4.1.4. Converter Transformers

The function of this basically is to transform the AC voltage to a level suitable for conversion, they are provided on both sides of the converter stations.

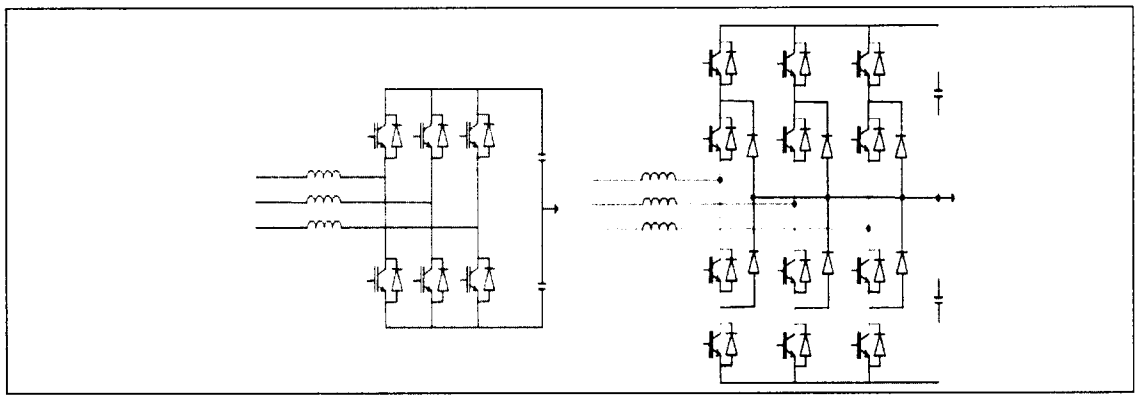

Figure 4.2 Two-Level and Three-Level VSC [35]

The VSC HVDC converters are composed of elementary converters and are arranged as a three level twelve pulse bridge or a two level six pulse bridge as shown in figure 4.2 above, some projects have been commissioned using this topology [36].

4.2 Advantages and disadvantages of VSC-HVDC

Despite the lower power capacity and higher switching losses of VSC HVDC there are numerous advantages of this system. A number of papers such as [37] and [38] have outlined the differences between the operation of a line commuted converter HVDC and voltage source converter VSC-HVDC and it is evident that it is an improvement on the classic HVDC system. The outstanding advantages of VSC HVDC systems as described in [35] are as follows:

Advantages VSC-HVDC

- It uses smaller filters and smaller space requirements, as well as reduced insulation requirement for its operation.
- It exerts independent control of active and reactive power without extra compensating equipment by using PWM. Whilst the transmitted power is kept constant, the AC voltage controller can control the voltage in the AC network. The reactive power generation and consumption of a VSC-HVDC can be used for voltage control to compensate the needs of the connected network within the rating of a converter.
- It leads to reduced risk of commutation failures. Study shows that disturbance in the AC system could lead to commutation failure in the classic HVDC system. VSC-HVDC uses self-commutating semiconductor devices, so there's no need for high AC voltage for it to operate.

- It is useful in feeding Islands and passive AC networks. The VSC converter is able to create its own AC voltage at any predetermined frequency without the presence of any rotating machine. This makes it useful in connection of large wind farms and industrial installations.
- It is useful in Mitigating power stability disturbance. The reactive power capabilities of the VSC-HVDC can be used to control the AC network voltage and thereby contribute to improvement in power quality. Also, due to faster switching capabilities of PWM the VSC-HVDC offers a new level of quality control regarding the issues of harmonics and flickers.
- Since the inverter side and the rectifier side operate independently there is no need for telecommunication connections as required in the classic HVDC system. This in turn improves the speed and the reliability of the controller.
- Multi-terminal HVDC grid can be realized. The VSC converters are suitable for creating a DC grid with a number of converters since little coordination is needed between the VSC-HVDC converters. One potential application of multi-terminal DC grids is to provide power supply to the city centers.

Disadvantages of VSC-HVDC

Despite the advantages of VSC-HVDC it has its disadvantages too; some of the advantages are as follows:

- High losses due to losses high energy dissipation at the converter stations
- Expensive for short distance transmission
- Its' power transfer is limited to the rating of the converter stations, and as such bulk power transfer is not yet feasible.
- Higher investment cost, the cost of the transmission line and the converter stations are high
- It is relatively a new technology

For more disadvantages of **VSC-HVDC** technology, see [39, 40].

4.3 Fundamentals of VSC-HVDC Transmission

The performance equations of the VSC-HVDC transmission can be explained as follows; each terminal of the system can be considered to be a voltage source connected to an AC transmission network via series reactors. Figure 4.2 shows line diagram of the VSC-

HVDC converter [35]. In the diagram the AC and the voltage source are connected through the phase reactor. Thus the converter is modeled as a controlled voltage source u_v (fundamental frequency voltage) generated by the VSC at the ac side and a controlled current source i_{DC} at the DC side. In this way the current source can be calculated based on the power balance at the DC and AC side of the converter station. The voltage source is obtained from the control system of the converter where the amplitude, the phase and the frequency can be independently controlled. As described in [35] the equation for the controlled voltage source is as follows:

$$u_v = \frac{1}{2} u_{DC} M \sin(\omega t + \delta) + harmonic \tag{4.1}$$

Where

M is the modulation index, u_{DC} is the controlled voltage source on the DC side, ω represents the frequency, δ is the phase shift of the output voltage. The variables δ, M and ω are adjustable by the controller.

Neglecting the losses of the phase reactor, the equation for the active and reactive power is given as:

$$P_f = \frac{u_f u_v \sin\delta}{X_v} \tag{4.2}$$

$$Q_f = \frac{u_f (u_f - u_v \cos\delta)}{X_v} \tag{4.3}$$

Where Q_f is the reactive power flow, u_f is the AC voltage on the secondary side of the transformer, X_v is the line reactance on the VSC network.

In a VSC-HVDC connection the active power on the AC side is equal to the active power transmitted from the DC side at steady state with losses neglected [35]. This is achieved when one of the converters controls the active power transmitted while the other converter controls the DC side voltage. Then the reactive power generation and consumption is used to control the AC voltage of the network. Many more properties of VSC-HVDC can be seen in [35]

The controlled current source from the DC side is given as

$$i_{DC}(t) = \frac{u_f^{(q)}(t) I_v^{(q)*}(t)}{u_{DC}(t)} \tag{4.4}$$

Where $I_v^{(q)*}$ represents the current reference

The use of the above parameters by the VSC-HVDC technology to control the active and reactive power of power system is the strength of the VSC-HVDC system and it has been found to improve the power quality supplied to the grid tremendously [35].

The VSC harmonics depends on topology used (whether its' 6 pulse or 12 pulse), and the switching frequency of the IGBT. The use of 12 pulse has been found to improve the harmonic condition on both the AC and DC sides, for this study the model of the VSC-HVDC system used utilizes the use of the 12 pulse system. The AC and DC harmonics have the following order

$Vdc = 12n; n = 1, 2.....$

$Vac = 12n + 1; n = 1, 2.....$

Under ideal condition all harmonics cancels out.

Chapter 5

Power System Stability

Power system stability is a problem that has challenged power engineers for ages. It was first recognized as a problem in 1920 [41]. Then it was seen as a problem normally associated with long transmission lines and over loaded networks. As power system evolved and interconnections between networks increased the complexity of the problem also increased. Power stability problem has been classified as an important phenomenon in the power industry due to many major blackouts caused by it [42]. In the past transient instability was identified as the major power stability problem but with the advent of new technologies, new methods of control and operation of power systems under stressed conditions, different kinds of instability of the power systems has emerged e. g., voltage stability, small signal stability and frequency stability. This has led to different classification of power stability as will be discussed later. For easy understanding, only the rotor angle stability will be discussed in this chapter while voltage stability is discussed in chapter 6

Definitions of power system stability

Power stability is broadly defined as that property of the power system that enables it to remain in a steady state of operating equilibrium under normal operating conditions and to regain an acceptable state of equilibrium after being subjected to a disturbance [1]. A more broad definition was given by IEEE-CIGRE Joint Task Force on Stability Terms and Definitions [5]. This definition provides a systematic basis for classifying power system stability, identifying and defining different categories, and providing a broad picture of the phenomena and it discussed the linkages relating issues like power systems reliability and security. The definition is given under leaf:

"*Power system stability is the ability of an electric power system, for a given initial operating condition, to regain a state of operating equilibrium after being subjected to a physical disturbance, with most system variables bounded so that practically the entire system remains intact*". This definition is all encompassing, it applies to an interconnected power grid as a whole, and therefore it has gained much acceptance in the power systems literature.

5.1 Classification of Power stability

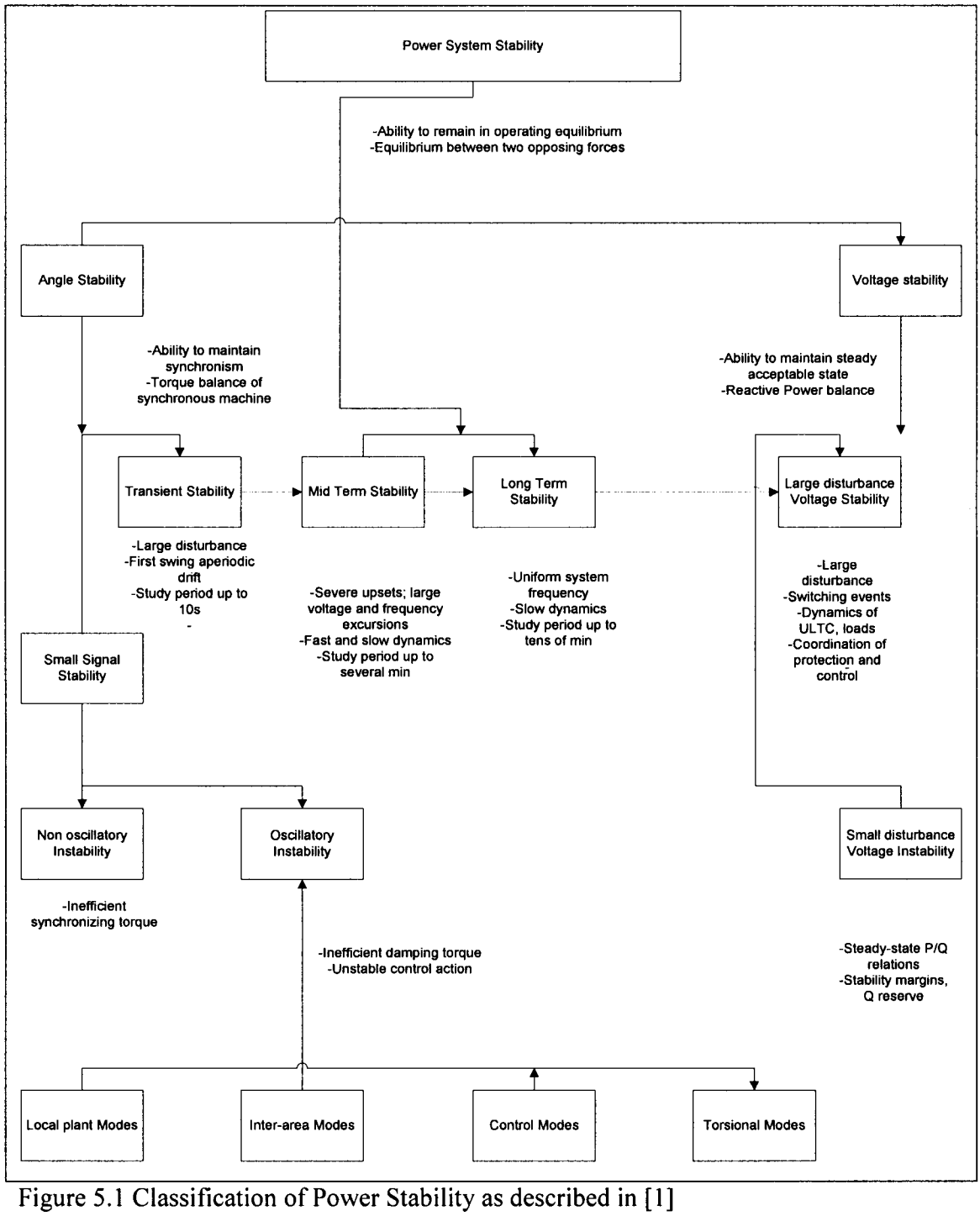

Figure 5.1 Classification of Power Stability as described in [1]

Power system stability encompasses voltage stability, transient stability, and small signal stability. From figure 5.1 above transient and small signal stability are both subset of rotor angle stability.

5.1.1 The challenge of power system stability

Contemporary events in the power industry have shown that the knowledge of the static safety limit of a power system is not enough measure to ensure a safe and reliable operation at varying load. It is of paramount importance to know and understand the system dynamics and stability. Not only should generator stability be tested but also voltage stability criteria need be taken into consideration. The stability problem that are more susceptible to the generator dynamics is the angle stability, comprising the transient and small signal stability.

5.1.2 Synchronous machine

The synchronous generator has two important elements: the field and the armature. The field is associated with the rotor and the armature with the stator of the generator. The rotor is driven by the prime mover; this movement causes the rotating magnetic field of the field winding to induce alternating voltages in the three-phase armature winding of the stator. The frequency of the induced alternating voltages and the resulting currents that flow in the stator windings when a load is connected depends on the speed of the rotor [1]. Therefore, when two or synchronous generators are interconnected, the stator voltages and currents must have the same frequency and the rotor mechanical speed of each generator must synchronize to this frequency.

5.1.3 Modelling of synchronous machine

Accurate modelling of synchronous machines is a very important issue in all kinds of electrical power systems. DigSilent power factory provides highly accurate models which are useful in wide arrays of analyses, starting from simplified models for load flow and short circuit calculation up to very complex models for transient simulations.

Synchronous generators are represented in two different ways as follows:

- The round rotor generator or turbo generator
- The silent rotor generator

Round rotor generators are used when the shaft is rotating at or close to synchronous speed of $1500\,\mathrm{min}^{-1}$, to $3000\,\mathrm{min}^{-1}$. Round rotor types of synchronous generators are normally used in systems like nuclear plants, thermal plants. Silent rotor generators rotate

at slower speed within the range of $60\,\text{min}^{-1}$ to $750\,\text{min}^{-1}$ and are employed in diesel or hydro power plants [34].

In this study DigSilent model of fifth order silent rotor machine was used for the different simulations scenarios. For stability studies RMS simulation model of 5^{th} order generator was used, according to [34]. In this type of model the stator as well as network transients are neglected. For more detailed studies, high order machine models will have to be used.

Figure 5.2 and figure 5.3 shows a schematic diagram of both types of machines.

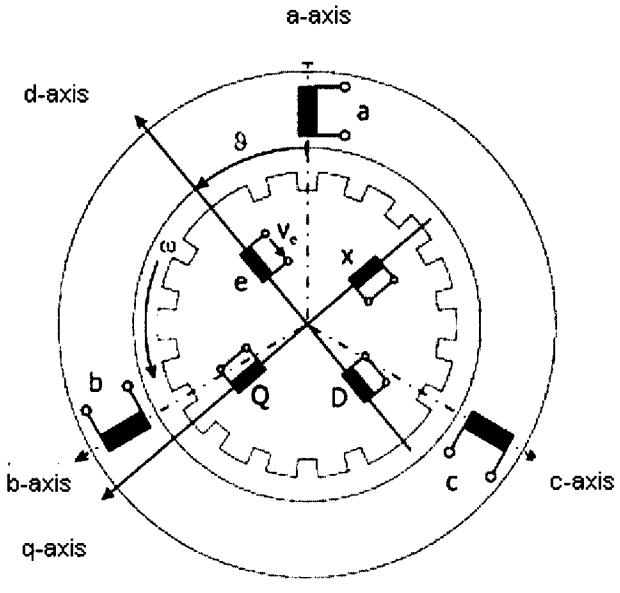

Figure 5.2 shows a schematic diagram of a three-phase round rotor synchronous machine [34]

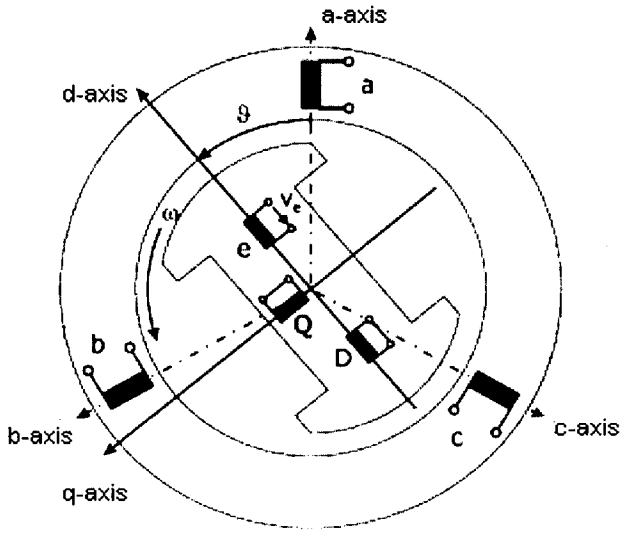

Figure 5.3 shows a schematic diagram of three phase salient rotor synchronous machine [34]

In the figures 5.2 and 5.3 three stator windings are shown as well as the rotor windings, the winding 'e' is the excitation winding fed by the excitation winding voltage'v_e'. Two damper windings are included in both axes. Damper wing D is represented in the d-axis and 2 Q damper windings is represented in the q-axis. The rotor rotates with the speed of its speed ω. The rotor angle ∂ is the angle between the d-axis and the stator field.

5.1.4 Voltage equations

Instantaneous values were used to describe generator's voltage equation. This leads to three dimensional problems in the, a, b, c coordinate system, and transformation of all values into a rotating reference frame is called dqo or parks transformation [1, 34]. The voltage equations for both the stator and rotor for round and salient rotor generators are given below as described in [1, 34] as follows:

$$u_d = r_s i_d + \frac{1}{\omega_r}\frac{d\psi_d}{dt} - n\psi_q \tag{5.1}$$

Equation 5.1: Stator voltage d-axis, round rotor

$$u_q = r_s i_q + \frac{1}{\omega_r}\frac{d\psi_q}{dt} - n\psi_d \tag{5.2}$$

Equation 5.2: Stator voltage q-axis, round rotor

$$u_0 = r_s i_0 + \frac{1}{\omega_r}\frac{d\psi_0}{dt} \tag{5.3}$$

Equation 5.3: Stator voltage, Salient rotor:

Rotor Voltage Equations:

Voltage d-axis:

$$u_e = r_e i_e + \frac{d\psi_e}{\omega_r dt} \tag{5.4}$$

$$0 = r_D i_D + \frac{d\psi_D}{\omega_r dt} \tag{5.5}$$

Voltage, q-axis

$$0 = r_x i_x + \frac{d\psi_x}{\omega_r dt} \tag{5.6}$$

Rotor Voltage equation, q-axis Salient rotor [34]

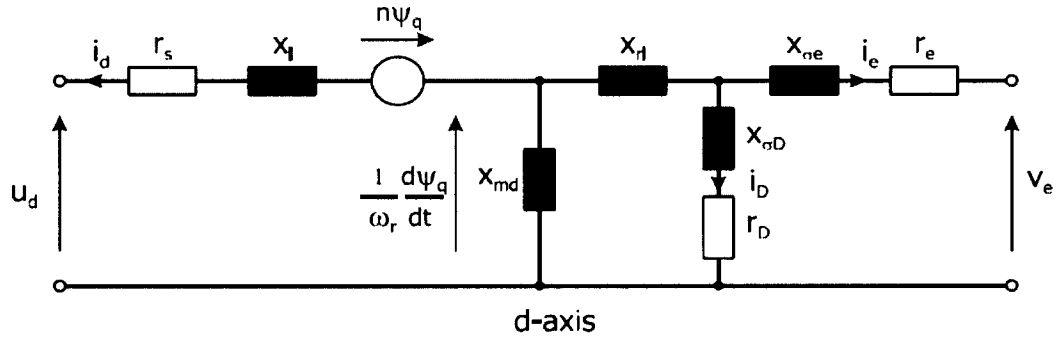

Figure 5.4 d-axis equivalent circuit for synchronous machine [34]

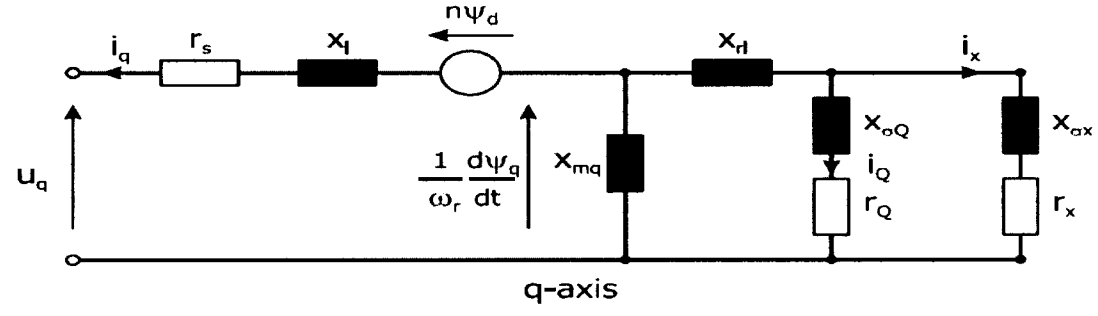

Figure 5.5 q-axis equivalent circuits for the synchronous machine [34]

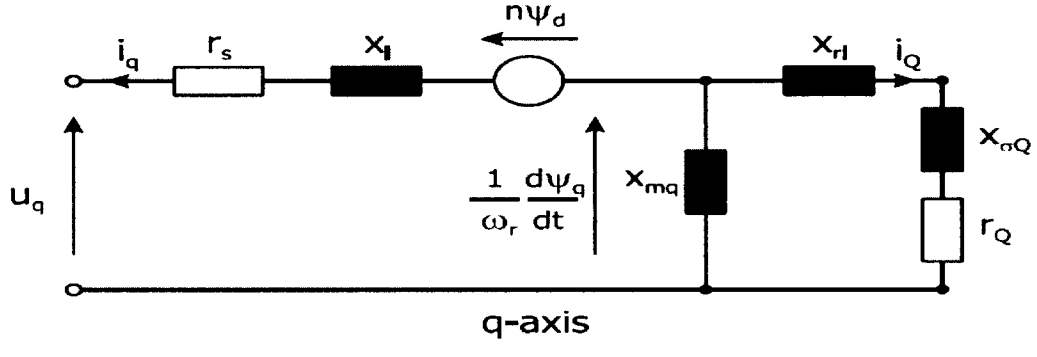

Figure 5.6 q-axis equivalent circuit for the synchronous machine (salient rotor)[34]

5.1.5 RMS Simulation

Under RMS Simulations the stator flux transients are neglected, the voltage, current, resistance and reactance relationship are as given [34]:

$$u_d = r_s i_d - x_q i_q + u''_d \tag{5.7}$$

$$u_q = r_s i_q + x_d i_d + u''_q \tag{5.8}$$

The Input/Output Definition of the synchronous machine model, output analysis, impedance definition in the equivalent circuit for RMS stability study are shown in the appendix A: Table A.2 and standard parameters for synchronous generators is given in Appendix B: B:1.

5.2 Rotor angle stability

When two or more synchronous machines are interconnected, the stator voltage and currents of all the machines must have the same frequency and the rotor mechanical speed of each is synchronized to this frequency. Therefore, for a stable operation the rotors of all the interconnecting machines must be in synchronism. The ability of interconnected synchronous machines to remain in synchronism is defined as rotor angle stability [1]. A necessary condition for satisfactory operation is that synchronous machines must remain in synchronism or colloquially" in step". This aspect of stability is influenced by the dynamics of generator angle and power angle relationships. Rotor angle stability involves the study of electromechanical oscillation inherent in power systems. In general, an initial generator rotor angle swing which does not exceed 160° is considered to be stable. A rotor angle which exceeds 160° has only a small margin before pole slipping (180°) an initial swing above 160° may result in pole slip or repeated pole slipping which is considered unstable [43].

Rotor angle swing in excess of 160° or transient voltage dip in excess of 25% can result in the following detrimental effects on the network [44].

Network voltage collapse

Motor load loss on under voltage

Oscillation damping

All electromechanical oscillations resulting from any small or large disturbance in power system shall be well damped and the power system shall return to a stable state of operation, the damping ratio of the oscillations should be at least 5%. For inter area oscillation a smaller ratio will be acceptable and the halving time should not exceed 5 seconds [1, 5].

A sudden change in electrical system is associated with a number of phenomena with varying time frames. First, the electrical properties adjust quickly to the state, this changes the share of power production between different generators and it also causes change in the load demand. Secondly, the imbalance between the electrical and mechanical output of the participating generators causes a change in the mechanical speed, the rate of speed change is dependent on the power deviation and the rotor inertia. This means that when generators changes speed at different rate the rotor angles deviates from the initial values and this causes a change in power flow to the grid. Thirdly, the control and protection phase disconnects any fault which further causes a new transient that tries to return the system to a steady state of operation or pre-disturbance state. These transitory and oscillatory phenomena is called Rotor angle Stability or Electromechanical Power Oscillations. The first swing oscillation is of interest in rotor angle stability study because it indicates that the generators do not swing too far from each other on the first oscillation [1]. Under steady state of operation there must be equilibrium between the input mechanical torque and the output electromagnetic torque of each generator, with the speed remaining constant. This balance is offset during perturbation causing the rotors of the machines to either accelerate or decelerate according to the laws of motion of a rotating body. When a machine runs faster than the rest as a result of fault, and the angular position of its rotor relative to the slower ones will advance, and the resulting angular difference transfers part of the load of the slower machines to the fast ones, this reduces the speed difference until a steady state is achieved. Beyond certain point, an increase in angle difference results in transfer of less power in such a way that the angular difference is further increased. At this point the system cannot absorb the kinetic energy corresponding to the rotor speed differences and instability is ensued.

5.2.1 Equations of motion of synchronous machines

Rotational inertia equation or the swing equation is of paramount importance in power systems stability study. It describes the effect of imbalance between the electromagnetic torque and the mechanical torque of individual synchronous machines. When there is an imbalance between torques acting on the rotor, the net torque causing acceleration or deceleration is given below as stated in [1].

$$T_a = T_m - T_e \tag{5.9}$$

Where

T_a = accelerating torque in N-m

T_m = mechanical torque in N-m

T_e = electromagnetic torque in N-m

In equation 6.7, torque T_m and T_e are positive for a generator and negative for a motor. The combined inertia of the generator and the prime mover is accelerated by the imbalance in the applied torque. The equation of motion is given thus as stated in [1, 29]:

$$J = \frac{d\omega_m}{dt} = T_a = T_m - T_e \tag{5.10}$$

Where

J = combined moment of inertia of generator and turbine, $Kg.m^2$

ω_m = angular velocity of the rotor, mech. Rad/s

t = time, s

N can further be normalized in terms of per unit inertia constant H, defined as the kinetic energy in watt-seconds at rated speed divided by the VA base. Using ω_{om} to denote rated angular velocity in mechanical radians per second, the inertia constant is given by:

$$H = \frac{1}{2}\frac{J\omega_{om}{}^2}{VA_{base}} \tag{5.11}$$

Moment of inertia J in terms of H is

$$J = \frac{2H}{\omega^2_{om}} VA_{base} \tag{5.12}$$

If δ is the angular position of the rotor in electrical radians with respect to a synchronously rotating reference and δ_0 is its value at $t = o$,

$$\delta = \omega_r t - \omega_0 t + \delta_0 \tag{5.13}$$

Taking the time derivative and substituting in the equation 5.12 we have,

$$\frac{2H}{\omega_0}\frac{d^2\delta}{dt^2} = T_m - T_e \tag{5.14}$$

Equation 5.14 above gives the swing equation; including the damping torque component we have

$$\frac{2H}{\omega_0}\frac{d^2\delta}{dt^2} = T_m - T_e - K_D\Delta\omega_r \tag{5.15}$$

Where

K_D is the damping torque coefficient or factor and ω_r is the angular velocity of the rotor

$\Delta\omega_r$ is the difference in angular velocity of the rotor and its rated value .

$\Delta\omega_r = \omega_r - \omega_0$ where ω_0 is the rated value [1].

5.3 Small Signal Stability

Small signal stability is concerned with the ability of a power system to maintain synchronism under small perturbation. For the purpose of analysis the disturbance is considered so small that linearization of the systems equation is possible [45, 46]

The ensuing instability under small signal disturbance can be of two forms: (1) increase in rotor angle through non oscillatory or aperiodic mode as a result of lack of sufficient synchronizing torque, (2) rotor oscillations due to increasing amplitude due to lack of sufficient damping torque. The time of interest for this study is with 10-20 seconds.

In power systems nowadays Automatic voltage regulators (AVR) have been able to reduce the instability due to lack of sufficient synchronizing torque. The change in the electromagnetic torque of a synchronous machine following a disturbance is given by the equation bellow [29]:

$$\Delta T_e = T_s \Delta\delta + T_D \Delta\omega \qquad (5.16)$$

Where

ΔT_e is the change in electrical torque

T_e is the electrical torque coefficient

$T_s \Delta\delta$ is the synchronizing torque component

T_s is the synchronizing torque coefficient

$\Delta\delta$ is the change in rotor angle

$T_D \Delta\omega$ is the damping torque component

T_D is the damping torque coefficient

$\Delta\omega$ is the change in rotational speed

Thus the change in the electrical torque can be resolved in two components, the synchronizing torque in phase with rotor angle deviation and damping torque component in phase with the speed deviation.

The stability of the system depends largely on these two. Lack of any results in one form of instability or the other as follows. Lack of sufficient synchronizing torque leads to aperiodic or non-oscillatory instability in the network and lack of damping torque leads to oscillatory instability in power systems. The rotor equation shown in equation 5.15 is governed by the laws of motion as described in [1, 29].

Torque equation:

$$T_{el} = E_q' i_q + E_d' i_d + (x_q' - x_d') i_d i_q \qquad (5.17)$$

(The parameters used in the simulation for the generator in this study are given in the **Appendix B: Table B.2)**.

5.3.1 Oscillation modes

The prevailing situation in power system suggests that small signal stability problems emanate largely from insufficient damping of oscillations. Small signal stability modes have been categorized as follows [1]:

5.3.1.1 Local mode: This happens when one or more generators in a station swings against the rest of the generators within a location. Their effects thus are localized.

5.3.1.2 Inter-area mode: This happens when a group of generators in the network in one location swings against the rest of the generators in the network. This is peculiar to networks with weak short circuit ratio (SCR).

Other modes are control modes due to control devices within the network i.e. HVDC controls, Static Var Compensator (SVC) and speed governors, etc. Also, torsional mode is another mode inherent in power systems, which could be attributed to turbine generator shaft system rotational systems. For more insights on the dynamics of rotor angle stability see [5, 47, 48, and 49] various techniques have been used to improve small signal stability following a small disturbance. Low frequency oscillation is a major problem for large interconnected systems. PSS is used for reducing local mode oscillations but less effective for inter-area oscillations of frequency less than 0.3 Hz [1]. On the other hand, due to its fast active and reactive power control VSC-HVDC can be used to mitigate such oscillations in the grid, by active and reactive power control. The ability of VSC-HVDC to control active and reactive power independently makes this possible. The best location for reactive power damping, is the electrical middle point between the oscillating generator groups, active and reactive power modulation are complementary, which

entails that VSC-HVDC will damp low frequency oscillations better than HVDC and PSS [2].

5.3.2 Small signal stability of a single machine infinite bus system.

Small signal stability analysis as stated in [48] are used in the study of single machine infinite bus (SMIB) system. Large system studies are as stated in [47, 49].

5.3.3 Analysis of small signal stability

There are various methods of analyzing small signal stability. One technique that has been of general acceptance in the power engineering literature is the Lyapunov technique, which is explained briefly as follows: For stability in the small (Lyapunov 1st method) states that, when the Eigenvalues have negative real part, the original system is asymptotically stable. When the Eigenvalues have at least a +ve real part the original system is unstable, when Eigenvalues have real part equal to zero, its not possible on the basis of first approximation to say anything in general. Stability in the large can be solved using non-linear differential equation using digital or analog computers. Method used for the computation of Eigenvalues of real non-symmetrical matrices is the QR transformation method originally developed by J.G.F Francis and described in [50].

5.4 Transient stability

Transient stability is also referred to as large disturbance rotor angle stability. It deals with the ability of the power system to maintain synchronism following a severe disturbance, such as a short circuit fault like three phase short circuit fault, loss of major load, or generating unit etc. The time frame for transient stability study is about 3 to 5 seconds, but could be extended to about 10 to 20 seconds in a large network with dominant inter-area swings [1]. Transient stability depends largely on the initial operating conditions and the severity of the transient disturbance. This instability occurs when rotor speed increases steadily until synchronism is lost within the first second. This situation is known as first swing instability and it is caused by lack of sufficient synchronizing torque. However, in large power systems, various oscillations that advance the rotor angle beyond the first swing can also lead to transient instability [5]. In this study Power Systems Stabilizer (PSS), HVDC, VSC-HVDC Were used to investigate transient stability following a disturbance in the network. Of special interest is the VSC-HVDC

which has been shown to be able to improve both the transient and small signal stability. The fast power run back capability of VSC-HVDC is very useful in helping the system from transient instability after a system's fault. As described above, the generator out-of–step is due to excessive kinetic energy accumulated in the generator rotor during fault. After the fault is cleared VSC-HVDC releases the energy to other healthy system [2].

5.4.1 Transient stability improvement by VSC-HVDC

The fundamental mechanism with this type of instability is that, the kinetic energy accumulated in the generator during the fault can not be released with first power swing if the fault is not cleared within reasonable period. The excessive energy causes lot of generators to go out of phase with the main grid after the fault is cleared. In the case of VSC-HVDC fast ability to release energy enables it to overcome these anomalies and the instant power reversal ability enables it to change up to two times the power of the rated value [2].

Chapter 6

Voltage Stability

Voltage stability problem has been responsible for many power network collapses over the years. It is the ability of power system to maintain stable voltages at all buses in the network after being subjected to a perturbation from the initial equilibrium operating condition. Low voltages can be associated with rotor angle going out of step, loss of synchronism of machines as rotor angles between two groups of machines approaches 180^0 causes' rapid drop in voltages at certain points in the network close to the electrical centre [1]. The type of voltage collapse related to voltage instability can occur where "angle stability "is not an issue. It depends on the system's ability to maintain and restore equilibrium between load demand and supply from the power system. Voltage stability is defined as:

"Voltage stability is the ability of a power system to maintain an acceptable power through out all the buses in the power system, under normal condition and after experiencing a perturbation in the power network" [1].

A system enters condition of voltage instability when a disturbance causes an increase in load demand or change in the system condition causes progressive and uncontrollable decline in voltage. The main factor causing instability is the inability of the power system to meet the demand for reactive power [1].

In the past voltage stability problems were associated primarily with weak systems and long lines. However, they are now also a source of concern in highly developed networks as a result of heavier loadings. A possible consequence of voltage stability problem in the power network is loss of load in a particular section of the network, or tripping of transformers and other control and protective equipment resulting in cascading outages. Loss of synchronism of some generators may result from these outages or from operating conditions that violate field current limit [5].

Voltage stability problems normally occur in a highly stressed system, whilst the cause of disturbance may vary from one event to the other. The factor causing voltage stability problems is inherent in the power network strength for transmission. Power transfer level also contributes to voltage collapse. Other factors are generator reactive power, voltage

control limits, load characteristics, characteristics of reactive compensation devices, and the action of voltage control devices such as transformer under-load tap changer (ULTC).

6.1 Principal causes of Voltage stability problems/Collapse

- Load on the transmission line is too high
- Voltage sources are too far from load centers
- The source Voltage are too low
- There is insufficient load reactive compensation
- Action of ULTC during low voltage conditions
- Poor co-ordination between various control and protective systems
- Large distances between generation and load
- ULTC action during low voltage conditions
- Unfavourable load characteristics e.g., induction motor
- Poor coordination between various control and protective units.
- Voltage instability may be aggravated by excessive use of shunt capacitor compensation. Reactive compensation is best with combination of shunt capacitors, static var systems and synchronous condensers.
- In addition to the strength of transmission network and power transfer levels, the principal factors contributing to voltage collapse are generator reactive power/voltage control limits, load characteristics of reactive compensation devices such as (ULTC) Under load tap changer

Research has shown that voltage instability can be caused by the actions of HVDC terminal links that is used for either long distance bulk power transmission or back to back applications [5]. Also, the actions of converter transformer tap changer controls can lead to voltage instability of the system [1].

6.2 Mitigations of Voltage Instability

Ever since voltage instability was recognized as a problem, power engineers have been trying to find a way of mitigating these problems. Some of the steps taken to address the problem are given below.

Stability margin should be ensured by proper selection of compensation schemes. The selection of sizes, ratings and locations of the compensation devices should be based on detailed study. Design criteria based on maximum allowable voltage drop following a contingency are often not satisfactory from voltage stability view point. The stability margin should be based on MW and Mvar distances to instability [1].

6.2.1 Use of Capacitors for the mitigation of Voltage instability

Shunt capacitors are used to extend voltage stability limits by correcting the receiving end power factor. They are also used to free up spinning reactive reserve in generators and thereby help to prevent voltage collapse in many situations.

6.2.2 Limitation of shunt capacitors in voltage stability

- Voltage regulation is poor in a shunt capacitor compensated network
- Stable operation is unattainable beyond certain level of compensation
- The reactive power generated by a shunt capacitor is proportional to the square of the voltage, at low voltage VAR support drops.
- A static var system (SVS) will regulate up to its maximum capacity, there are no problems within this range. When pushed beyond limits it acts as a simple capacitor and prone to instability problems

Synchronizing condenser unlike SVS has an internal source of voltage and it improves the systems performance [1].

Series capacitors are self regulating devices. The reactive power supplied by series capacitor is proportional to the square of the line current and independent of the bus voltages [1]. This is favourable for the mitigation of voltage instability. Series capacitors reduces both the characteristics impedance Z_c and power transmission angle as a result both voltage regulation and stability are improved [51].

6.2.3 Use of VSC-HVDC for the mitigation of Voltage instability

Other studies have shown the use of VSC-HVDC for the improvement of voltage stability [35, 2, and 52]. VSC-HVDC uses its ability to control active and reactive power independently to achieve this. The advantages of using VSC-HVDC for the improvement of voltage stability are as follows: VSC-HVDC in parallel with HVAC has better damping ability than the reactive shunt compensation, during grid restoration. It controls voltage and stabilizes frequency when active power is available at the remote end; during grid restoration frequency control is not limited.

6.2.4 The Use of VDCOL for the mitigation of Voltage Instability

Voltage dependent current order limit or VDCOL automatically reduces the reference current (Id_ref) set point when VdL (Vd line) decreases i.e., during a DC line fault or a severe AC fault [1] VDCOL helps to recover normal commutation and thus power transfer may resume during fault. It is most effective in faults involving weak receiving-end AC system.

6.2.5 Prevention and Analysis of Voltage Instability

With the improvement in technology, various means of detecting weak points that are vulnerable to voltage instability in the network are now available. Devices like Supervisory control and data acquisition (SCADA) system in real time is continually analyzing the impact various contingencies would have on the power system. This analysis is known as real time contingency analysis, and it reports what the post contingent loading on the system would be and what the post contingent system voltages would be, if a contingency occurred at that time. Real time contingency analysis has two components as described in [53]. The first is the use of energy management system (EMS) power flow application which applies Newton Raphson load flow solution to determine what system component loadings would be for number of nominated contingencies. This application then reports if the system components are at the risk of exceeding their capability due to post contingent loading. The second part uses voltage stability assessment tool (VSAT) application uses a static PV analysis to determine the post contingent system voltage for the same nominated contingent events. This analysis identifies the point at which post contingent voltage is likely to become unstable i.e. the

system is at risk of voltage collapse should contingency occur. By monitoring real time the system operators are able to ensure security standards for post contingent equipment loading, and post contingent system voltage, are maintained all times. When there is an alert that voltage limit or loading limit would be violated a standard procedure is followed to correct the situation. These standards ensure that the system is being operated at maximum capability before further corrective action is taken depending on the originating situation [53].

6.3 Using VP and QV Curves to analyze voltage stability

In this study both curves were used to investigate the voltage stability of a weak hybrid HVAC/HVDC and HVAC/VSC-HVDC systems. The study identifies the buses that are sensitive to voltage collapse. It shows the improvement of voltage stability using VSC-HVDC system and also the weaknesses of HVDC system when integrated with a weak HVAC system. Voltage instability is a localized problem but its impact on the system can be wide spread as it depends on the relationship between transmitted active power (P), injected reactive power (Q) and the receiving end voltage (V). This analysis is commonly referred to PV and QV curves.

1. PV Curve

This analysis involves the transfer power P from one region of the system to another and monitoring of the effect on the voltage magnitude of the system.

2. QV Curve

Voltage stability depends on how the variation of P and Q affects the voltage at the load buses. In this analysis the influence of reactive power characteristics of devices at the receiving end (loads or compensating devices) is more apparent in a QV relationship. It shows the sensitivity and variation of bus voltage with respect to reactive power injection or absorptions [1].

6.4 Voltage collapse

Voltage collapse has drawn attention since the last 15 years in the power community [54]. Voltage collapse phenomena are important in determining system's security and performance. This will continue to increase due to continued interconnections of bulk power in the network, necessitated by economic and environmental pressure. The

blackout following voltage collapse in the interconnected Chilean system (CIS) in May, 1997 was caused by lack of reactive power, and also report shows that saturation of the excitation control in some key generating units of the system, is the main cause of the voltage collapse [55] The system was recovered after about 30 minutes after fault and about and about 80% of the system's load was lost during the fault.

Voltage collapse is defined as "*a process by which sequence of events accompanying voltage instability leads to a low unacceptable voltage profile in a significant part of the power system*" [1].

6.4.1 Reasons for voltage collapse

- Loss of heavily loaded line, this will transfer load and stress to other lines causing a heavy reactive power demand on the system.
- Abnormal operating condition of the systems in the network, such as the ULTC, converter station controller's e.t.c could cause generating units near the load centre to be out of power for a reasonable period, thereby putting more stress on the network.

6.5 Criteria for voltage stability

If the voltage at the bus is rising at the same rate as the injection of reactive power into the bus, the system is stable if:

$$\frac{\partial Q}{\partial V} > 0 \qquad (6.1)$$

The system is unstable if:

$$\frac{\partial Q}{\partial V} < 0 \qquad (6.2)$$

The system is said to be at critical voltage point if;

$$\frac{\partial Q}{\partial V} = 0 \qquad (6.3)$$

Where, Q represents reactive power injected into the system and V represents voltage injected into the system. These conditions above is known as Bruck-Markovic criterion [56]

The system is unstable as long as there exist in the system a bus which does not fulfill these requirements as shown above in equations 6.1, 6.2 and 6.3.

Chapter 7

Description of the power system models and the case studies

This chapter covers the simulations used in analyzing the transient stability, and small signal stability and voltage stability of the power system network. The power system models were implemented using DIgSILENT Powerfactory version 14.0.515. Most of the parameters used and the power system models were obtained from [1]. Five case scenarios were investigated.

7.1 Case studies

- The first being the system using a single machine infinite bus (SMIB) system to analyze power flow and the effect of transmission distance on the power network.
- The second scenario deals with the transient and small signal stability of the two-area power network interconnected with HVDC link was investigated. Three case studies were used for the small signal stability investigation. And two case studies were used for the transient stability investigation.
- The third scenario investigated the rotor angle stability of the two-area power network by studying the effects of AVR and PSS on the power network.
- The fourth scenario covers the study of transient stability enhancement of power systems using the HVDC and VSC-HVDC technology.
- The fifth scenario investigated the voltage stability of two-area HVAC power system using HVDC and VSC-HVDC links

7.2 Scenario 1: SMIB power system model

A single machine infinite bus system (SMIB) was used this consists of two generators, G1 on the left hand side denoted as (Area A). This represents the reference bus (SLACK bus) and G2 on the right (Area B) represent the PV bus as shown in fig. 7.1. Both generators are rated 20kv and 900MVA. Also identical transformers of 20kv/230kv were

used on both sides. HVAC transmission line (between bus 3 and bus 4) was set at 600 km, HVDC line was set at 600 km, with rectifier set at current control and inverter at gamma control. Power flow was carried out and it converges after the 3rd iteration. The generators were loaded as follows G1 (P= 700MW and Q=185Mvar) G2 (P= 719MW and Q=176Mvar). Capacitors C1 and C2 of values 400 Mvar each were used for the compensation of the reactive power in the system. During the transient stability investigation, a 3 phase fault was applied at the middle of the HVAC of the hybrid network at 3 seconds and was cleared after 3.05 seconds. The fault was cleared by opening the two breakers at the end of the transmission line. The bus bars (bus 3 and bus 4) links the HVDC converter stations as shown in figure 7.1.The frequency of operation used for the system is 60Hz and the MVA base is 100MVA.

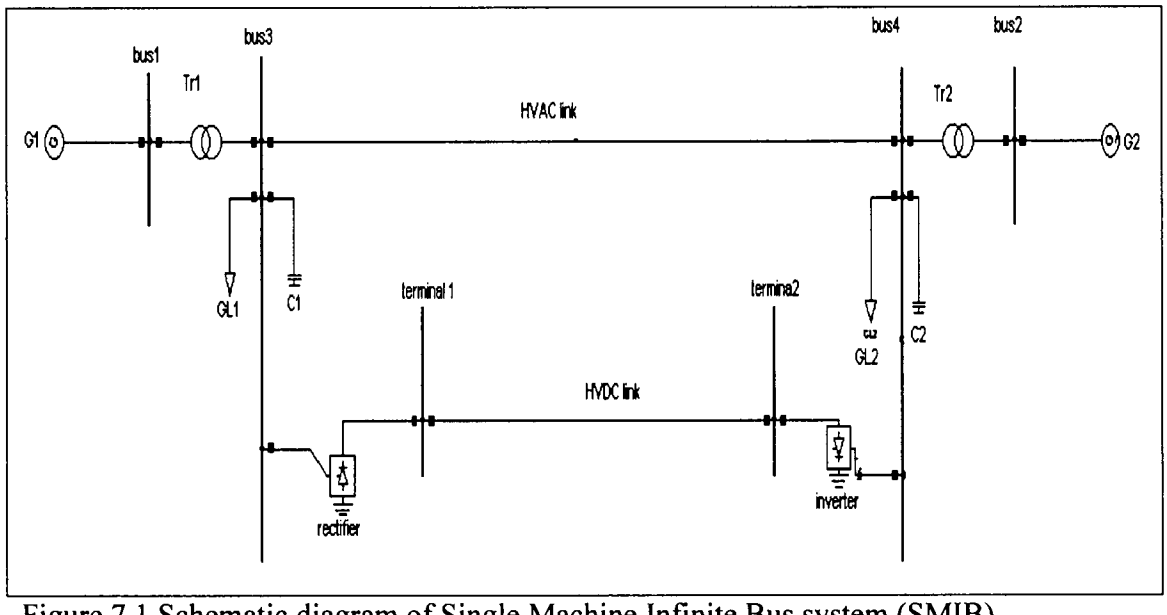

Figure 7.1 Schematic diagram of Single Machine Infinite Bus system (SMIB)

7.2.1 Load flow results using DIgSILENT

The first study was on the power flow for the single machine infinite bus system. This power flow calculation was obtained using the DIgSILENT Powerfactory simulation software.

Load flow calculation were obtained using DIgSILENT, the result of the load flow is shown in Table 7.1 below.

Table 7.1 Power flow for the hybrid HVAC-HVDC network

	Active Power (MW)	Reactive Power (Mvar)
G1A	684.06	55.53
T1A	684.06	55.53
GL1A	500.00	350.00
C1A	0.00	-398.73
L1A	74.50	-21.18
T12A	-684.06	-39.82
GL2B	900.00	350.00
C2B	0.00	-395.89
C1A	0.00	-397.85
L1B	-71.44	-7.01
G2B	719.00	71.69
T2B	-719.00	54.28
REC-A	-109.56	0.00
REC-B	109.56	0.00

From the load flow results total power generated in the network stood at is 1408.82 MVA or 1403.06+j127.22 MVA, (comprising the total input active power from G1A and G2B (see row 2 and 12 table 7.1). Installed capacity is around 1710 MW. In the AC link 74.50-j21.18 MVA was available for transmission (see row 6 L1A in table 7.1) however, due to the losses on the transmission link only -71.44-j7.01 was delivered to area B (see row 11 table. 7.1).

In the DC link 109.56 MVA of power flowed from area A on the DC line to augment with 719.00-j71.69 MVA from generator G2 area B in order to meet the demand of the load in area B (900+j350) MVA, which was greater than the generated power in area B, the additional reactive power requirement was met by the capacitor (C1 and C2). The total load in Area A is 500+j350 (see row 4 GL1A) and the total load in area B is 900+j350 (see row 8 GL2B in Table. 7.1)

Generator1 area A supplied (684.06+j55.53) MVA again the additional reactive power requirement was compensated by capacitor C1. Therefore in this network, power flowed from Area A to Area B to augment the generation of area B in order to meet the demand through the HVDC link and the HVAC link.

7.2.2 Investigation of the effects of increasing line length on the power network

In this study, the distance of HVAC transmission line was increased in steps of 100 starting from 100 km until the load flow fails to converge. Their effect on the active power and reactive power of the system was observed. This investigation was done for the HVAC transmission scheme, the HVDC transmission scheme as well as the hybrid HVAC-HVDC system. The result obtained for the HVAC link is presented in Table 7.2

Table 7.2 Effect of line length of HVAC transmission

Distance	L1A		L1B	
	P (MW)	Q (Mvar)	P (MW)	**Q (Mvar)**
100	184.19	-6.57	-181.00	28.18
200	187.62	4.76	-181.00	41.00
300	191.50	18.88	-181.00	55.76
400	196.27	37.87	-181.00	75.16
500	203.59	70.18	-181.00	107.94
550	84.94	119.71	-181.00	158.28
600	0	0	0	0

From table 7.2 above it is noticeable that more power is required to transmit the same amount of power to the receiving end from L1A to L1B as the distance between them increases, also Newton Raphson's iteration converges with more number of iterations as the line length increases. The result shows that losses in transmission of power increases with distance in the HVAC transmission scheme. The area of concentration is on the AC line L1A and L1B. From the load flow results it is observable that as the line length increases both the active power and reactive power increases at the sending end LIA, whilst the same amount of active power (-181.00 MW) is transmitted to the receiving end L1B, also from the result, the reactive power increases as the transmission length

increases. This brings to the fore the limitations of HVAC system, for the same amount of active power supplied to the load more power is needed from the sending end to maintain it as the transmission length increases. Beyond 550 km the system collapses, due to the fact that generation and compensation was not able to meet the reactive power requirement. To achieve this, the system needs higher voltage gradient [57].

The same test was carried out using HVDC link alone, the line length was increased from 100 km to 2000 km with little or no effect on the power transmitted (not shown here since there was no noticeable effect).

Table 7.3 the effect of line length on a hybrid HVDC and HVAC network

Distance (KM)	L1A		L1B	
	P (MW)	Q (Mvar)	P (MW)	Q (Mvar)
100	71.98	-9.14	-71.49	4.47
200	72.47	-11.72	-71.48	2.41
300	72.97	-14.12	-71.47	0.17
400	73.48	-16.47	-71.46	-2.15
500	73.99	-18.81	-71.45	-4.54
600	74.50	-21.18	-71.44	-7.01
650	74.77	-22.39	-71.44	-8.29
700	0	0	0	0

For the hybrid network it is observable that the power flows from area A to area B. Furthermore, it is observable that as the distance increases less active power is transmitted to area B, due to the fact that more reactive power is needed to support the active power as the transmission distance increases. This led to the collapse of the system at a distance of 650 km. The result shows that the hybrid network HVAC-HVDC transmitted more power at a longer distance beyond the limit of HVAC system. The HVDC system improved the transmission length of the HVAC link from 550 km to 650 km, which represents about 18% increase. Also, of interest here is the increase in the number of iteration as the transmission distance increases. In practice the maximum limit for quality power transfer is about 500 km, beyond this point, increase in the power level with reactive power compensation is needed [1].

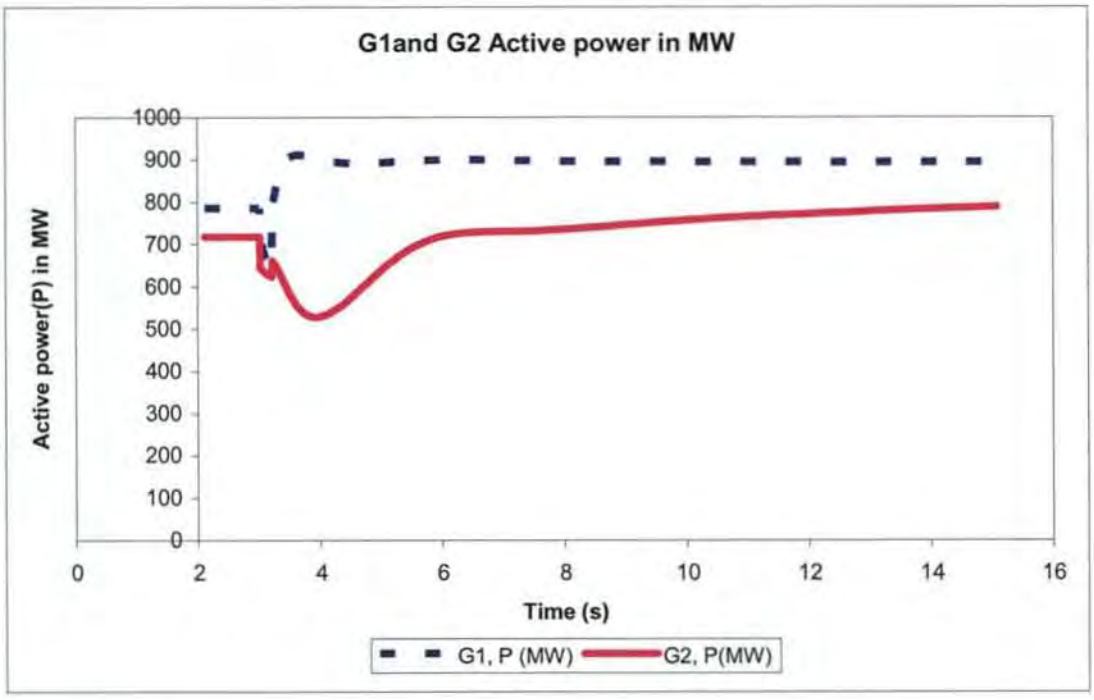

Figure 7.2 the active power in (MW) of generators G1 and G2

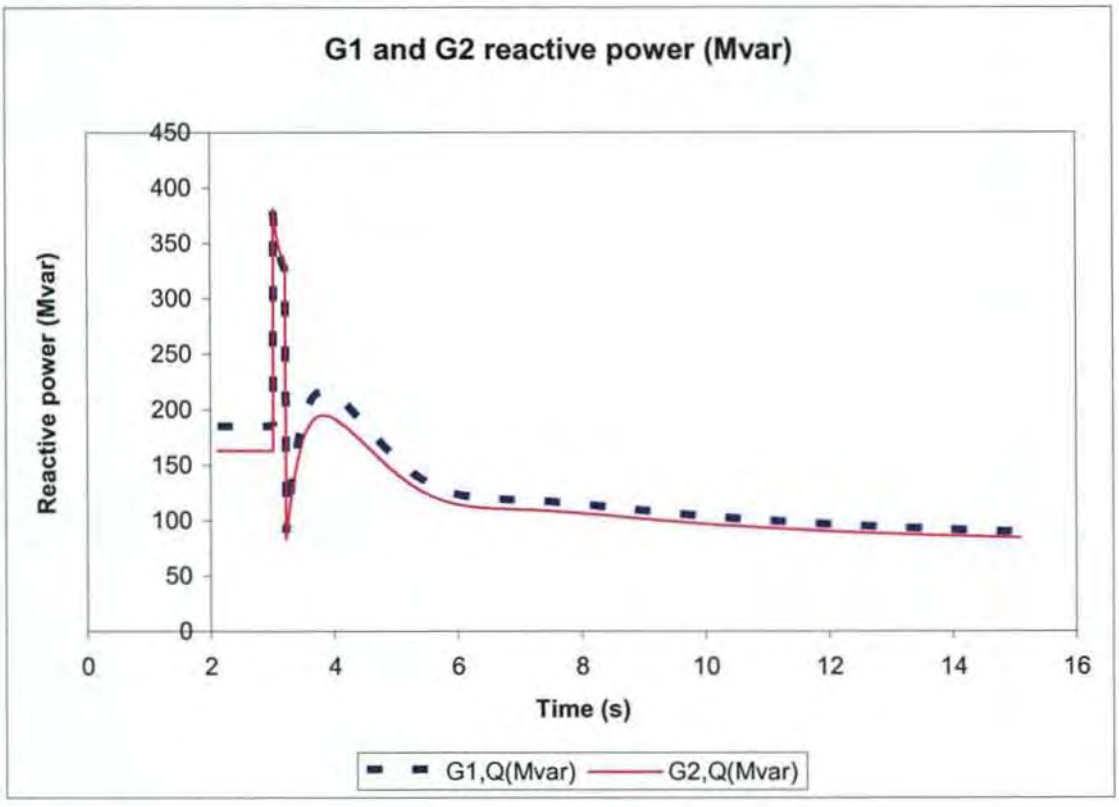

Figure 7.3 the reactive power of generators G1 & G2

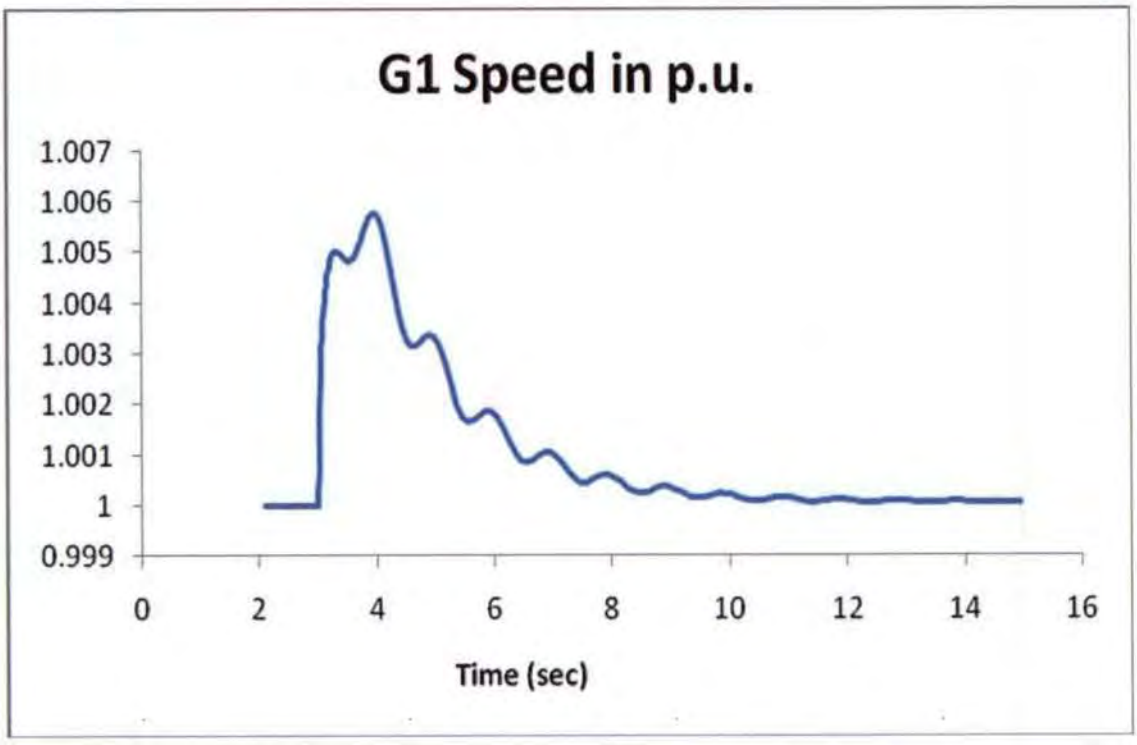

Figure 7.4 the speed of generators G1

Please note the y-axis in figure 7.4 represents the generator speed in p.u

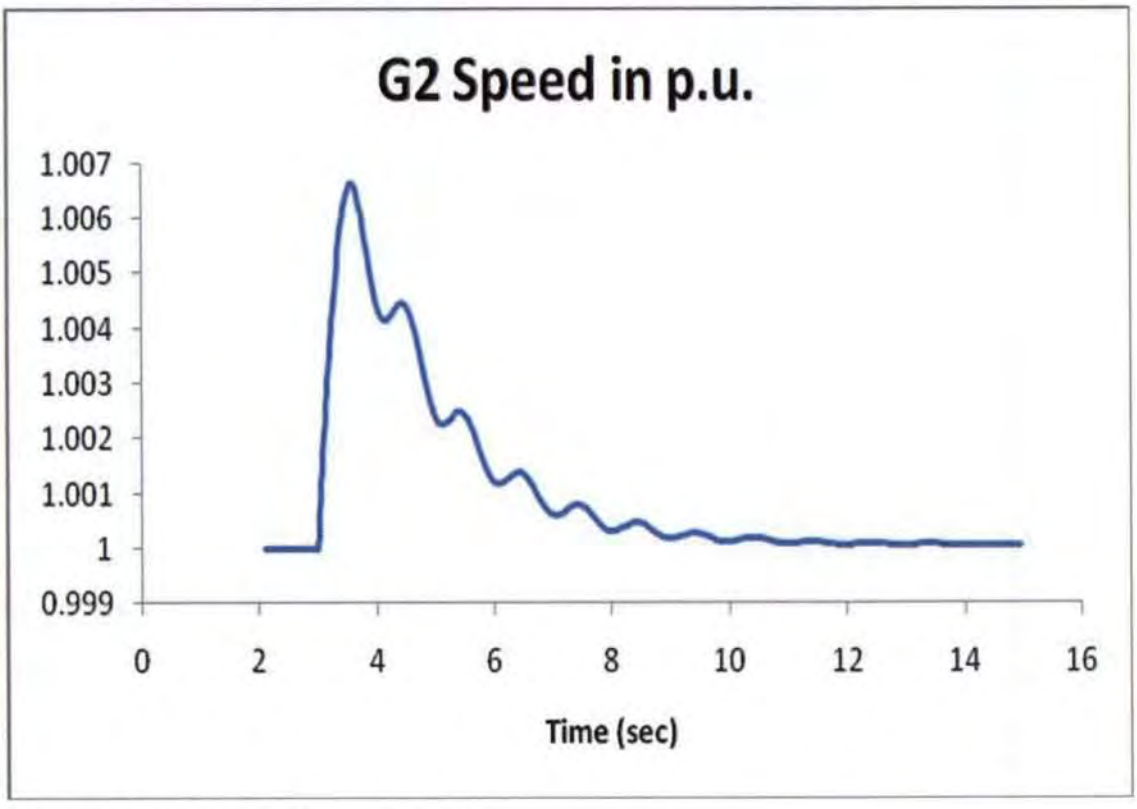

Figure 7.5 the speed of generators G2

Please note also, the y-axis in figure 7.5 represents the generator speed in p.u

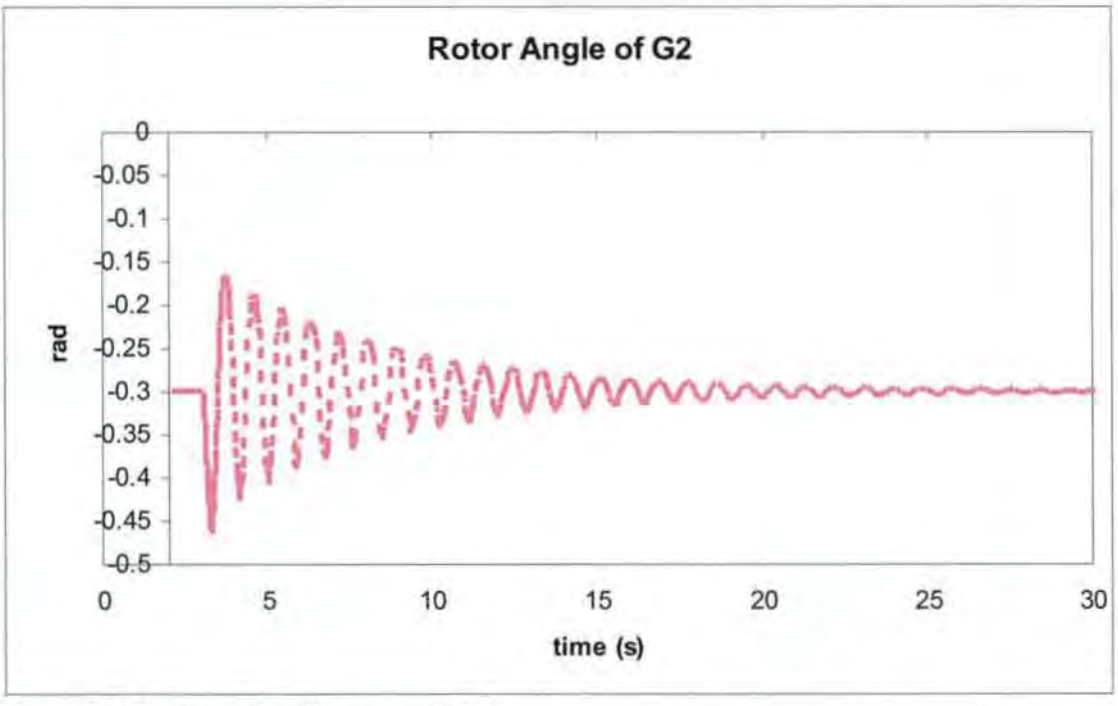

Figure 7.6 Rotor angle of generator G2

Note in plotting the above graph (figure 7.6) the time on the x axis was extended to 30 seconds to capture the period of coming to steady state.

From figures 7.2, 7.3, 7.4, 7.5 and 7.6 above the transient study shows that the system was stable under the large disturbance; in figure 7.2. The active power G1 and G2 takes about 5 seconds to settle after the perturbation, G1 at rest was operating at 800 MW, but dipped to about 650 MW (about 18.75% drop) and G2 dipped from 719 MW to about 500 MW (which is about 30.46%) whilst the reactive power in figure 7.3 settles in about 10 seconds after the disturbance, after having a surge of about 100% for G1 and G2 had a surge of about 138%. Figure 7.4 and figure 7.5 shows the generators G1 speed. The first swing on the speed of the generators G1 shows that it moved up from1.000 p.u to 1.0058 p.u and G2 rose from 1.0 p.u to about 1.0067 p.u before coming to rest after about 7 and 10 seconds respectively. Also, figure 7.6 shows that the rotor angle of G2 was stable. The disturbance caused a swing in both directions with the first swing coming down with decreasing amplitude from -0.3 rad to about -0.47 rad, the upward swing moved to about -0.17 rad before settling within 20 seconds after the disturbance. The result shows that generator G2 is affect more by the impact of the fault than generator G1 (slack bus).

7.3 Scenario 2: Transient and Small Signal Stability of the two-area power network

In this study, the transient and small signal stability of a weak (with low effective short circuit ratio ESCR) two area network is investigated. The following three transmission schemes are used for the small signal stability study, namely, High Voltage Alternating Current (HVAC) Link, High Voltage Direct Current (HVDC) Link and the hybrid HVAC/HVDC link. The transient stability was investigated on the hybrid HVAC/HVDC by applying a three-phase short circuit fault at the middle of the line L9 of HVAC line on the hybrid power network. This study shows that even when the parent networks HVAC and HVDC are stable, their interaction could affect the stability of the power network if the tie-line between them is weak.

HVAC/HVDC Hybrid Network Model

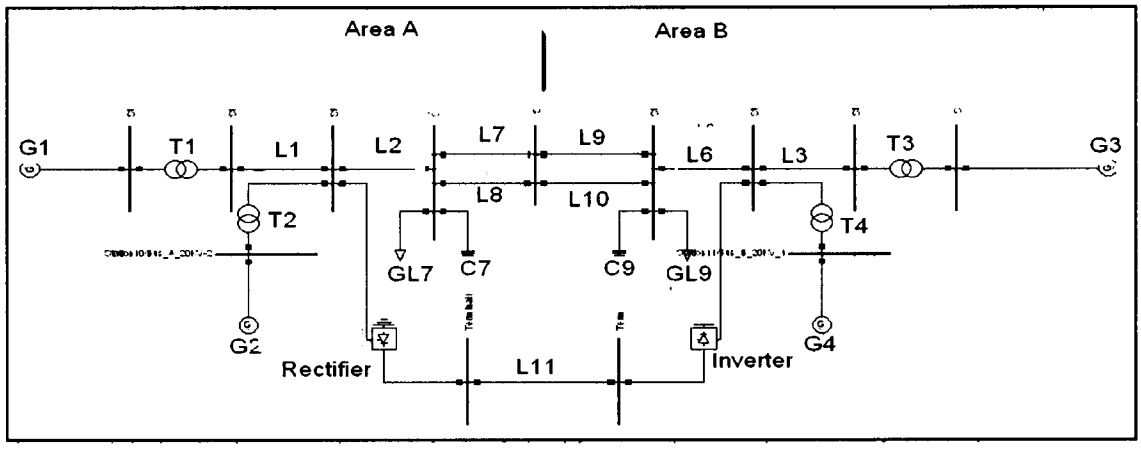

Figure 7.7 a two area hybrid HVAC and HVDC power network.

A two-area power system model taken from [1] is used for the simulations as shown in Fig.7.7. The AC network parameters as given in the above reference were used under a 60 Hz system in this study. CIGRE bench mark parameters are also used for the converter stations for DC network. The rating of the generators and HVDC lines, the current setting of the converters and the duration of the three-phase fault used for this simulation is given below and the complete parameters of the system are given in Appendix B: Table B: 2.

(i) Generators rated values are 20KV, 900MW, 100MVA base value, 60 Hz.

(ii) The total HVAC line length is set at 420km and HVDC line was set at 2000km.

(iii) The rectifier station is set at constant current control; the rated current is 2 kA whilst the inverter station is set at gamma (Constant extinction angle) control.

(iv) A three phase short circuit fault was applied at 50% of the line length (L9) on the HVAC link at 3 seconds and cleared after 3.05 seconds.

(v) The Generator (G1) on the left area A is the slack bus and the one on the right (G3) in area B was set as a PV bus and G2 and G4 are set as PQ bus.

7.3.1 Transient stability study of the HVAC system

Under the transient stability study the rotor angle of G3 and rotor angle difference of G1 were investigated, also the G3 speed, terminal voltage of G3, the active and reactive powers of G1 and G3 were equally investigated. G3 and G1 were chosen because G1 is the slack bus and G3 is close to the fault and they represent generators on different areas of the power network. In [58] rotor angle difference is defined as "*the difference between the rotor angle of the synchronous generators and the rotor angle of the synchronous motors*" when a fault occurs, the system is less able to transfer power from the synchronous generators to the synchronous motors, since the instantaneous power input did not change. The generators will begin to speed up while the motors slowed down; this further increases the rotor angle difference.

In this study a three-phase short circuit fault was applied half the length of the AC link L9 as shown in figure 7.7 above. The results of the transient stability study are given in Figures 7.8 to 7.13. The load flow results are given in Appendix C: Table C: 1.

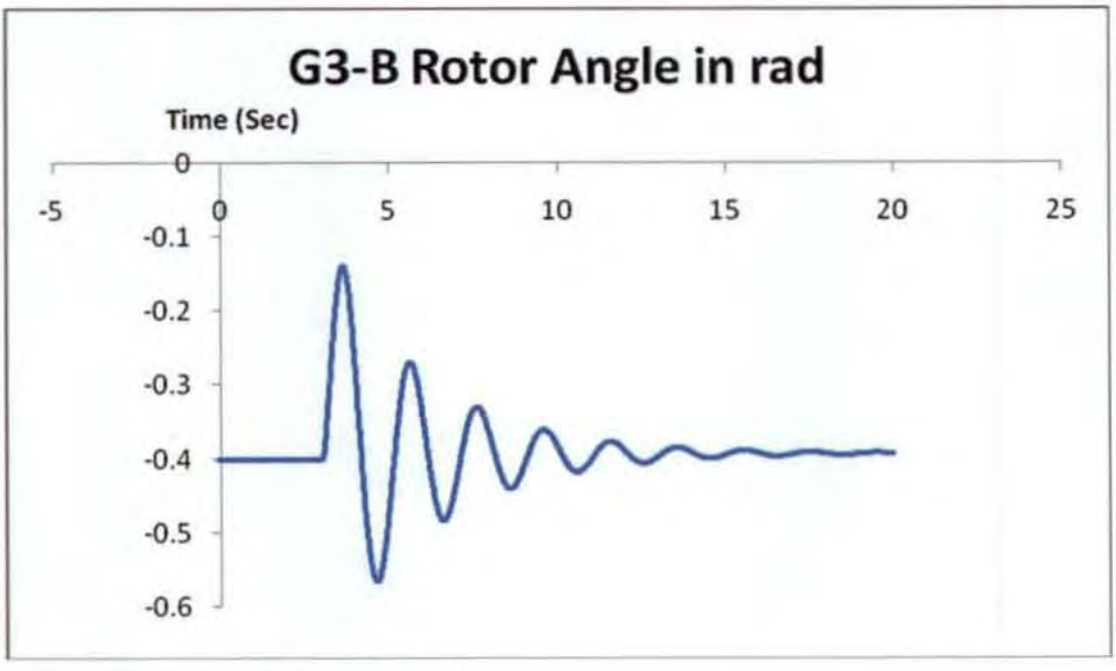

Figure 7.8 Generator (G3) Rotor Angle

Please note the y-axis in figure 7.4 represents the generator rotor angle in rad

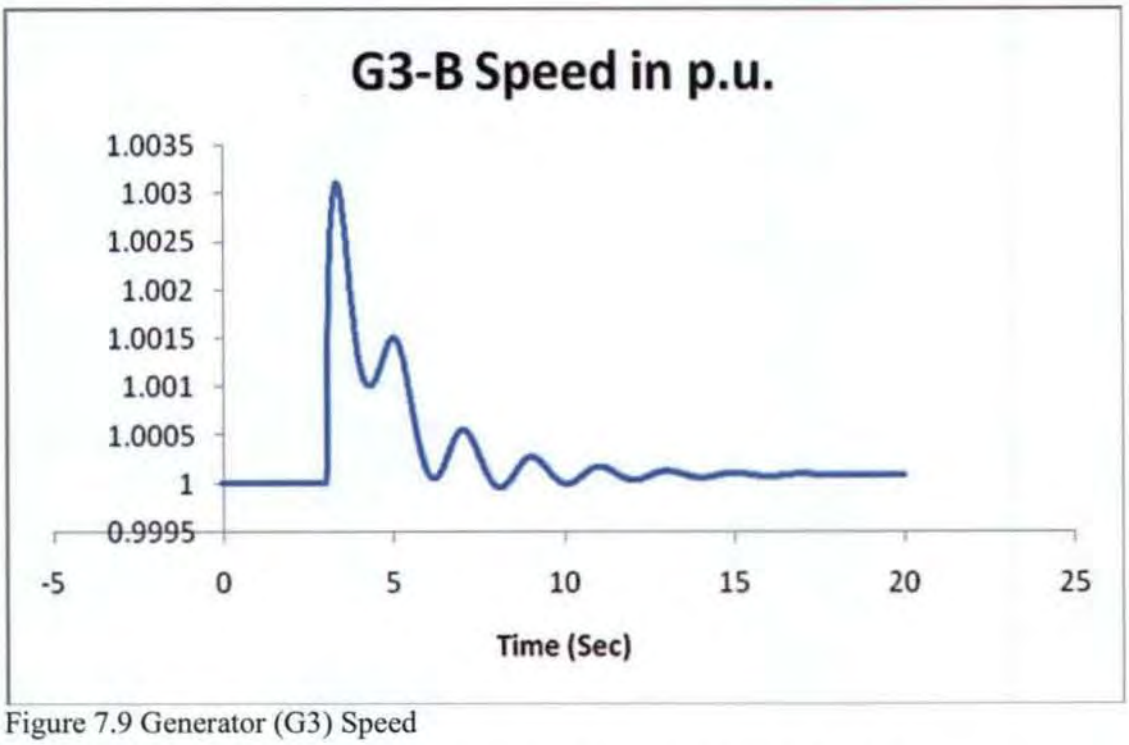

Figure 7.9 Generator (G3) Speed

Please note the y-axis in figure 7.4 represents the generator speed in p.u

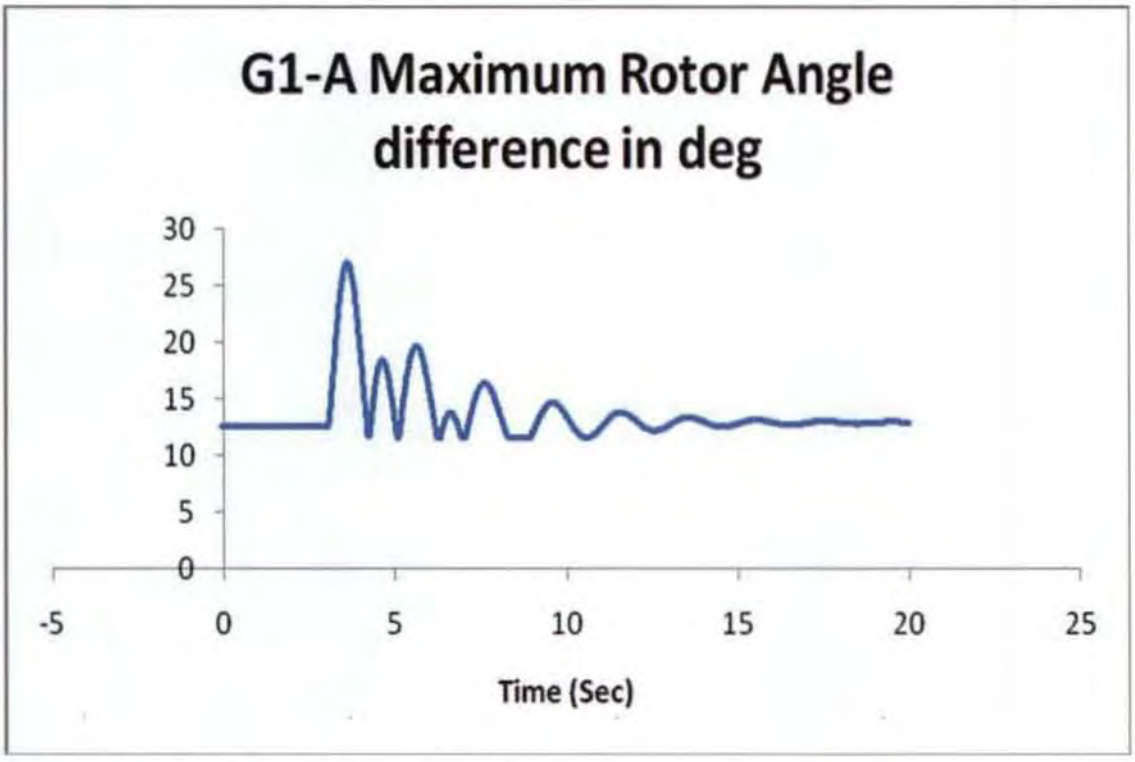

Figure 7.10 Rotor Angle difference (G1)

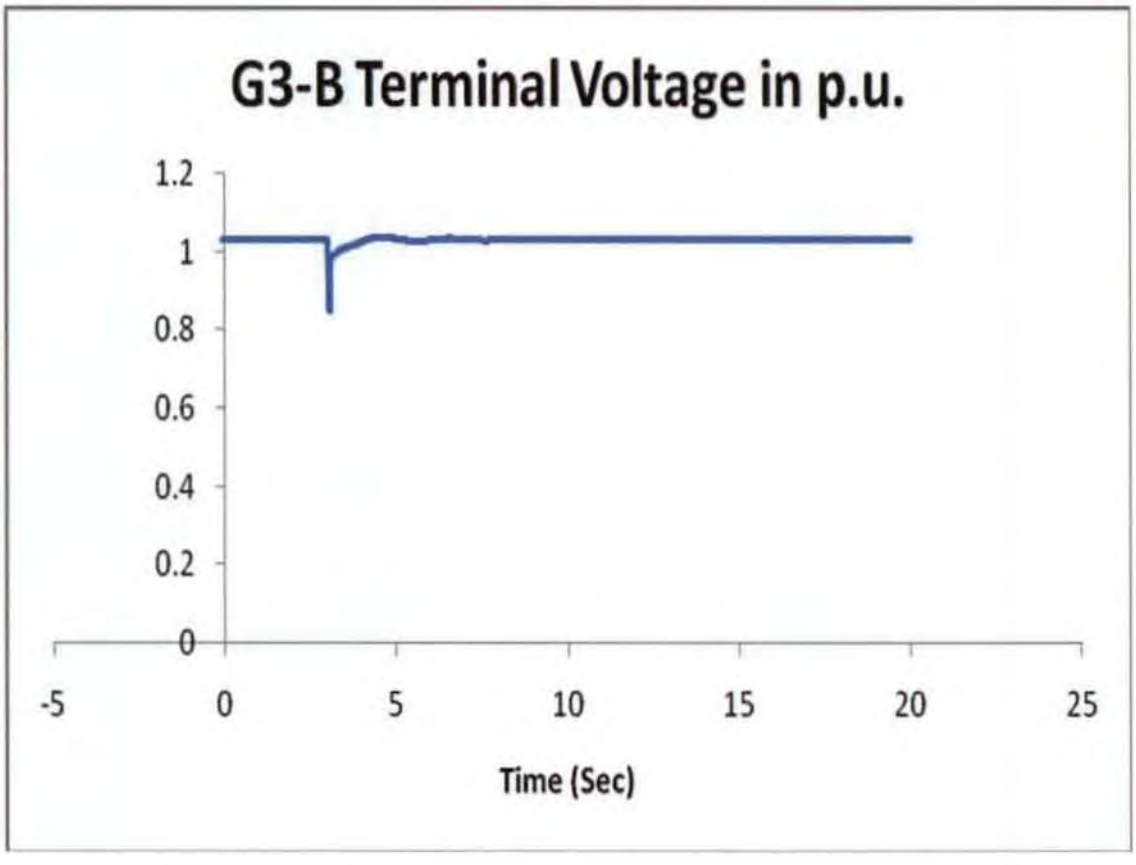

Figure 7.11 Terminal Voltage of Generator (G3)

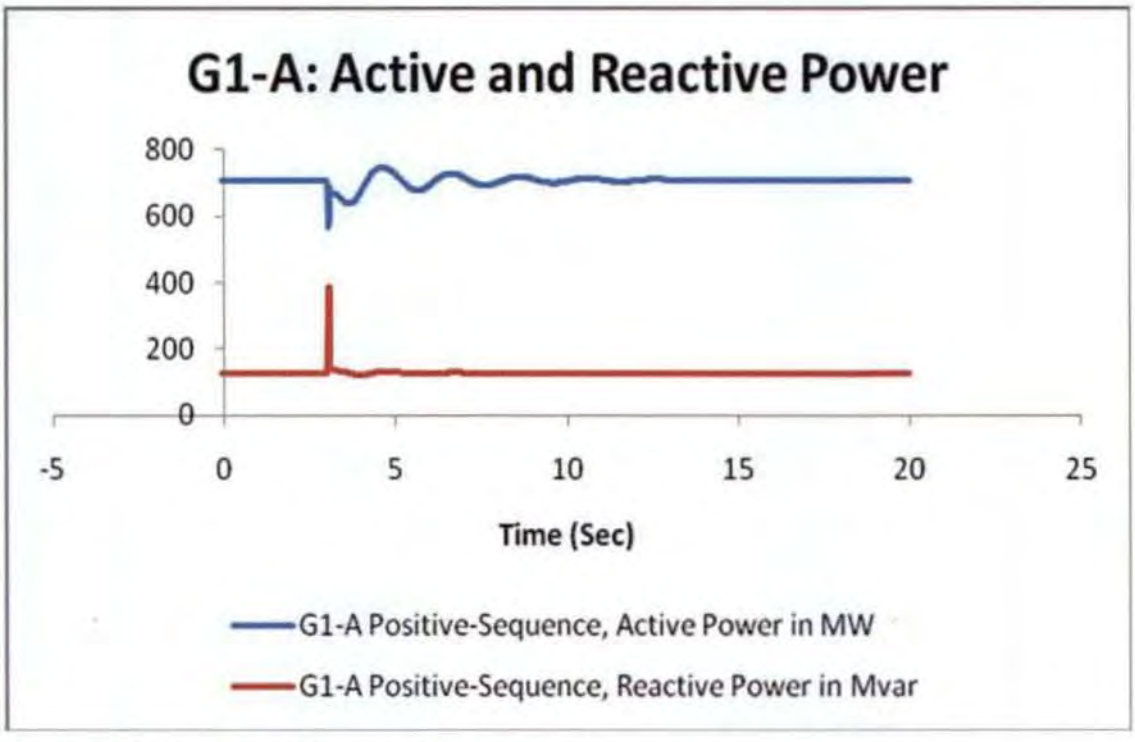

Figure 7.12 Active and Reactive Power of (G1)

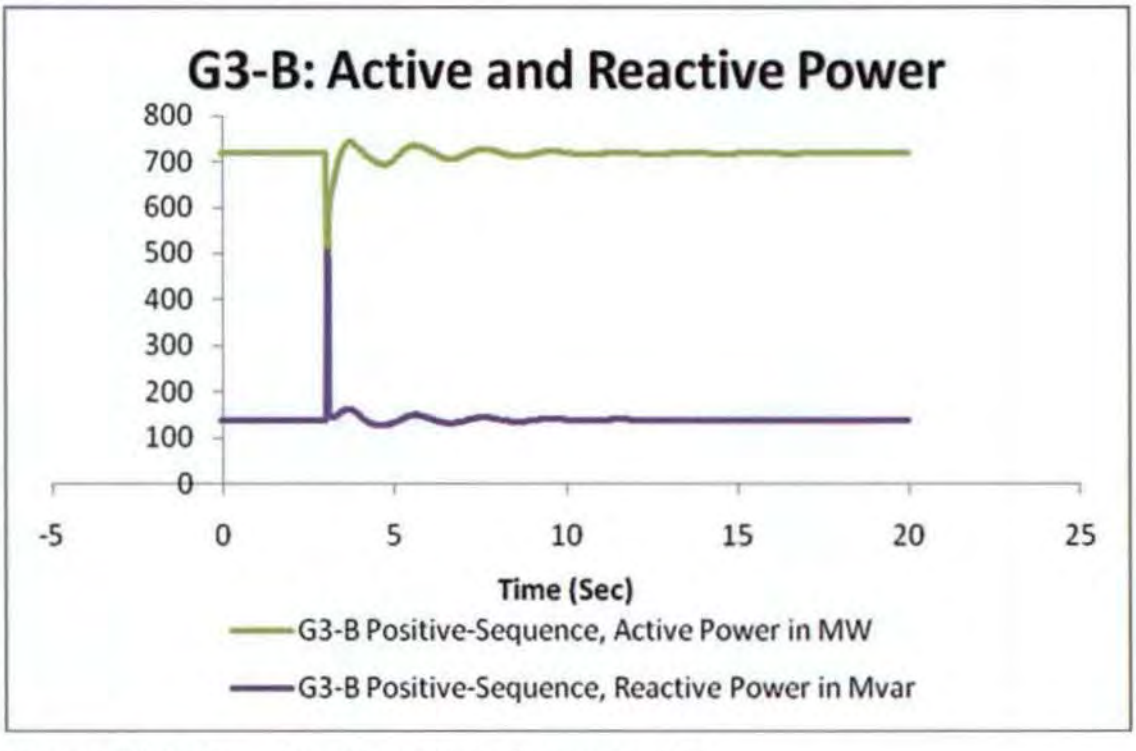

Figure 7.13 Active and reactive power of generator (G3)

Transient stability is investigated using the hybrid link as the. Figures 7.8 to 7.31 above showed the effects of three-phase short circuit fault at the middle of line L9) with regard to the responses of the rotor angle, generator speed, maximum rotor angle difference, terminal voltage, active and reactive power of the system to the fault.. Figure 7.8 shows generator G3's rotor angle response to the perturbation. In the first swing it dipped from -0.485 rad to about -0.538 rad and then up to about –0.463 rad before returning to a steady state of operation in about 10 seconds after the perturbation.

Figure 7.9 shows that the speed of the generator (G3) swing from 1.0 p.u. (pre-fault steady state operating condition) to about 1.0045 p.u. before coming to a steady state of operation after about 10 seconds following the transient disturbance. It is to be noted that G3 is investigated because it is close to the fault. Figure 7.10 shows that the rotor angle difference of generator G1 was at 60° before the fault, but swings to about 61.9° and then dipped to about 58.5° before coming to equilibrium at 60° after about 10 seconds post fault situation. Figure 7.11 shows the behavior of the terminal voltage of generator G3 following the fault. The system was initially operating at about 1.038 p.u before the fault, but dipped after the fault to about 0.997 p.u. during the fault, before recovering to a stable state of operation at about 8-9 seconds after the fault.

Following the fault, active and reactive powers of generators 1 and 3 were temporally perturbed as indicated by Figure 7.12 and figure 7.13. G3's active power had a downward swing from about 700 MW to about 500MW before returning to a steady state after about 11 seconds. The reactive power followed similar pattern but in opposite direction. The first swing was upward from about -125 Mvar operating state to about 500 Mvar (representing a surge of about 130%) before coming to rest. G1's first swing is downwards from about 700 MW to about to 550MW representing a drop of 29% before returning to steady state of operation within 8 seconds after the disturbance. The reactive power of G1 had an upward swing following the fault from about 125 Mvar to about 400 Mvar following the first swing and returns to a steady state after about 8 seconds following the fault. With the above result the system is said to be stable under a transient disturbance of a three phase short circuit fault. The result showed that generator G3 is affected more by the fault than generator G1.

7.3.2 Small Signal Stability Analysis

Theoretically the inter-area oscillation frequency ranges from 0.1 to 0.3 Hz for very low frequency and from 0.4 to 0.8 Hz for low frequency. Local modes and inter-machine modes are is within the range of 0.8 to 2 Hz. Frequency of oscillation depends on the strength of the system and on the moment of inertia of the generator rotors [1]. Using Lyapunov 1st method, when the eigenvalues of a system have negative real part, the original system is asymptotically stable. When the eigenvalues have at least a positive real part the original system is unstable and when eigenvalues have a real part equal to zero, it is not possible on the basis of first approximation to say anything in general about the stability [59]. Small signal stability was investigated using three case transmission line schemes, HVAC, HVDC, and the hybrid HVAC/HVDC systems and the results obtained are as shown by tables 7.4-7.6. The tables show the modes with electromechanical oscillations in the three transmission schemes, for easy analyses of the results. The complete results of the small signal stability investigation are shown in the Appendix D: Table D: 1, Appendix D: Table D: 1 and Appendix D: Table D: 1

7.3.3 Interpretation of results of HVDC/HVAC Link

Table 7.4 lists the real and imaginary parts of the eigenvalues as well as the system frequency and damping ratio for the hybrid HVAC-HVDC network. Eigenvalues 2 to 5, 14 to 16 and 18 to 20 are real eigenvalues with damping ratio of 1 and these represent stable eigenvalues which are said to be critically damped. Eigenvalues 6 and 7 are conjugate pairs with collective damping ratio of 0.9999 and damped frequency of 0.0056Hz. Similarly, modes 8 and 9 are conjugate pairs with damping ratios of 0.1694 and damped frequency of 1.1034Hz. Also, modes 10 and 11 have damped frequency of 1.0788 Hz and damping ratio of 0.1765 eigenvalues 12 and 13 are conjugate pairs with a lower damping ratio of 0.0955 and damped frequency of 0.5039. It shows that the eigenvalues are stable with decaying oscillations. These are the dominant eigenvalues in the system. In analyzing the above result, electromechanical oscillations of the system plays a major factor. The result shows that the system is poorly damped and most likely prone to instability.

7.3.4 Interpretation of results of HVDC Link

In Table 7.5: Shows the result of small signal stability investigation under the HVDC system. Eigenvalues 2 to 6, 9 to 10 and 13 to 18 are critically damped. The dominant mode of oscillation here is local mode. There are no inter-area oscillations but there are traces of control mode of oscillation at the 19 and 20 modes as a result of the HVDC converter control actions which were well damped. To this end, the system can be said to be very stable under small signal disturbance.

7.3.5 Interpretation of results of HVAC Link

From this Table 7.6: Eigenvalues 2 to 6 and 14 to 20 are real eigenvalues with damping ratio of 1. This represents the highest eigenvalues that can be achieved. Eigenvalues 8 and 9, and 10 and 11 are conjugate pairs with damping ratios 0.1704, 0.1747 and damped frequencies 1.1166Hz and 1.0966Hz respectively. This represents local mode of oscillation in the system. Also, eigenvalues 12 and 13 are conjugates and represent inter-area oscillation with damped frequency of 0.5789 and damping ratio of 0.1159 which indicates that the system is damped. On the other hand the hybrid HVAC-HVDC network can be considered to have a poorly damped inter-area mode.

From the above analysis, the HVAC system is stable. Systems fault excites both local and inter-area modes of oscillation in area A of generators G1 and G2. Also, area B

With generators G3 and G4 have both oscillations, but the local oscillations that results into inter area modes. This is justified by the fact the local mode has higher damping factor than the inter-area mode.

Table 7.4 Eigenvalues result for HVAC/HVDC network

Eigenvalues	Real Part	Imaginary part	Damped Frequency	Damping Ratio
6	-9.9288	0.0355	0.0056	0.9999
7	-9.9288	-0.0355	0.0056	0.9999
8	-1.1919	6.9331	1.1034	0.1694
9	-1.1919	-6.9331	1.1034	0.1694
10	-1.2157	6.7780	1.0788	0.1765
11	-1.2157	-6.7780	1.0788	0.1765
12	-0.3038	3.1662	0.5039	0.0955
13	-0.3038	-3.1662	0.5039	0.0955

Table 7.5 Eigenvalues result for HVDC system

Eigenvalues	Real Part	Imaginary Part	Damped Frequency	Damping Ratio
7	-1.2483	6.8623	1.0922	0.1790
8	-1.2483	-6.8623	1.0922	0.1790
9	-9.1161	0	0	1
10	-4.0000	0	0	1
11	-1.7562	6.3687	1.0136	0.2658
12	-1.7562	-6.3687	1.0136	0.2658

Table 7.6 Eigenvalues result for HVAC link

Mode	Real part	Imaginary part	Damped Frequency	Damping Ratio
8	-1.2129	7.0157	1.1166	0.1704
9	-1.2127	-7.0157	1.1166	0.1704
10	-1.2222	6.890	1.0966	0.1747
11	-1.2222	-6.890	1.0966	0.1747
12	-0.4244	3.6371	0.5789	0.1159
13	-0.4244	-3.6371	0.5789	0.1159

7.4 Scenario 3: Effects of AVR and PSS on the transient and small signal stability of the two-area network

This study shows the analysis of transient and small signal stability of a two-area multi machine power system as shown in figure 7.14.The same network and parameters as described previously where used for this study with the exclusion of the HVDC Link. In other words only the HVAC transmission scheme was investigated. This was achieved by investigating the impact of a three-phase short circuit fault on the generator speed, the terminal voltage, the excitation flux, the rotor angle and active power transmitted after the large disturbance. Furthermore, the study shows the damping effect of a power system stabilizer (PSS) with automatic voltage regulator (AVR) on small signal stability of power systems. As well as its improvement on power transmitted following a major fault in the power system. The power system stabilizer provides additional input signal to the regulator to damp power system oscillations the voltage regulator responds to network disturbance by increasing the generator field voltage, which invariably improves the transient stability also; small signal stability is improved by increasing the synchronizing power [1]. The PSS sometimes is referred to as a supplementary excitation control. Power systems dynamic performance is improved by PSS by using auxiliary stabilizing signals to control the excitation system. The block diagram of the PSS and AVR and their inputs are given in the Appendix F: Table F.1 and table F.2 respectively, also their parameters are given in the Appendix G: Table G.1 and table G.2 in the same order. The PSS and the AVR were integrated in the generators G3 and G4 in area B to the fault.

7.4.1 The simulation case studies

The small signal stability study is conducted on the High Voltage Alternating Current (HVAC) system. The cases with and without PSS have been considered. In case one a PSS was integrated into the system, whilst in case two the study is without PSS. This study shows that the generators in the area close to fault area are mostly perturbed by the effect of the fault; therefore, the analysis was based on the study of these generators i.e. G3, G1, G4 also G2 was analyzed to show the difference in effects between Area A and

Area B. This is evident from the results of the oscillations of generators in the two areas of the network as shown in the figures below.

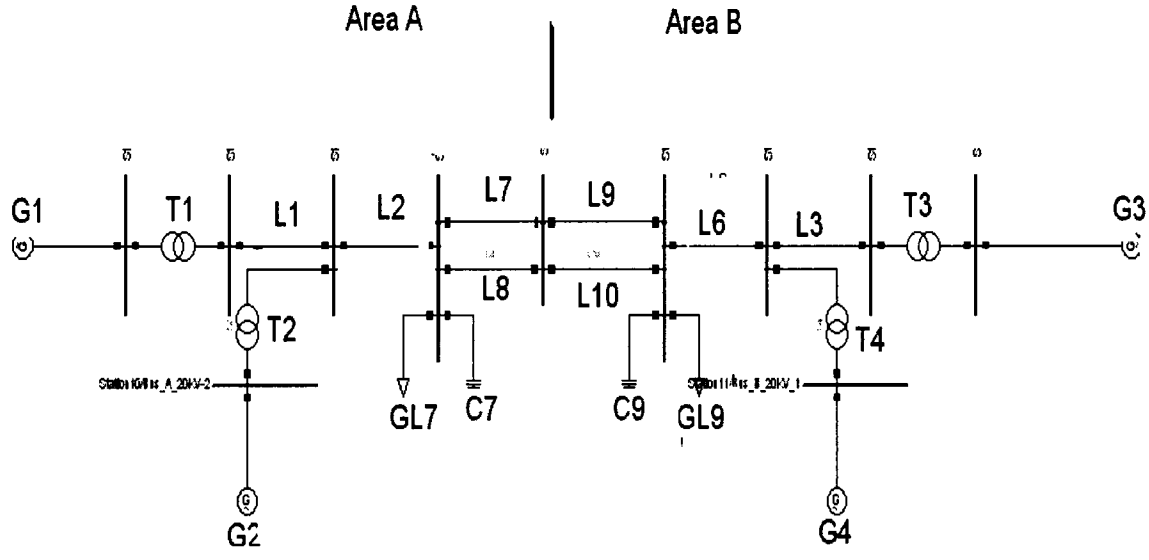

Figures 7.14 Two area HVAC power network

7.14 Transient Simulation

Figures 7.15 to 7.19 Shows the results of transient simulation with and without PSS system. Please note that, the y-axis in figures 7.15.1 and 7.15.2 represents rotor angle in rad, and the x-axis represents time in seconds.

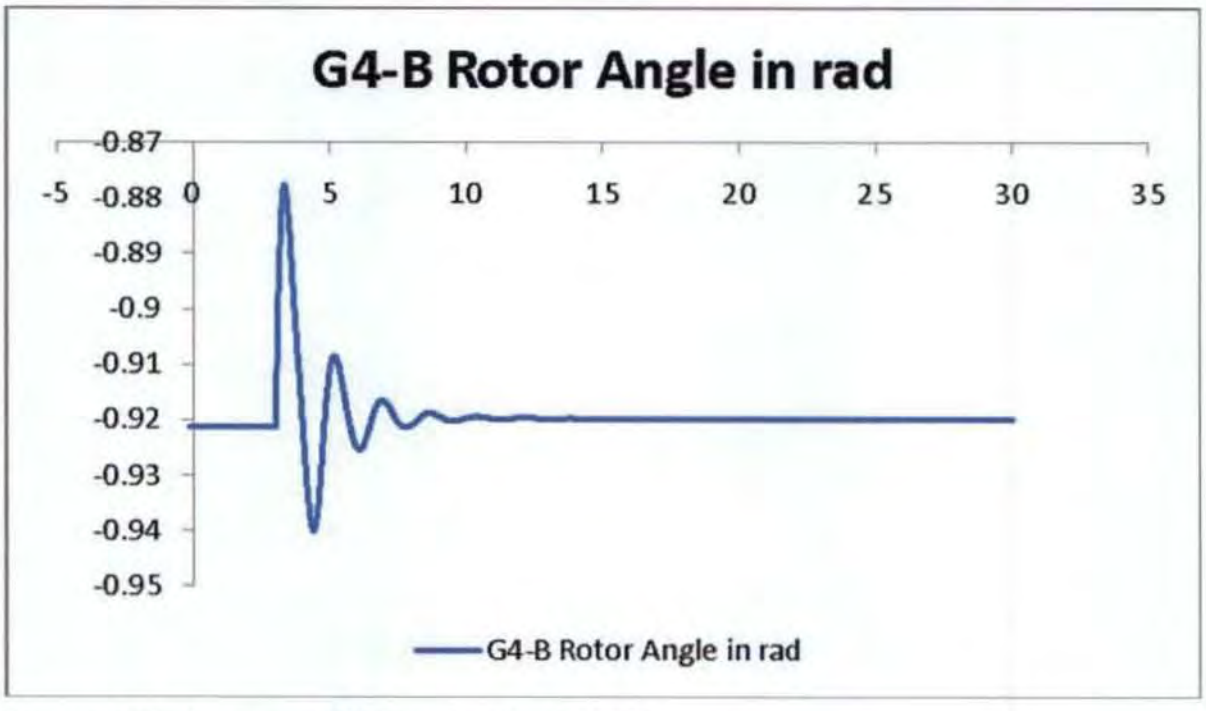

Figure 7.15.1 Generator (G4) Rotor angle with PSS

Please note the y-axis represents rotor angle in rad

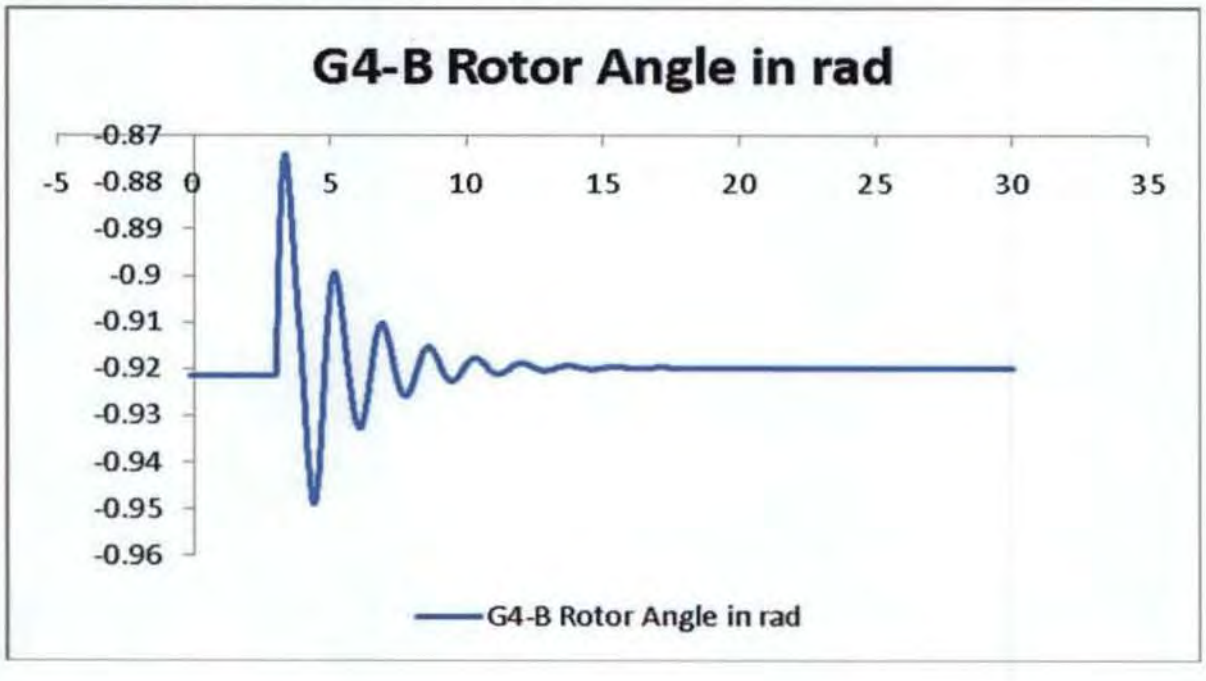

Figure 7.15.2 Generator (G4) Rotor angle without PSS

Please note the y-axis represents rotor angle in rad

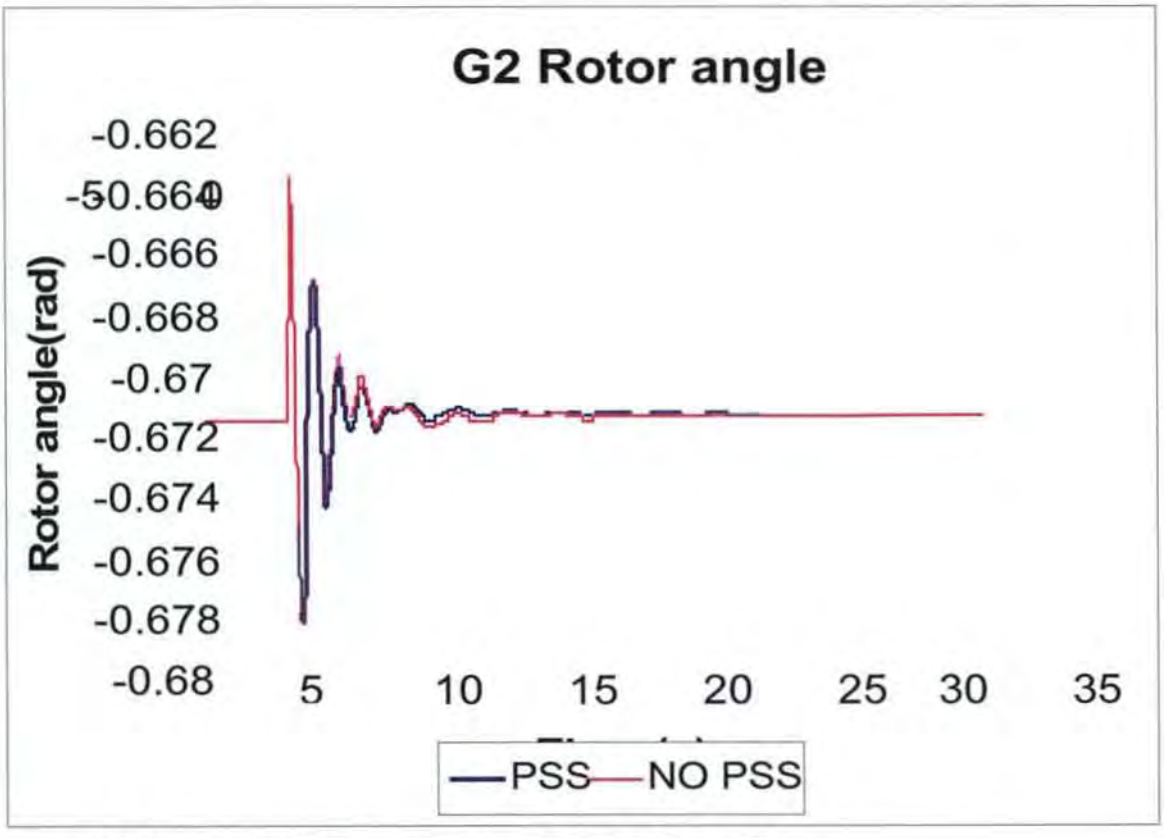

Figure 7.16 Generator (G2) Rotor Angle with and without PSS

Please note that, the y-axis in figures 7.17.1 and 7.17.2 represents rotor angle in rad, and the x-axis represents time in seconds.

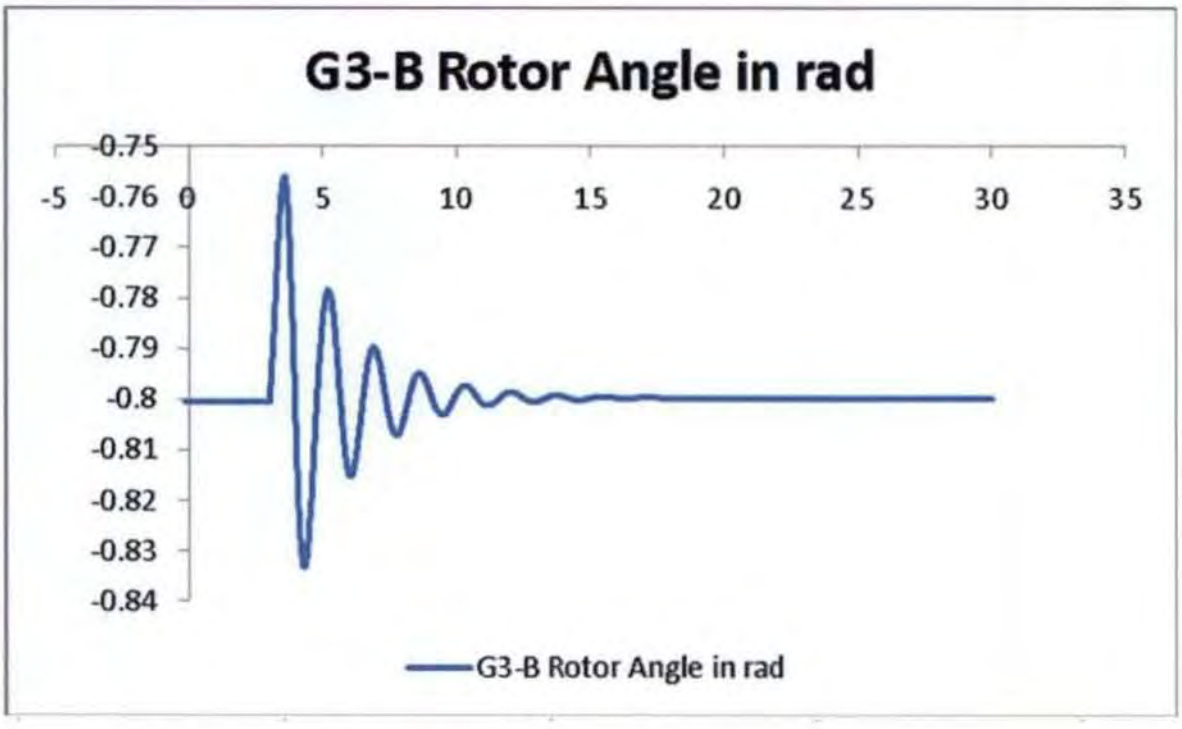

Figure 7.17.1 Generator (G3) rotor angle without PSS

Please note the y-axis represents rotor angle in rad

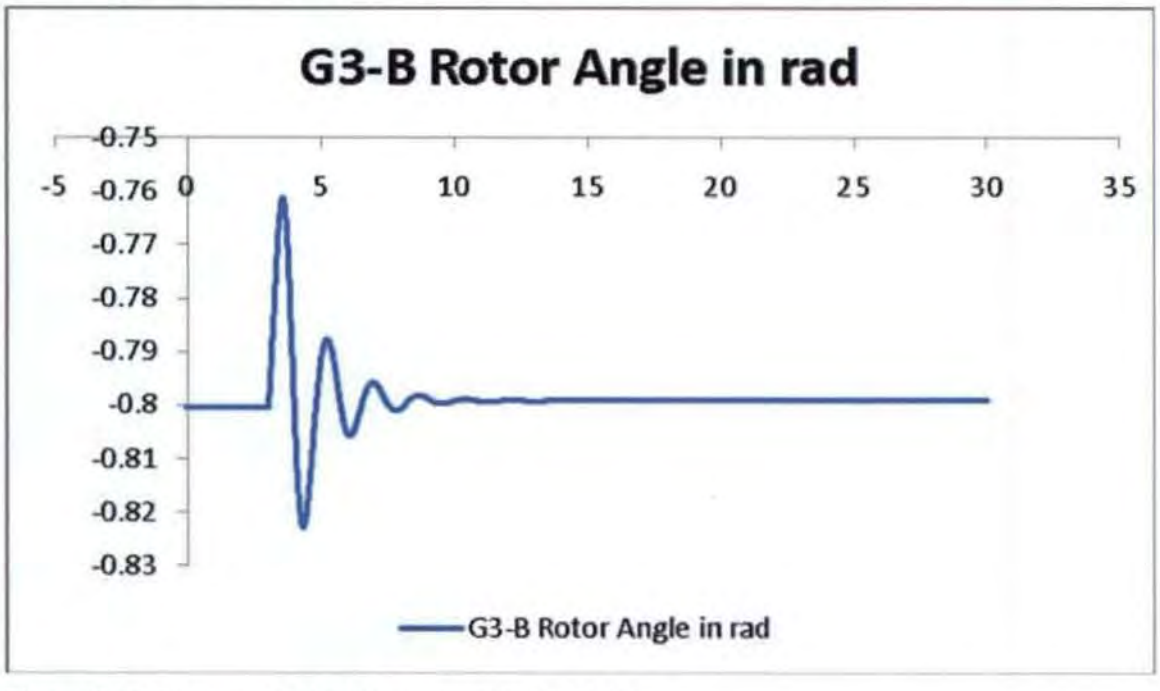

Figure 7.17.2 Generator (G3) rotor angle with PSS

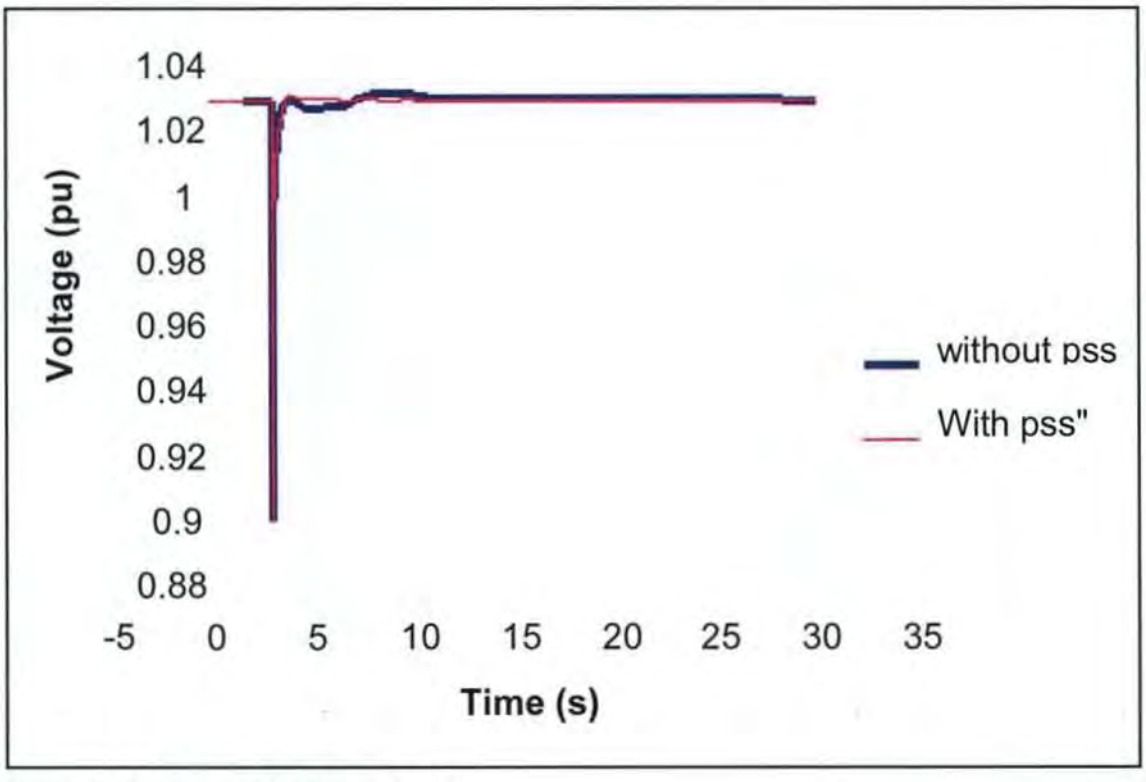

Figure 7.18 Terminal Voltage of (G3)

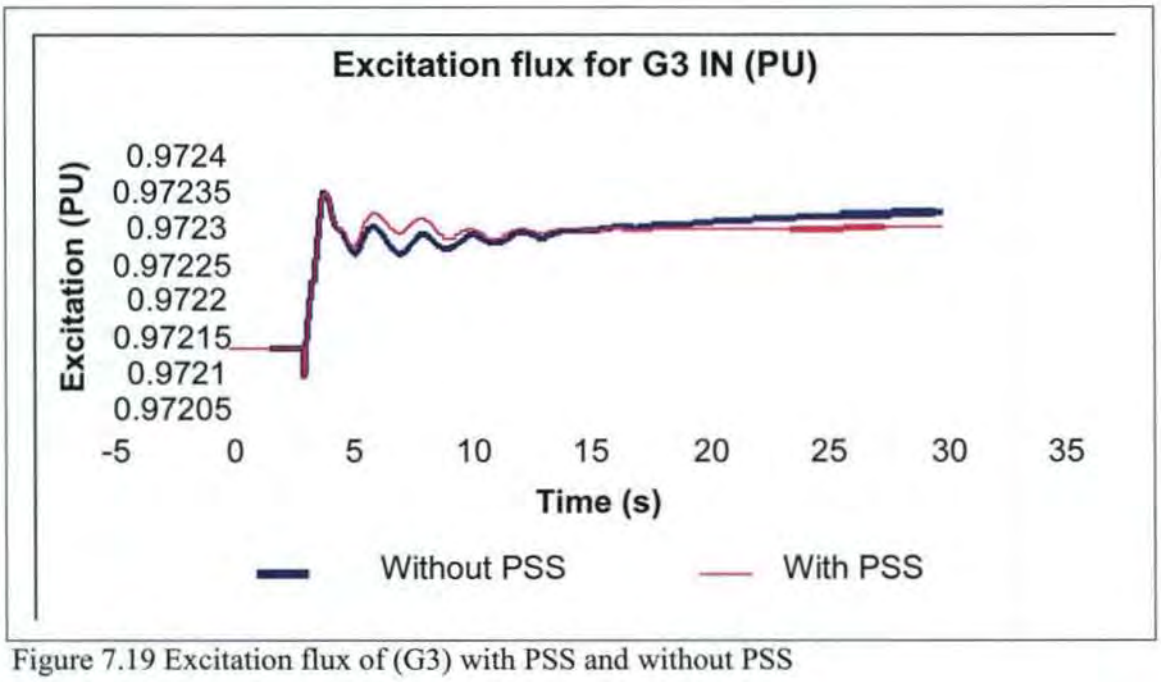

Figure 7.19 Excitation flux of (G3) with PSS and without PSS

Figures 7.15 to 7.19 above shows the effects of a three phase short circuit fault applied at the middle of line L9 as shown in figure 7.14. Figure 7.15.1 shows generator G4's

rotor angle responses to the fault when the PSS was integrated in the network. In the first swing it surged upward from about -0.922 rad to about -0.88 rad and then dipped to about –0.94 rad before returning to a steady state of operation with decreasing amplitude in about 6 seconds after perturbation. When operated without the PSS as seen in figure 7.15.2 the generator's first swing was upward from -0.922 rad to about -0.875 rad and dipped to -0.950 rad before settling with decaying in oscillations in about 13 seconds, this shows that system is marginally better damped with the PSS system. Figure 7.16 shows the response of generator G2 rotor angle following the fault. With out PSS the first swing amplitude rose from -0.672 rad upward to -0.664 rad before moving down to -0.670 rad and decays to a steady state at about 5 seconds after perturbation. With PSS the first swing was upward also, but the oscillation was better damped it came to steady state in about 8 seconds after disturbance. Figure 7.17.1: shows rotor angle responses of generator G3, without PSS. The first swing was from -0.80 rad rose to about -0.755 rad before coming down to about -0.835 rad and then returns to a steady state after 14 seconds it came to the same equilibrium state as it was before the disturbance. Without any PSS figure 7.17.2 the first swing followed the same pattern, during the fault, the first swing rose from -.0.80 rad to -0.78 rad and dipped to -0.824 and settled in 7 seconds. From the above results the generators close to the fault in Area B are more perturbed during the fault, they oscillates at higher amplitude and took more time to return to steady state after the fault. Generator G2 had little impact following the disturbance from area B. Figure 7.18: shows the responses of the terminal voltage of generator G3 with and without the PSS. The system was operating at about 1.03 p.u. before the fault, but dipped after the fault to about 0.9 p.u. during the fault, before recovering to a stable state of operation at about 5 seconds with PSS system, without the PSS the system dipped to 0.9 p.u and rose to about 1.045 p.u before coming to rest in about 8 seconds after the fault.. Figure 7.19 shows the excitation flux of G3. The system dropped from its initial steady state of about 0.97218 p.u to 0.97210 and then up to 0.97235 before settling at a new steady state of 0.9723 p.u with PSS. Without PSS the flux had an upswing without settling to a steady state after 30 seconds of operation.

7.4.2 Small Signal Stability simulation

The small signal stability study was conducted by considering the cases with and without PSS. The results obtained are discussed below.

7.4.3 Interpretation of results of HVAC with power system stabilizer

Table 7.7 gives the eigenvalues that represent the states of the generators in the system and the Eigenvalues are represented by the real and imaginary parts. Eigenvalues 1 to 12, 17, 20-22 and 25-30 are real eigenvalues with damping ratio of 1and these represent stable eigenvalues which are said to be critically damped, since they are not dominant modes they are left out in the table. Modes 13 and 14 are conjugates pairs with collective damping ratio of 0.1704 and frequency of 1.1167Hz. Similarly, modes 15 and 16 are conjugate pairs with a damping ratio of 0.1747 and frequency of 1.0965Hz this shows that the eigenvalues are stable with decaying oscillations. These modes represents local area oscillation in the system, modes 18 and 19 are conjugate pairs with damping ratio of 0.1164 and 0.5792Hz frequency. Modes 23 and 24 also conjugate pairs with damping ratio of 0.2564 and frequency of 0.15273 Hz, this mode is poorly damped, further investigation was carried out to ascertain whether it's a control mode or electromechanical, investigation shows that, although it's an electromechanical mode with G1-A and G2-A having participation in this mode (Appendix H: Figure H: 1 for the result of the participation of this mode). They are stable with decaying oscillations. These modes are the dominant eigenvalues in the system. They represent the electromechanical modes in the system, whilst modes 32 and 33 represent control modes which are well damped with a damping ratio of 0.9872 and as such not dominant. The system is therefore stable under the small signal stability study.

7.4.4 Interpretation of results of HVAC without power system stabilizer

From Table 7.8, modes 1 to 7 and 14 to 20 are real eigenvalues with damping ratio of 1. This represents the highest eigenvalues that can be achieved, and are said to be critically damped, therefore are left out of the table likewise. Modes 8 and 9, and 10 and 11 are conjugates pairs with collective damping ratios of 0.1704 and 0.1747 respectively and frequencies of 1.1166Hz and 1.0327Hz respectively. This represents local mode of oscillation in the system. Also, modes 12 and 13 are conjugates and represent inter-area oscillation with damped frequency of 0.5789 and damping ratio of 0.1139 which indicates that the system is poorly damped. However it represents stable eigenvalues with decaying oscillations. From the above analysis, the HVAC system is stable. Applied fault

excites both local and inter-area modes of oscillation in Area A of generators G1 and G2. Also, Area B with generators G3 and G4 having oscillations, but the local oscillations originates the inter area modes. This is justified by the fact the local mode has higher damping factor than the inter-area mode. This study shows the presence of the PSS improved the damping of the system; therefore the small signal stability of the system was enhanced with the PSS. From tables 7.7 and 7.8 the increase in the number of modes in table 7.7 was due to the presence of the PSS system and the AVR system in the network. The base case (HVAC system) was configured with four fifth order generators making the number of modes to be twenty.

7.4.5 Eigenvalues results for HVAC with and without PSS

Table 7.7: Small signal stability for HVAC with PSS

Eigenvalues	Real Part	Imaginary part	Damped Frequency	Damping Ratio
1	0	0	0	0
2	0	0	0	0
3	0	0	0	0
4	-1000.04	0	0	1
5	-50.0004	0	0	1
6	-33.2352	0	0	1
7	-31.2952	0	0	1
8	-31.3802	0	0	1
9	-28.7833	0	0	1
10	-28.1416	0	0	1
11	-9.9625	0	0	1
12	-9.8756	0	0	1
13	-1.2134	7.01652	1.1167	0.1704
14	-1.2134	-7.01652	1.1167	0.1704
15	-1.2222	6.8898	1.0965	0.1747
16	-1.2222	-6.8898	1.0965	0.1747
17	-5.5046	0	0	1
18	-0.4266	3.6391	0.5792	0.1164
19	-0.4266	-3.6391	0.5792	0.1164
20	-0.4266	0	0	1
21	-3.4710	0	0	1
22	-2.5009	0	0	1
23	-0.2546	0.9596	0.15273	0.2564
24	-0.2546	-0.9596	0.15273	0.2564
25	-1.0000	0	0	1
26	o.9999	0	0	1
27	-0.9968	0	0	1
28	-0.6364	0	0	1
29	-0.0041	0	0	1
30	-0.0381	0.0062	0.0010	0.9872
31	-0.0381	-0.0062	0.0010	0.9872
32	-0.0328	0	0	1

Table 7.8 Small signal stability for HVAC without PSS

Eigenvalues	Real Part	Imaginary part	Damped Frequency	Damping Ratio
1	0	0	0	0
2	-31.2941	0	0	1
3	-31.3799	0	0	1
4	-28.7799	0	0	1
5	-28.1394	0	0	1
6	-9.9626	0	0	1
7	-9.8757	0	0	1
8	-1.2129	7.1197	1.1166	0.1704
9	-1.2129	-7.1197	1.1166	0.1704
10	-1.2222	6.8898	1.0955	0.1747
11	-1.2222	-6.8898	1.0955	0.1747
12	-0.4244	3.6371	0.5789	0.1159
13	-0.4244	3.6371	0.5789	0.1159
14	-5.5045	0	0	1
15	-3.7750	0	0	1
16	-0.9892	0	0	1
17	-0.0015	0	0	1
18	-0.0390	0	0	1
19	-0.0333	0	0	1
20	-0.0293	0	0	1

Chapter 8

Voltage Stability Studies

This chapter investigates the voltage stability of the weak two-area HVAC power network, the hybrid HVAC-HVDC and the hybrid VSC/HVDC-HVAC systems. The voltage stability study was conducted on buses 4,5,7,8 and 12 used for transmission of power from area A to area B in the HVAC network (see figure 8.1), from the results of the voltage profile, voltage angle, voltage magnitude and the maximum load-ability point it is evident that bus 7 at the centre of transmission line has the highest proximity and sensitivity to voltage instability. The voltage stability was improved by the VSC-HVDC link, whilst the HVDC link improved transient stability as shown in chapter 7. It was problematic with voltage stability as a result of the effect of control actions of the (under load tap changers) converter stations on the weak HVAC link and the consumption of reactive power by the HVDC converter stations

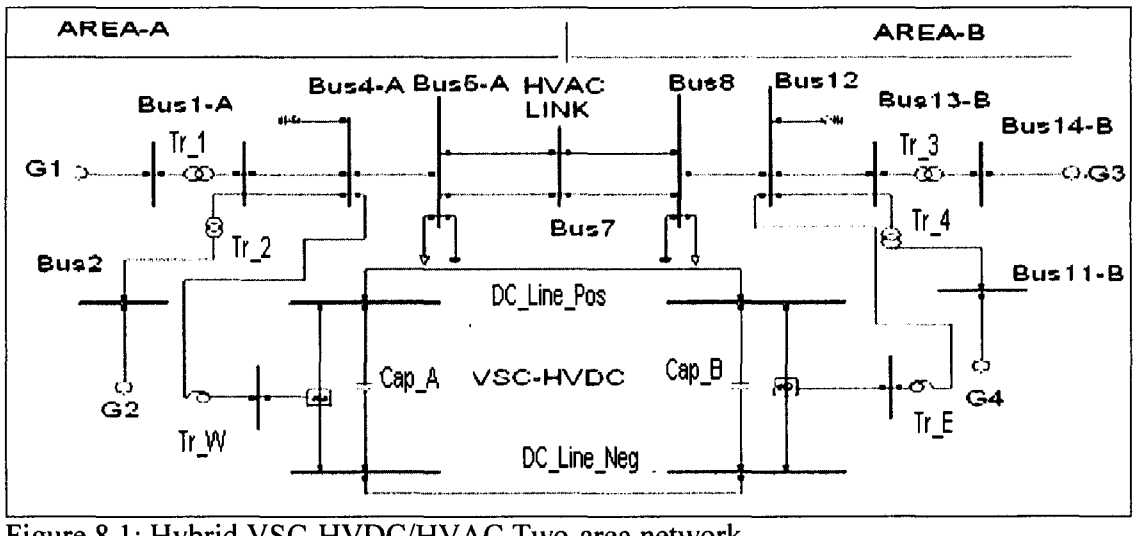

Figure 8.1: Hybrid VSC-HVDC/HVAC Two-area network

For the voltage stability study, QV curve was used to analyze the sensitivity and proximity of the system to voltage collapse, whilst PV curve was used to describe the maximum loading point (MLP) of the system, both curves were produced using series of power flow solutions for different load levels. The investigation was conducted using

three transmission schemes, namely, the HVAC system, the HVAC-HVDC hybrid network, and the hybrid HVAC-VSC/HVDC network.

8.1 Voltage stability analysis for the HVAC System

The simulation under HVAC was done using same network, same configuration and parameters of figure 7.14 (see chapter 7)

8.1.1 Voltage profiles at steady state

Figure 8.2 below shows the voltage profile of buses 4, 5, 7, 8, and 12 the HVAC transmission link, used for the transfer of power from area A to area B.

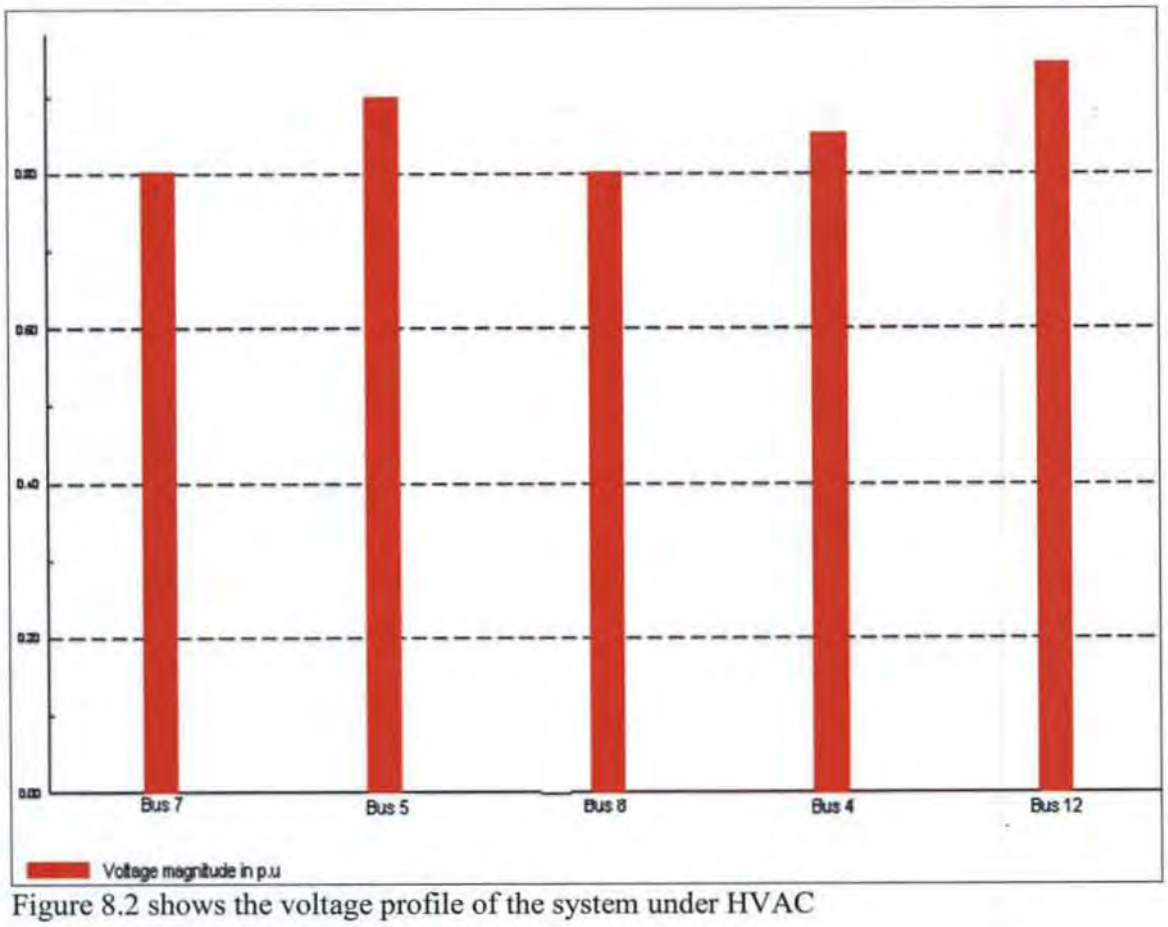

Figure 8.2 shows the voltage profile of the system under HVAC

The voltage profiles above show that under the HVAC transmission link, the voltage magnitude at the buses at the center of transmission line (buses 7 & 8) was lower than the buses at the sending and receiving end of the transmission line (bus 12 and 4

respectively). Note that power was supplied from both ends of the transmission line, but within the link from area A to area B power flowed from bus 5 through 7 to 8.

8.1.2 Voltage angles after a three phase fault

For simplicity only buses 5, 7, and 8 has been chosen here in analyzing the system since they are the principal buses linking area A to area B.

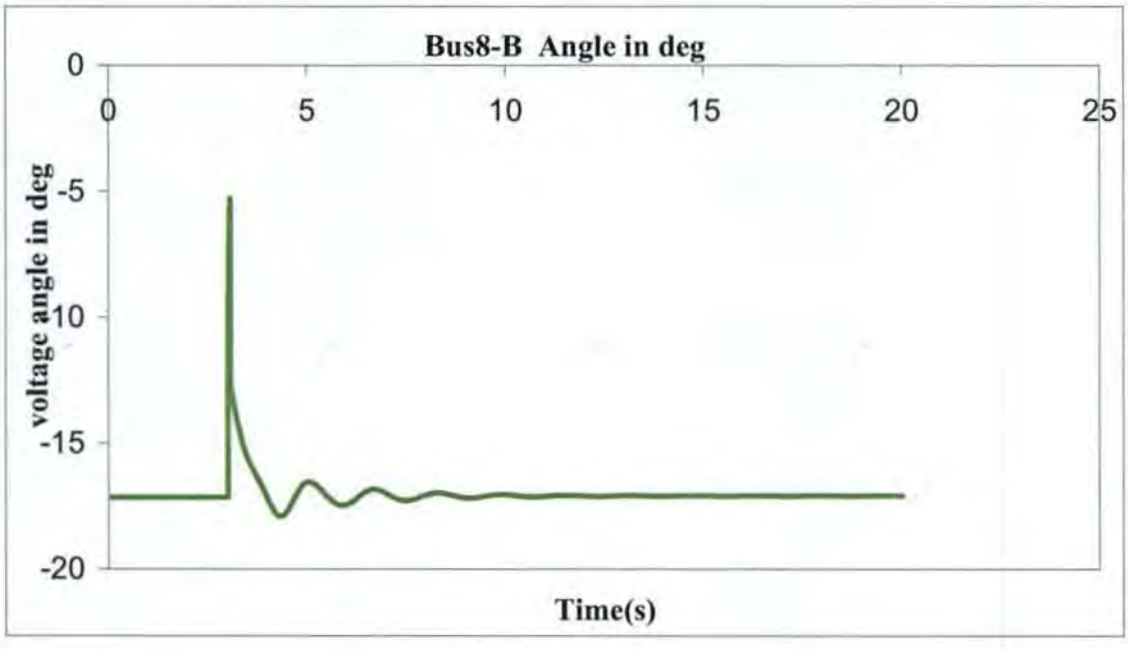

Figure 8.3: Voltage angle in deg for bus 8

Figure 8.3 shows that the voltage angle for bus 8 before the fault was -17.5^0 it rose to -5^0 during the fault before settling to a steady state in about 6 seconds. In figure 8.4: Bus 7 was at -7^0 before the fault and rose to 10^0 during the fault before coming to equilibrium in about 7 seconds. From the result bus 7 was impacted more by the fault having a higher first swing magnitude of about 15^0 during the disturbance, followed by bus 8 with 12.5^0 and bus 5 with 12^0 as shown bellow in figure 8.5: At steady state bus 5 was operating at 4^0 but rose to 16^0 during the fault and comes to equilibrium after 9 seconds. The result shows that the system was stable under HVAC link.

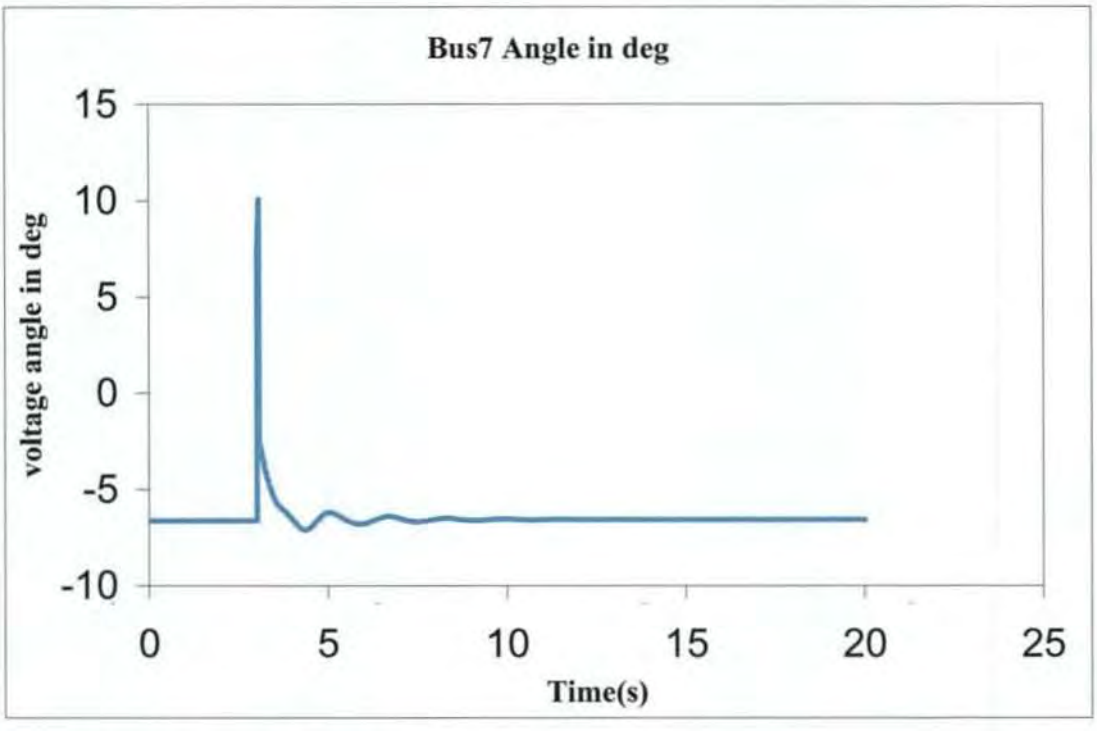

Figure 8.4 Voltage angle in deg for bus 7

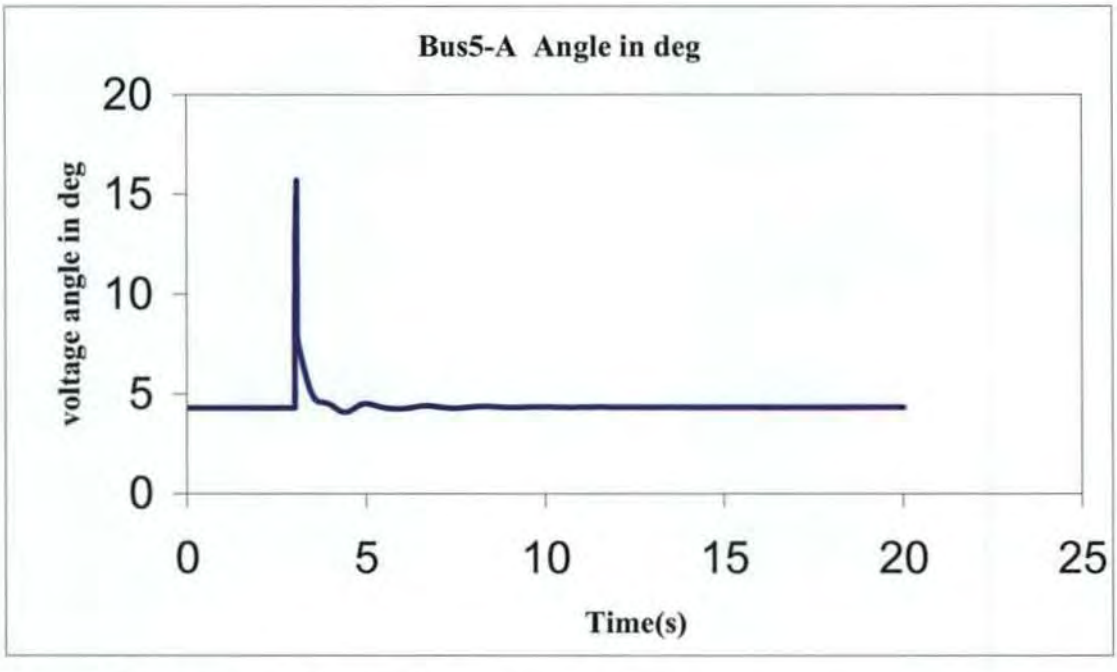

Figure 8.5 Voltage angle in deg for bus 5

8.1.3 Voltage magnitude for HVAC

Figure 8.6 shows that Bus 8 had the highest voltage magnitude at equilibrium; this is understandable since power flowed from area A to area B in the network. Figure 8.7 shows that Bus 7 was mostly perturbed with the disturbance coming down from voltage magnitude of about 1.0p.u to 0.4 p.u but settled in less than 2 seconds; In figure 8.8 bus 5 was the least perturbed since it came down from 1.0 p.u to 0.75 p.u, bus 8 dropped from 1.05 p.u to about 0.55 p.u. the bus had the highest voltage magnitude this is due to the fact that it is at the transmitting end of the network. It can therefore be deduce that the system is stable following the perturbation.

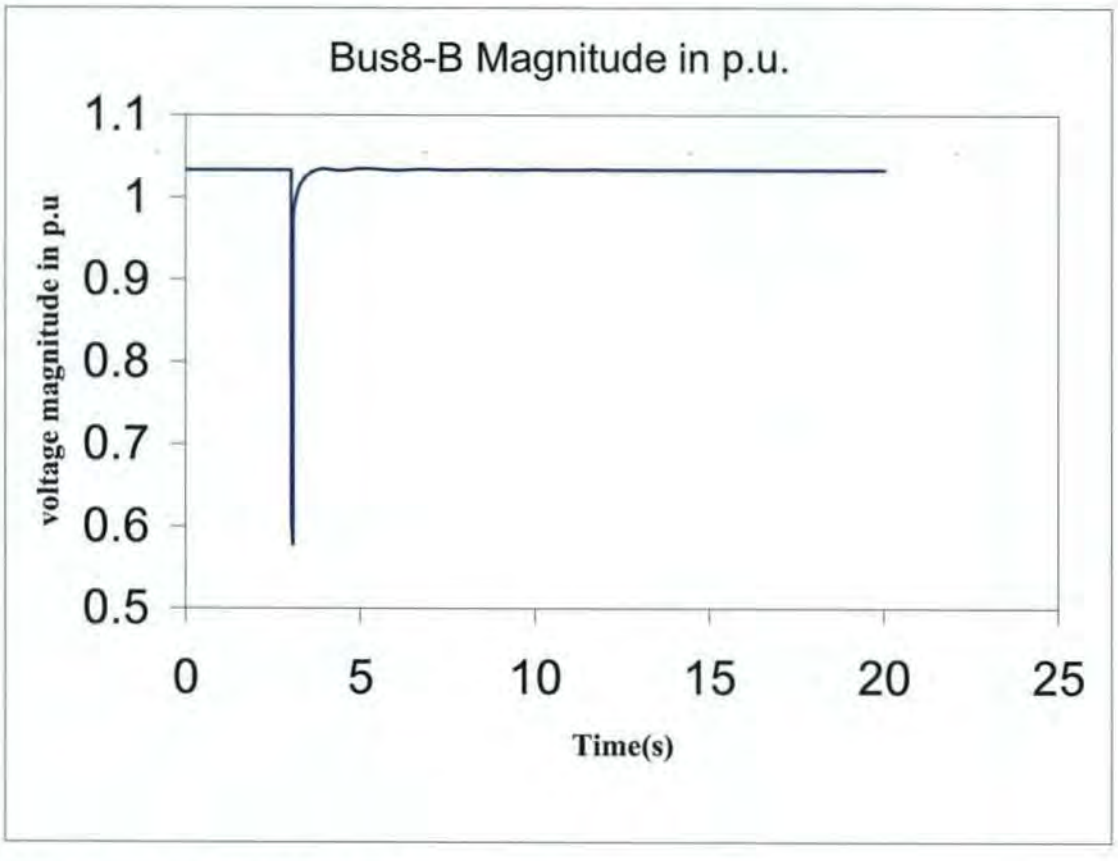

Figure 8.6 voltage magnitude in p.u for bus 8

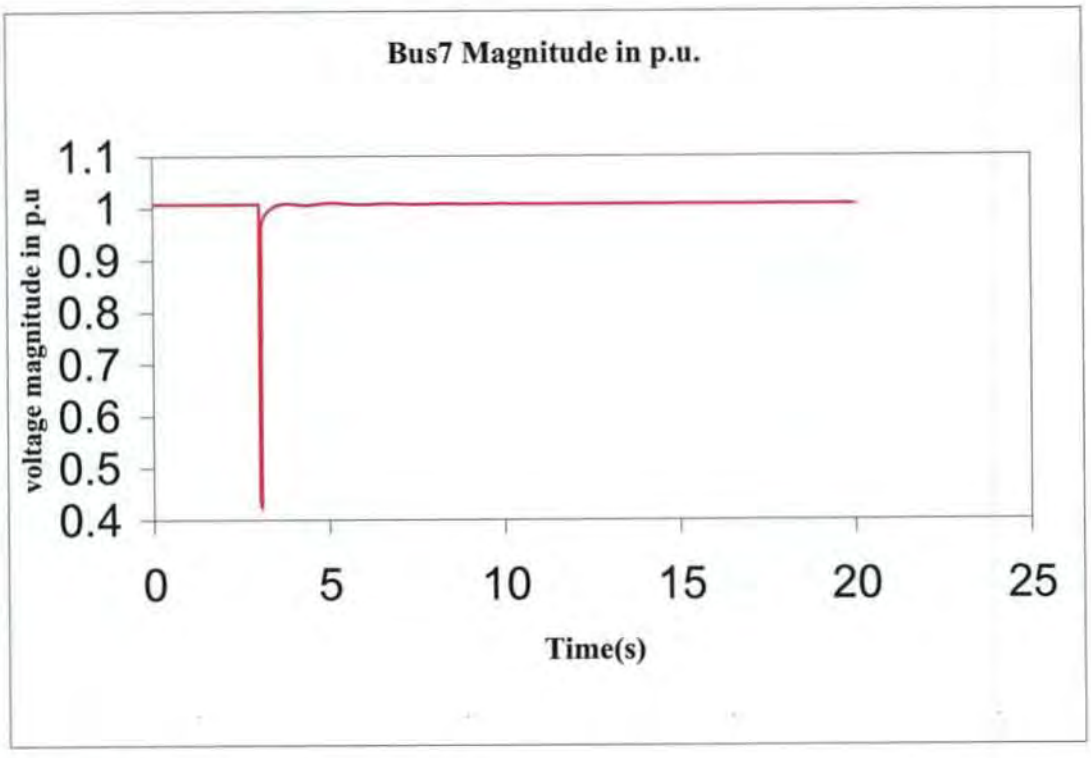

Figure 8.7 voltage magnitude (p.u) for bus 7

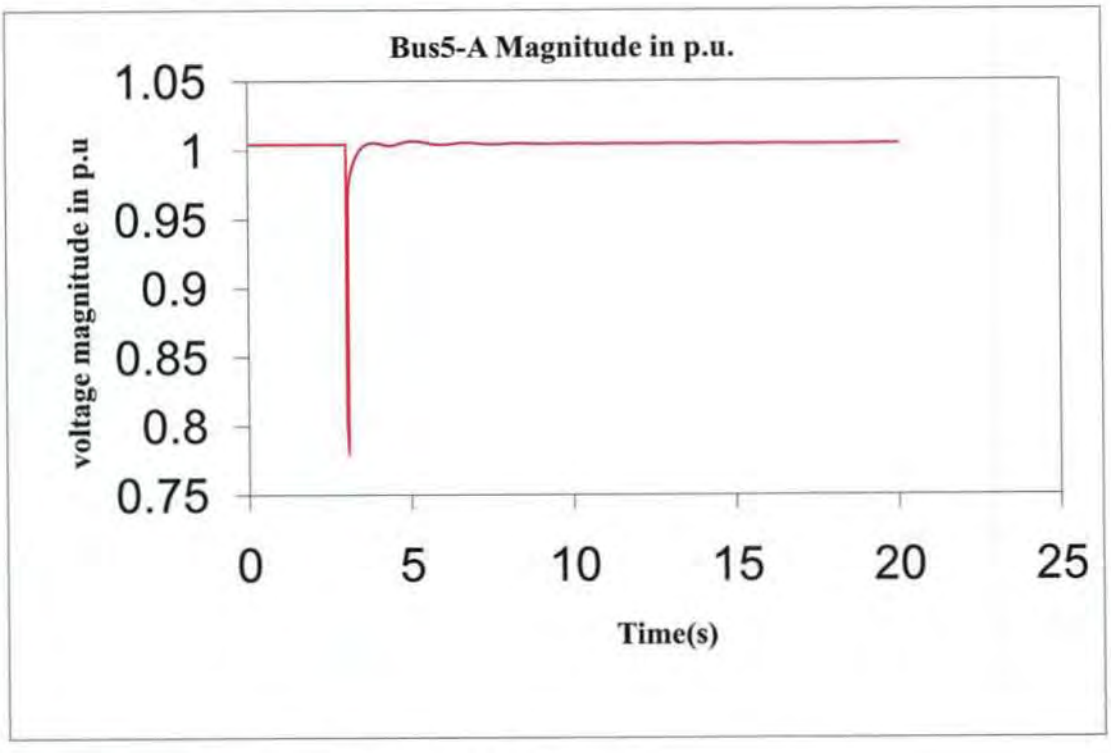

Figure 8.8 voltage magnitude (p.u) for bus 5

8.1.4 PV curve and VQ curves for voltage stability of HVAC system

QV curve of HVAC system

Figure 8.9: Shows the critical operating conditions for buses 7, 8, 5, 4 and 12. The sensitivity to voltage collapse was shown by the graph and it shows that the weakness of bus 7 is higher than the rest buses under investigation. It has higher sensitivity to voltage collapse with a critical operating point of 0.8353p.u (voltage magnitude), -456.13 Mvar (reactive power), followed by bus 8. the second critical bus is bus 8 (0.7453p.u, -464.6246Mvar) and the third critical bus is bus12 (0.7653p.u, -515.8819Mvar) in that order. Buses 4 and 12 have lower sensitivity to voltage collapse followed by bus 5.

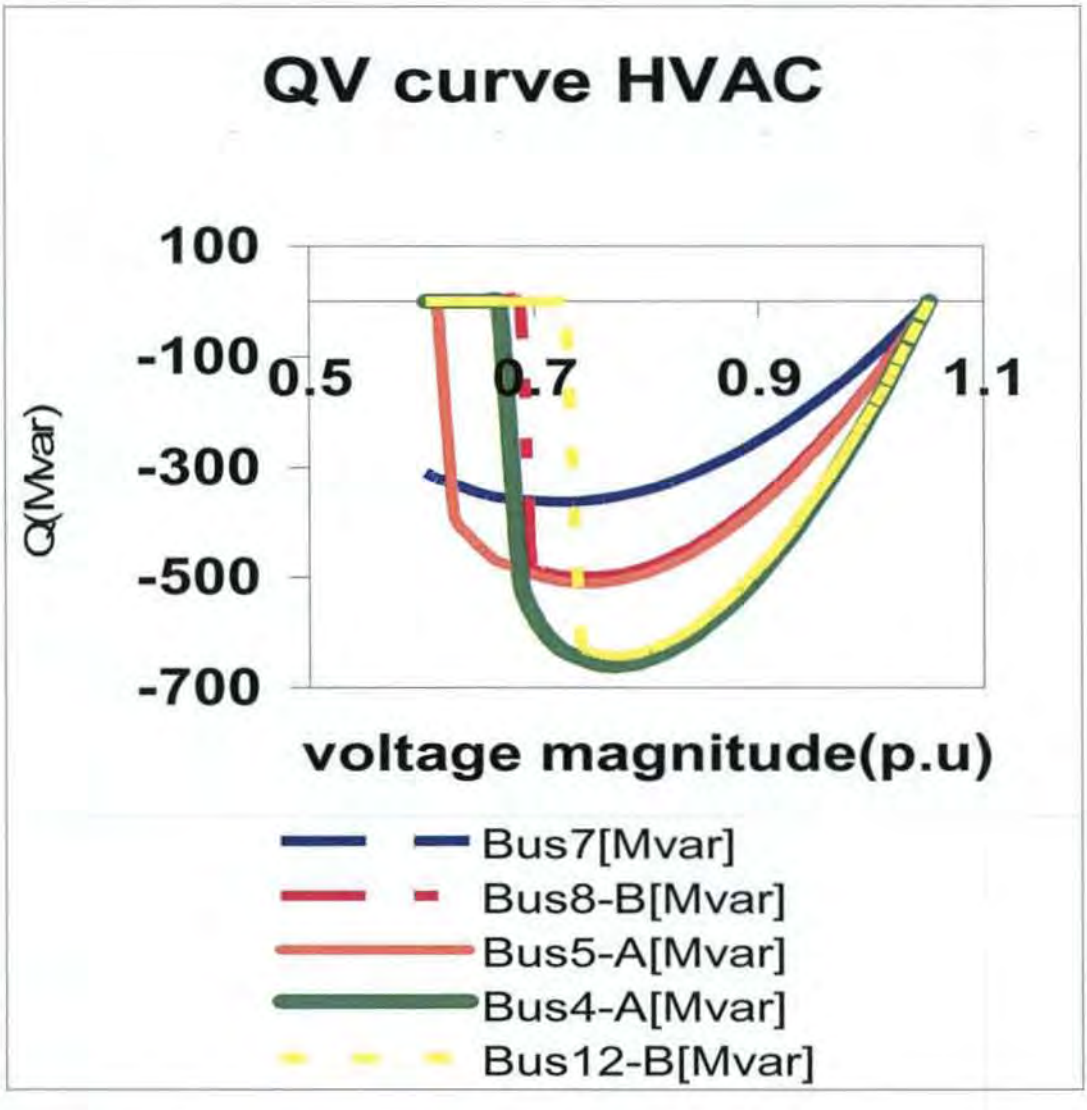

Figure 8.9 VQ Curve under HVAC

VP curve of HVAC system

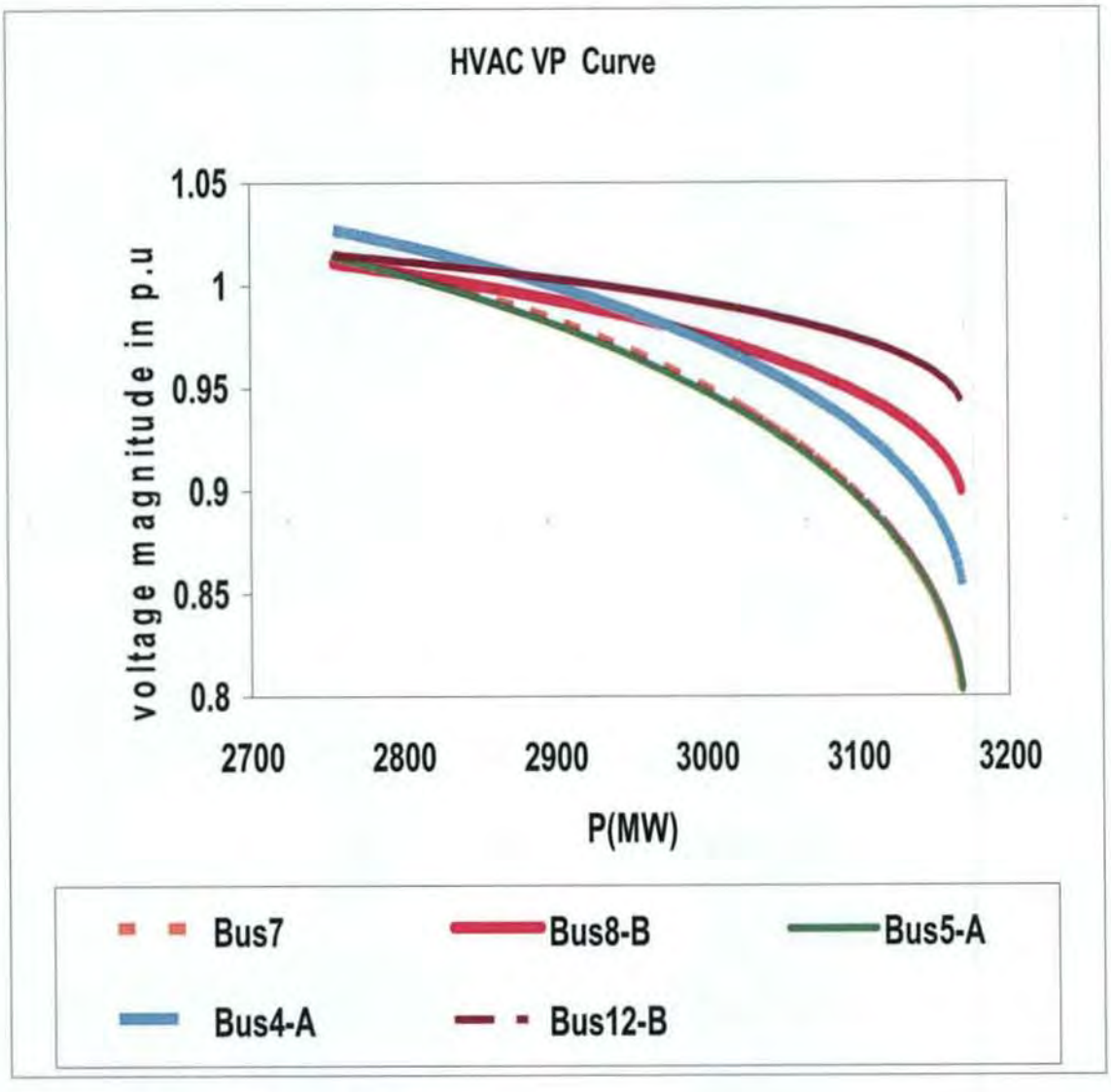

Figure 8.10 PV Curve under HVAC

Figure 8.10 show that the maximum MLP achievable under the HVAC was 3168.25MW. Further explanation is given when the results of various networks were compared.

8.2 Voltage stability Analysis for hybrid HVDC-HVAC system

8.2.1 Voltage profiles at steady-state

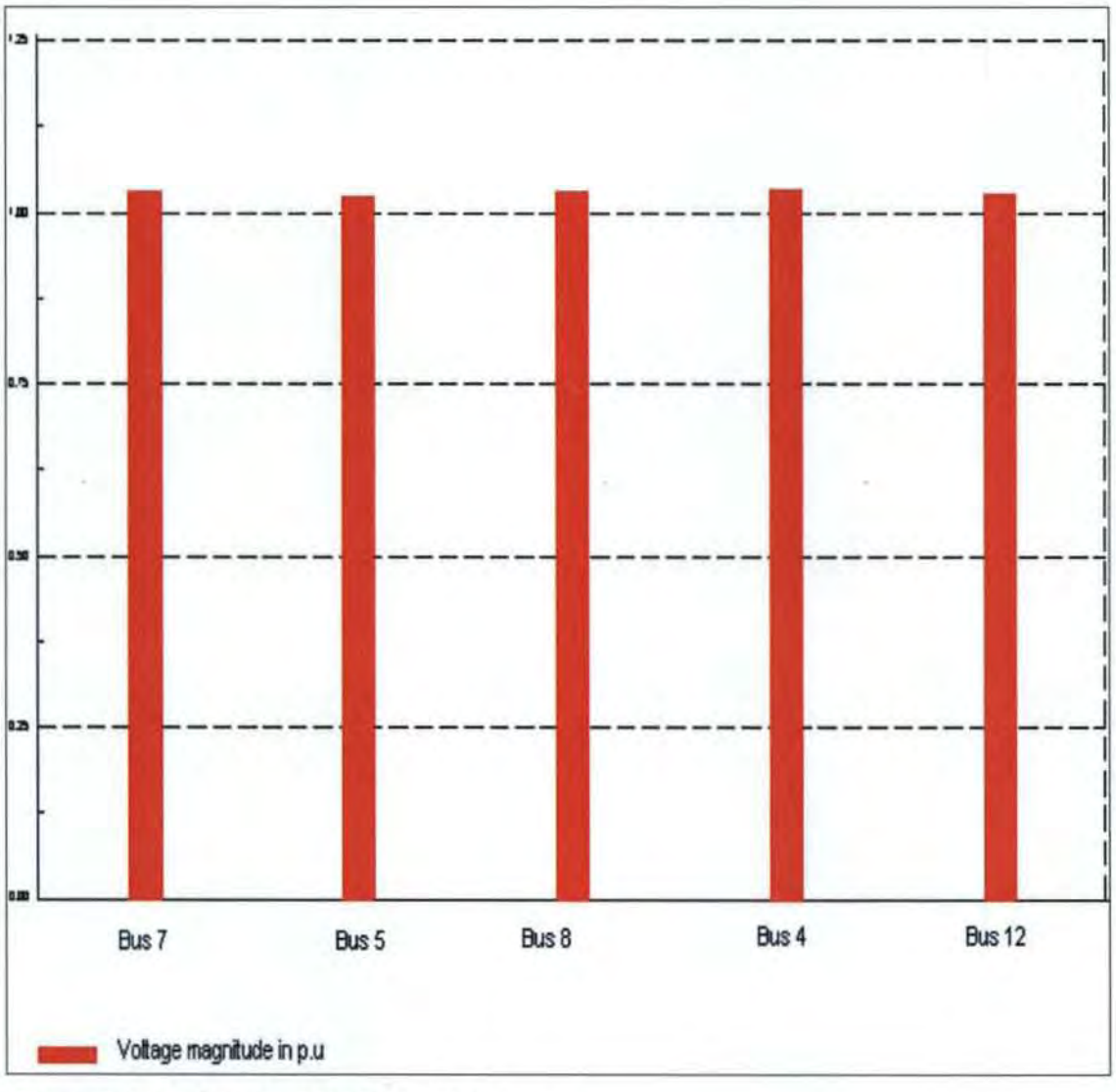

Figure 8.11 Voltage profile for HVDC System

The voltage magnitude was maintained at equilibrium from the sending end to the receiving end of the network, before the fault under the HVDC system.

8.2.2 Voltage angles after a three-phase fault

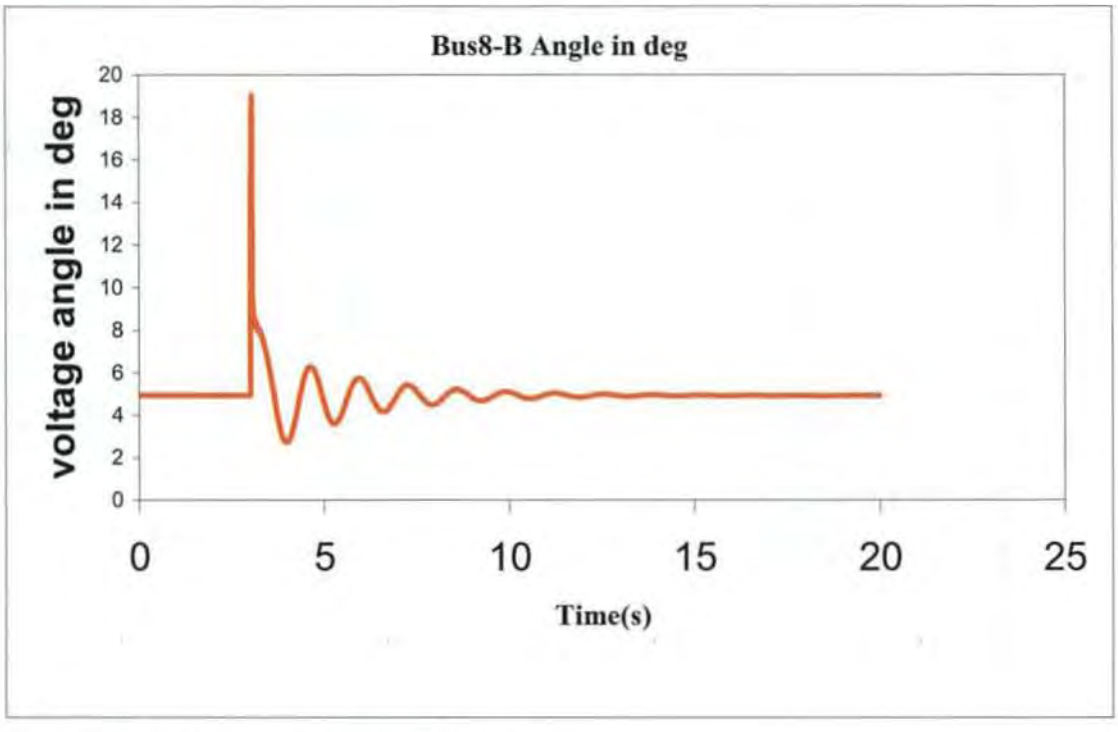

Figure 8.12 Voltage angle in deg for bus 5

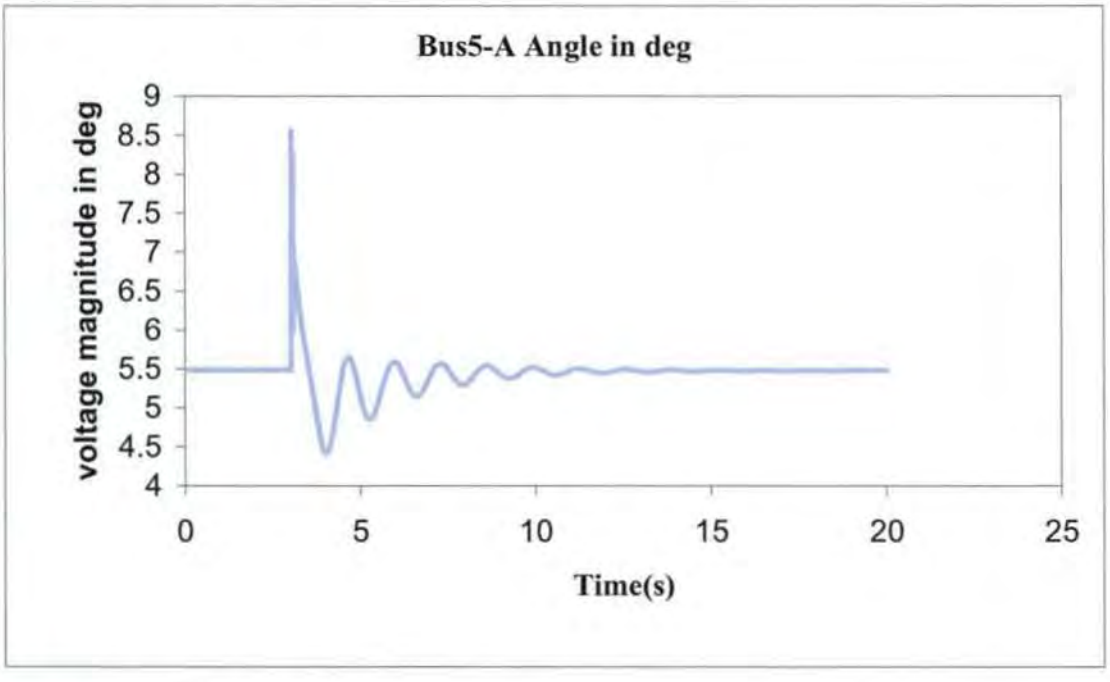

Figure 8.13 Voltage angle in deg for bus 8

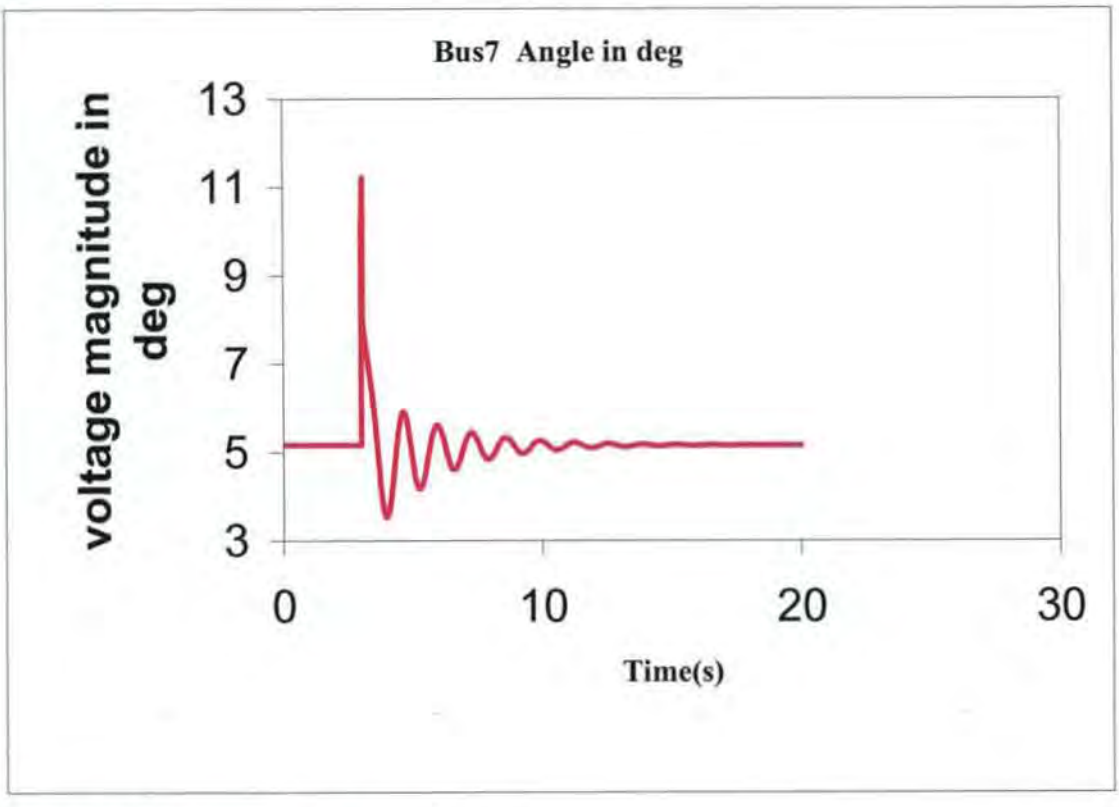

Figure 8.14 Voltage angle in deg for bus 7

Buses 5, 7, & 8 were also used to explain this system, before the perturbation bus 8 was operating at a steady state at voltage angle 4.4^0 deg as shown above in figure 8.12. During the fault but had an upswing to about 19^0 deg. It came down with decreasing amplitude to equilibrium after about 8 seconds. Bus 5 in figure 8.13 operated at a higher voltage angle at equilibrium with voltage angle of 5.5^0 deg, this bus was less perturbed by the fault than the rest, at the first swing it rose to about 8.5^0 deg and regain equilibrium in less than 7 seconds after the fault. In figure 8.14 Bus 7 operated from 5^0 deg at rest before the fault, it rose to about 11^0 during the fault and later regained equilibrium after about 10 seconds.

8.2.3 Voltage magnitude

Figures 8.15-8.17 shows the voltage magnitudes of buses 8, 5, and 7 after the three-phase fault in the network

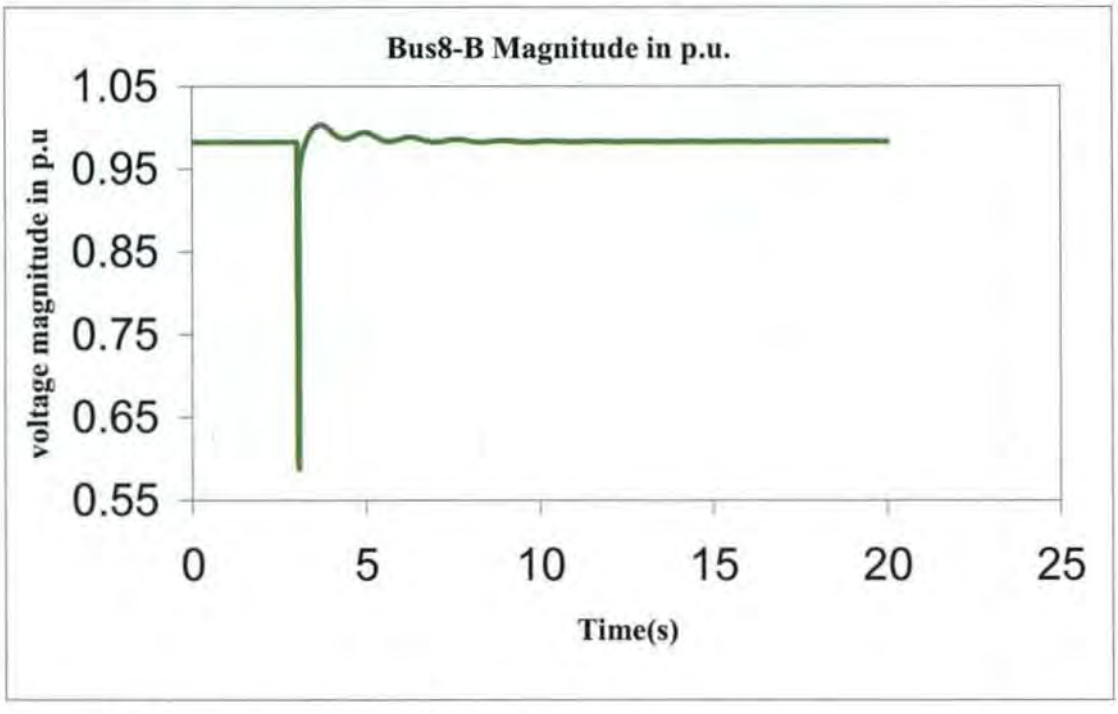

Figure 8.15 Voltage magnitude (p.u) bus 8

Bus 8 in figure 8.15 shows that the voltage magnitude dipped from 0.95 p.u operating condition to about 0.75 p.u during the fault in the first swing and regained equilibrium after about 3-4 seconds, again bus 5 shown in figure 8.17 was the lest perturbed during the fault, under steady state it operated with 1.0 p.u and dipped to 0.75 p.u it also settled after about 3 seconds. From figure 8.16: The voltage magnitude of bus 7 was more perturbed by the fault, although operating at a voltage magnitude of 1.0 p.u at steady state it dipped to 0.4 p.u during the fault but regained equilibrium in less than 2 seconds,.

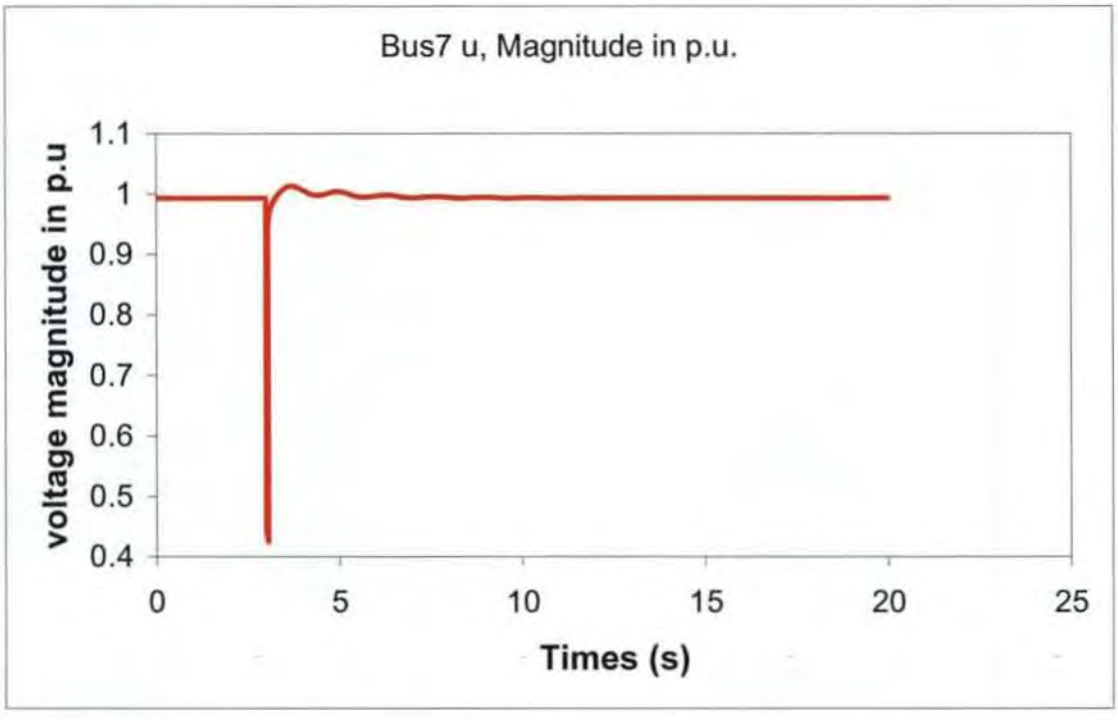

Figure 8.16 Voltage magnitude (p.u) bus 7

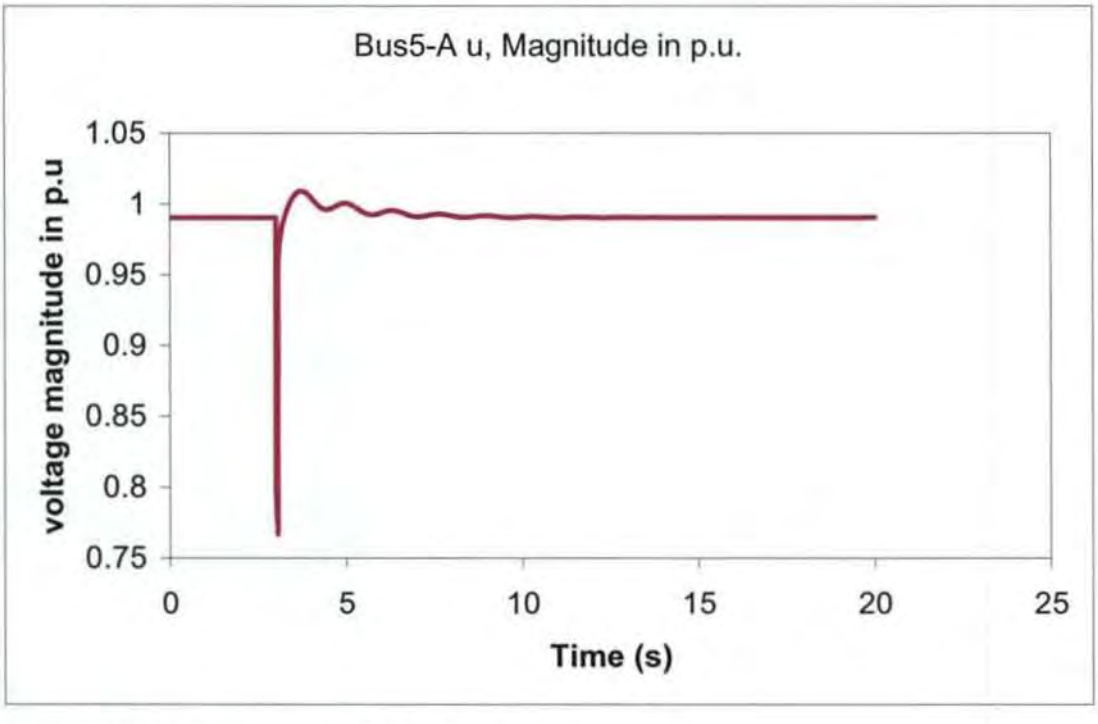

Figure 8.17 Voltage magnitude (p.u) bus 5

8.2.4 VP curve and QV curves for voltage stability of the hybrid HVDC-HVAC network

Figure 8.18: Shows the sensitivity of the system to voltage collapse, bus 7 the effects of the insufficient the reactive power is shown in buses 7, 5 through 5 this more pronounced in these buses due to the fact that these buses are closer to the HVDC converter station. The HVDC adsorbs reactive power and the control actions of the converter station results in insufficient supply of reactive power leading to voltage collapse in these buses.

QV curve for HVDC-HVAC network

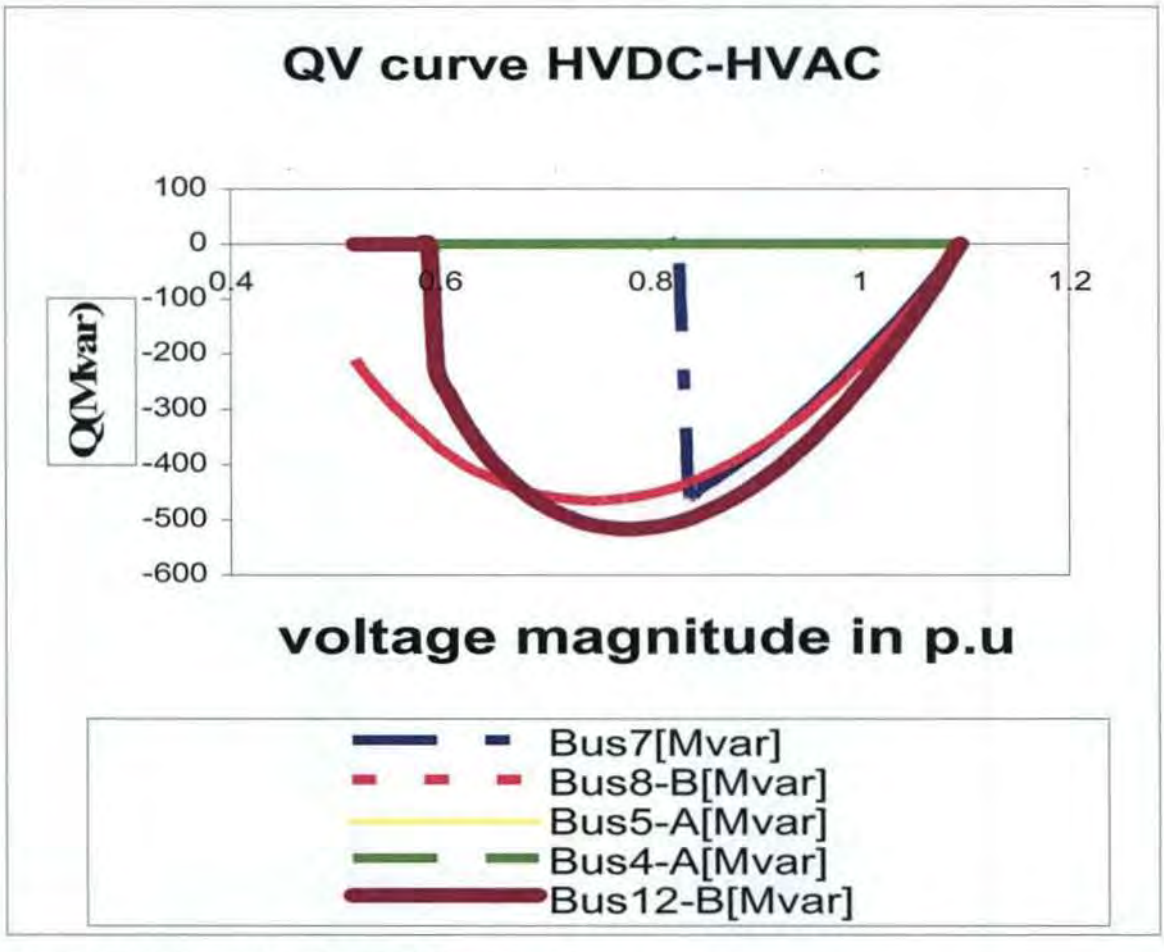

Figure 8.18 QV curve under HVDC Interaction

VP curve for HVDC-HVAC network

Figure 8.19 below shows the VP curves for buses 5, 7, 8, 4 and 12, under the hybrid HVAC-HVDC network.

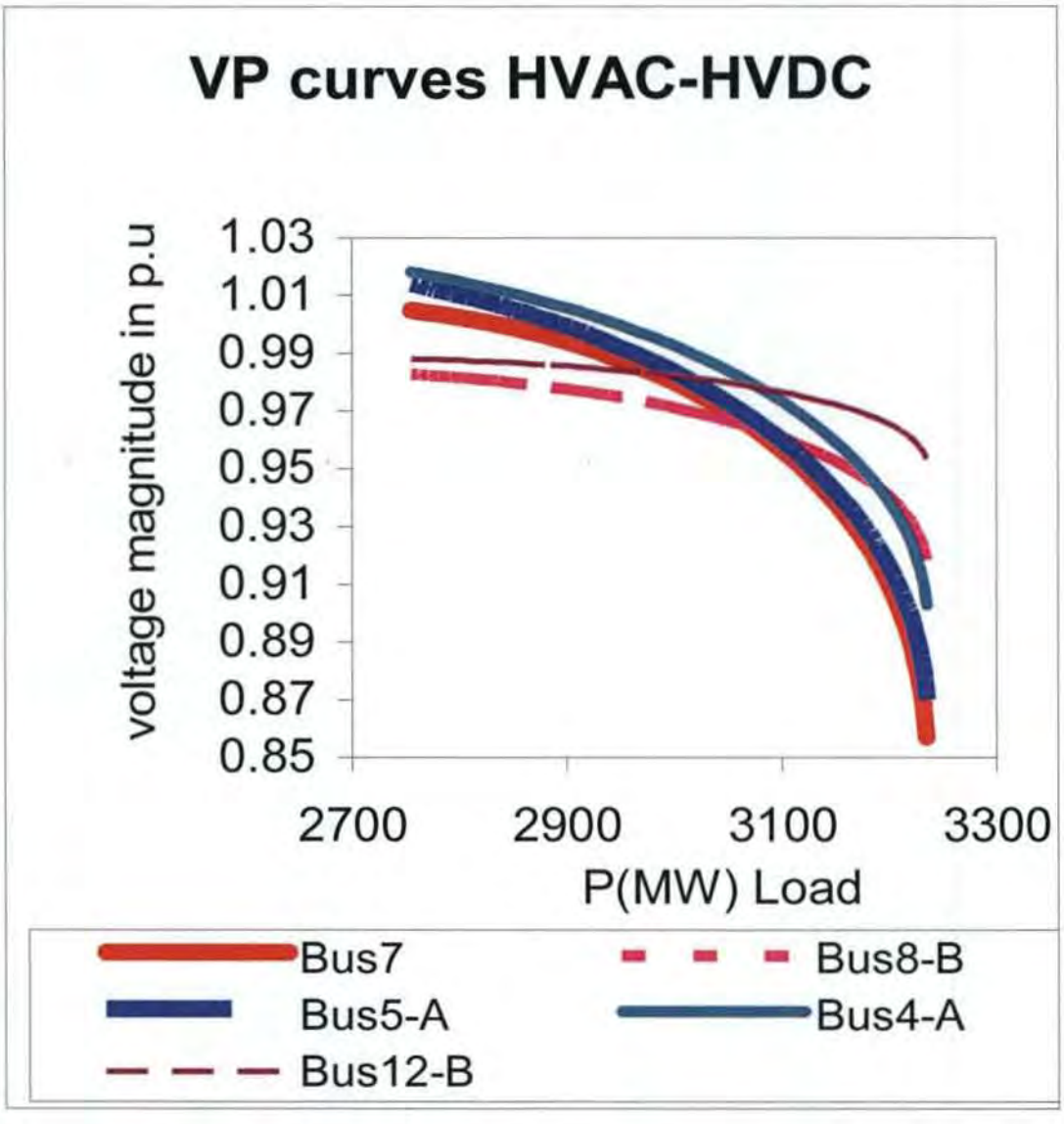

Figure 8.19 PV curve under HVDC Interaction

Figure 8.19: Shows the maximum loading points for buses 7, 5, 12, 8 and 4 The MLP achievable here was 3234.37MW. Further explanation is given later in the study.

8.3 Voltage stability study for the hybrid HVAC-VSC-HVDC system

This section shows the voltage, the voltage profile, voltage magnitude, voltage angle, as well as the PV and QV curves for the hybrid HVAC-VSC-HVDC system.

8.3.1 Voltage profiles at steady state

Figure 8.20 shows the voltage profile under the HVAC-VSC-HVDC network. Instead of depletion of voltage at the buses at the middle of the transmission line the voltage magnitude actually increased as shown in buses 7 & 8 as was the case with the HVAC link figure 8.2 refers, this is due to the ability of the VSC-HVDC to control active and reactive power independently [2].

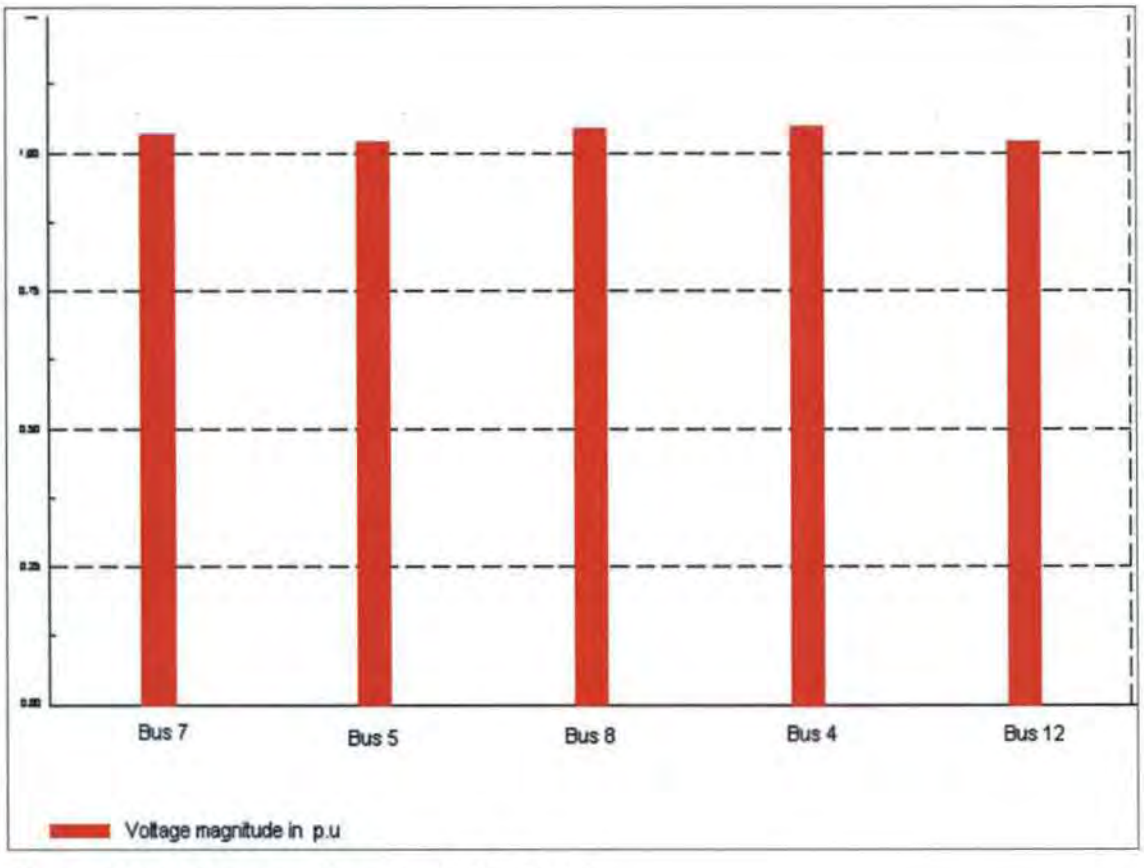

Figure 8.20 Voltage profile under VSC-HVDC

8.3.2 Voltage Magnitude

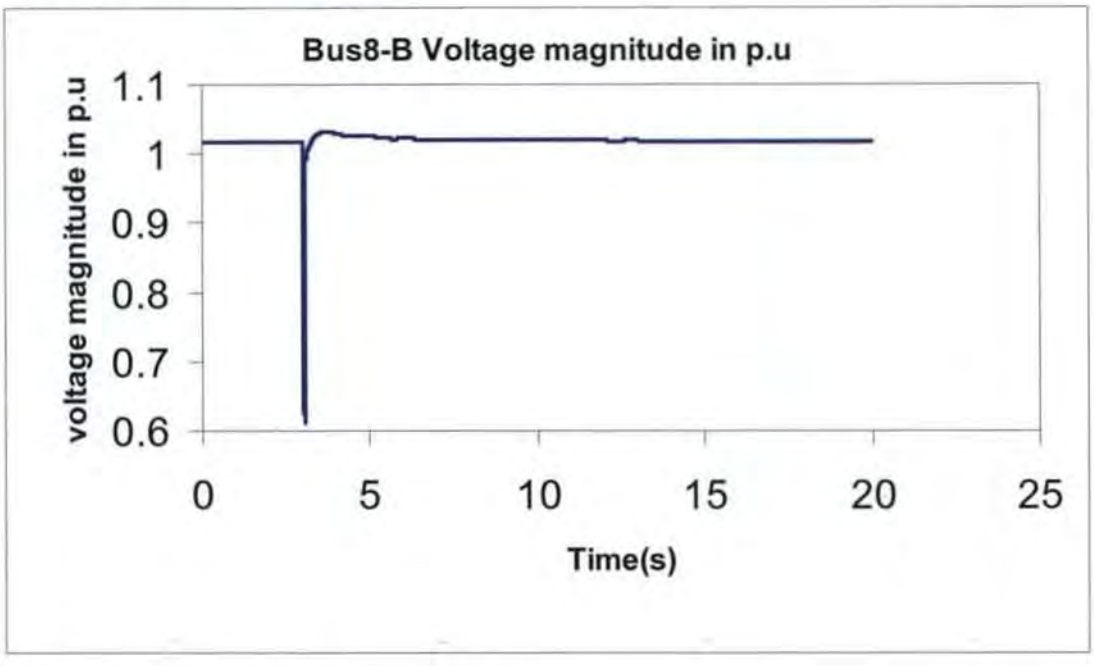

Figure 8.21 Voltage magnitude (p.u) for bus 8

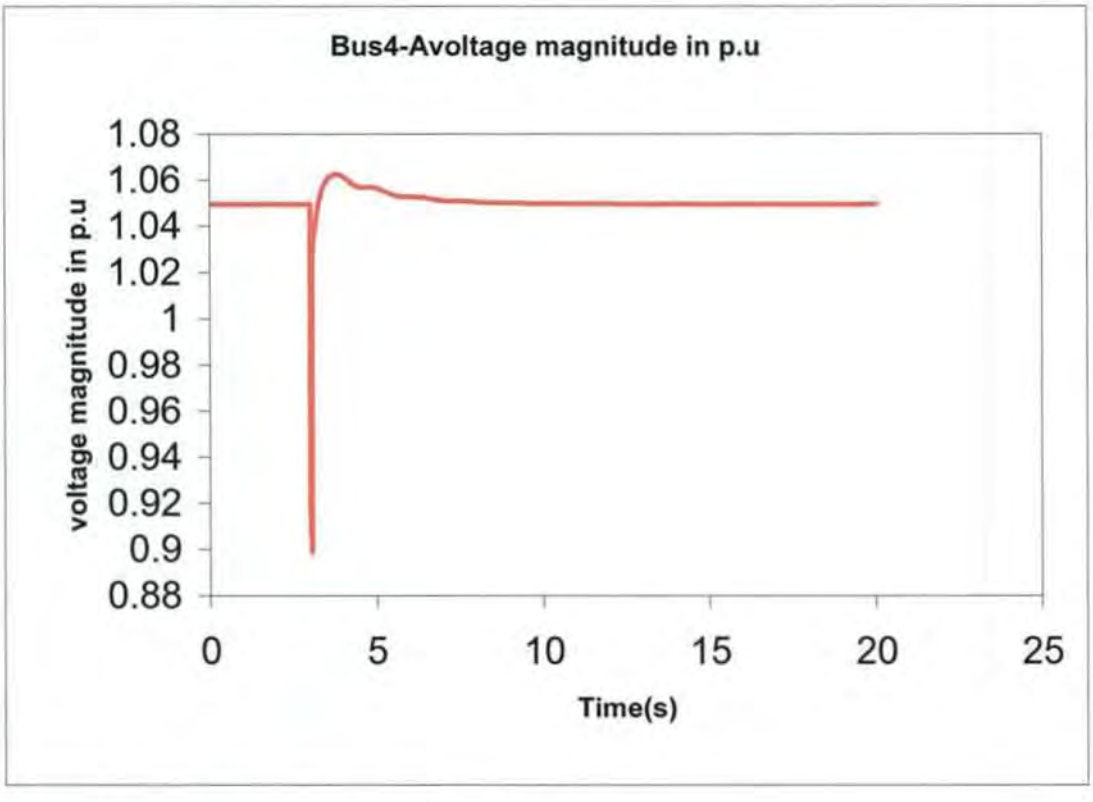

Figure 8.22 Voltage magnitude (p.u) for bus 4

The voltage magnitude of buses 5, 7and 8 have been chosen here for the analysis of the voltage magnitude under the HVAC-VSC/HVDC hybrid network. The voltage magnitude in figure 8.21 shows that bus 8 at rest before the fault was at 1.0 5 p.u, but dipped to 0.6 p.u during the fault and settled to equilibrium in about 3 seconds after the fault. In bus 7 figure 8.23 at equilibrium the voltage magnitude was 1.05 p.u also before the fault it dropped to 0.45 p.u during the fault and returned to steady state in less than 3 seconds after the fault. Figure 8.25 shows that in bus 5 the voltage magnitude was 1.05p.u before the fault but dipped to 0.85 p.u during the fault and also settles to equilibrium in less than 3 seconds likewise. From the results VSC-HVDC maintained the same voltage profile from one end of the network to another and the effect of the fault was more felt in the buses closer to the fault. Therefore the voltage magnitude was stable in the hybrid system following the three-phase fault.

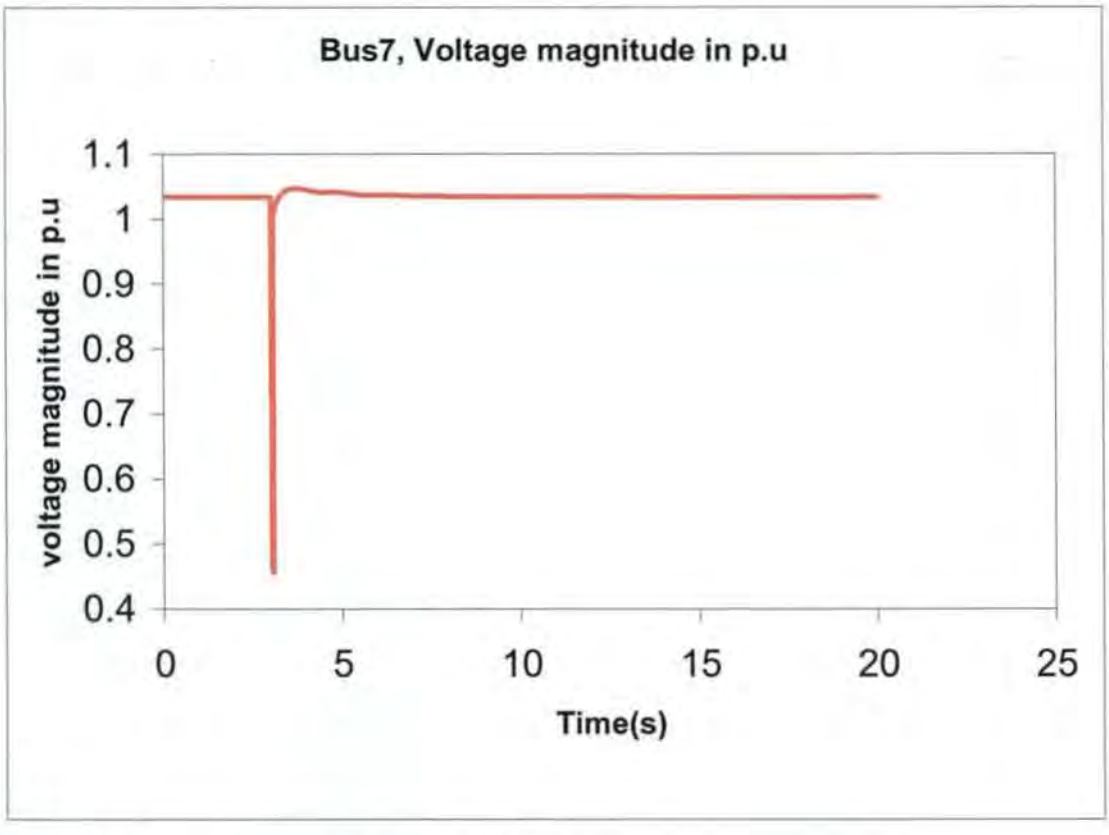

Figure 8.23 Voltage magnitude (p.u) for bus7

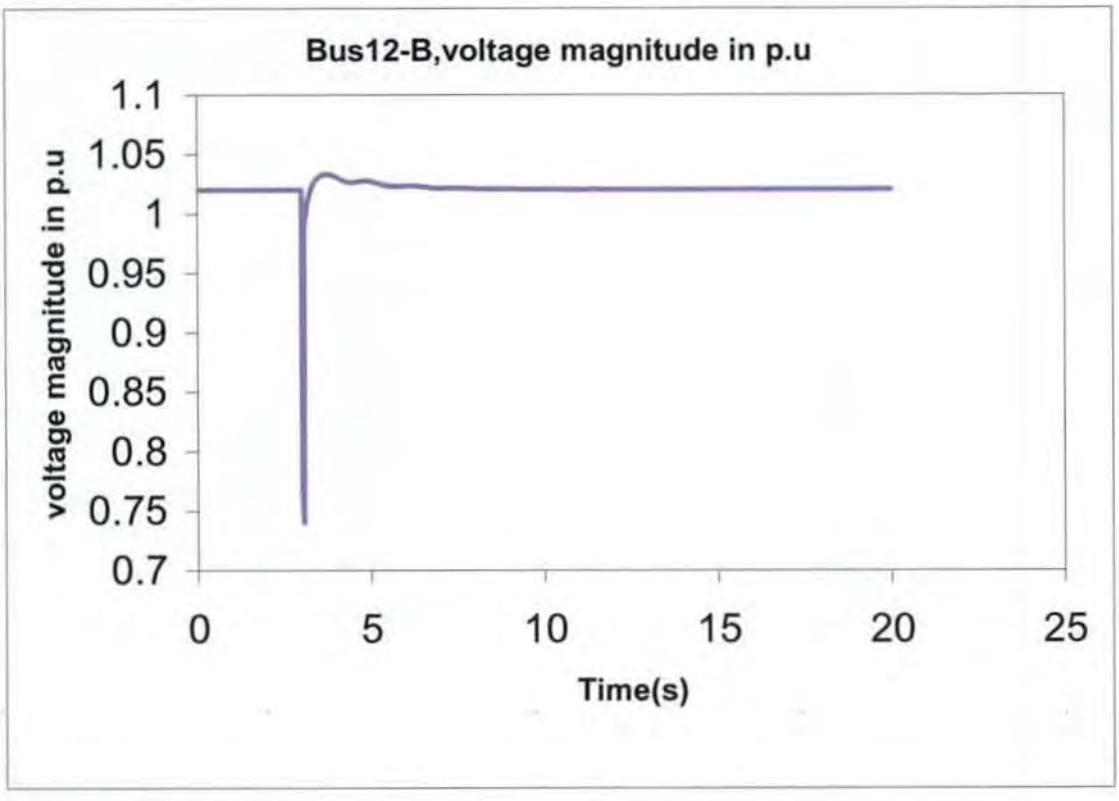

Figure 8.24 Voltage magnitude (p.u) for bus12

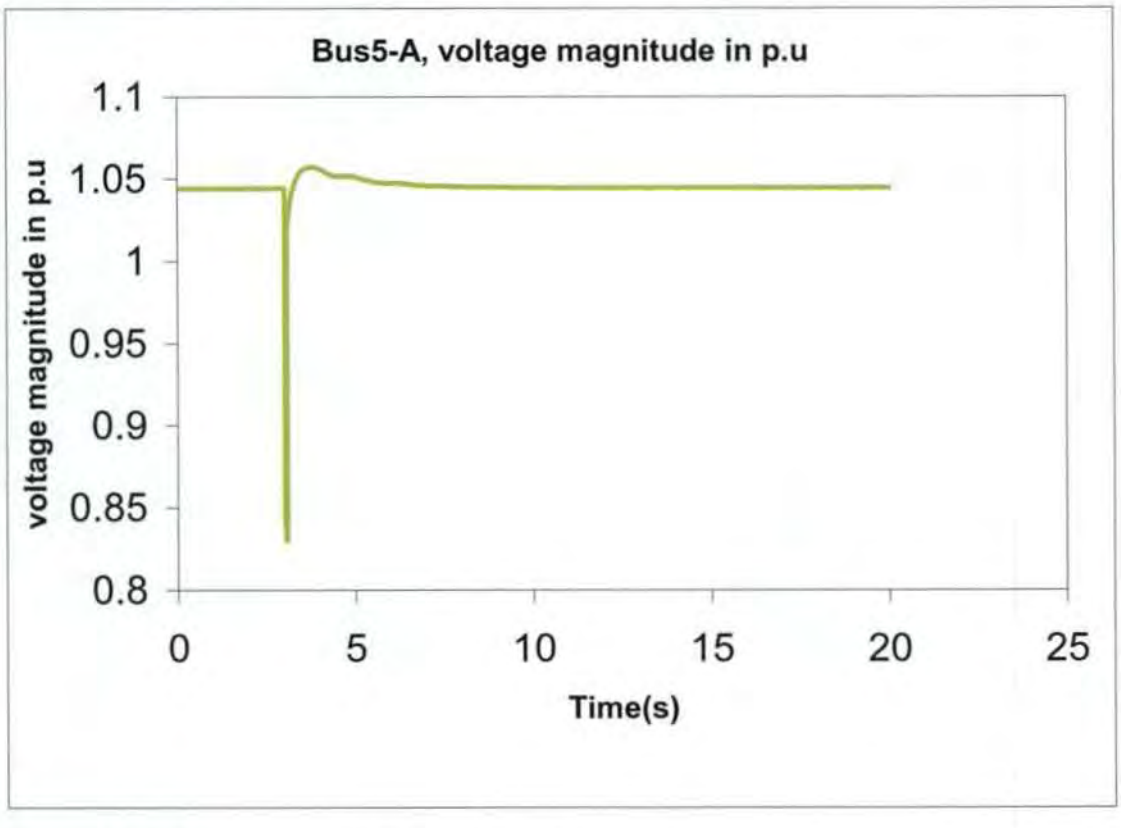

Figure 8.25 Voltage magnitude (p.u) for bus 5

8.3.3 Voltage angle VSC-HVDC-HVAC

Figure 8.27 below shows the bus 7 voltage angle, the voltage angle of bus 7 and bus 8 in figure 8.26 are the most affected buses within the link from area A to area B bus 7 at steady state was almost at 1^0 deg but increased to 10^0 during the first swing but was quick to regain steady state in less than 3 seconds after the fault. Bus 8 at steady state was operating at -5^0 before the fault but rose to 5^0 deg during the fault, it settled to a steady state in less than 4 seconds after the fault. Bus 5 in figure 8.3.9 before the fault was at 5.5^0 deg it rose to about 11^0 during the fault and settles in less than 7 seconds after the fault. From the above the systems' voltage angle is said to be stable under the transient disturbance. The voltage angle for buses 4 and 12 are given in the appendix E: Figure E.2 and Figure E.1 respectively.

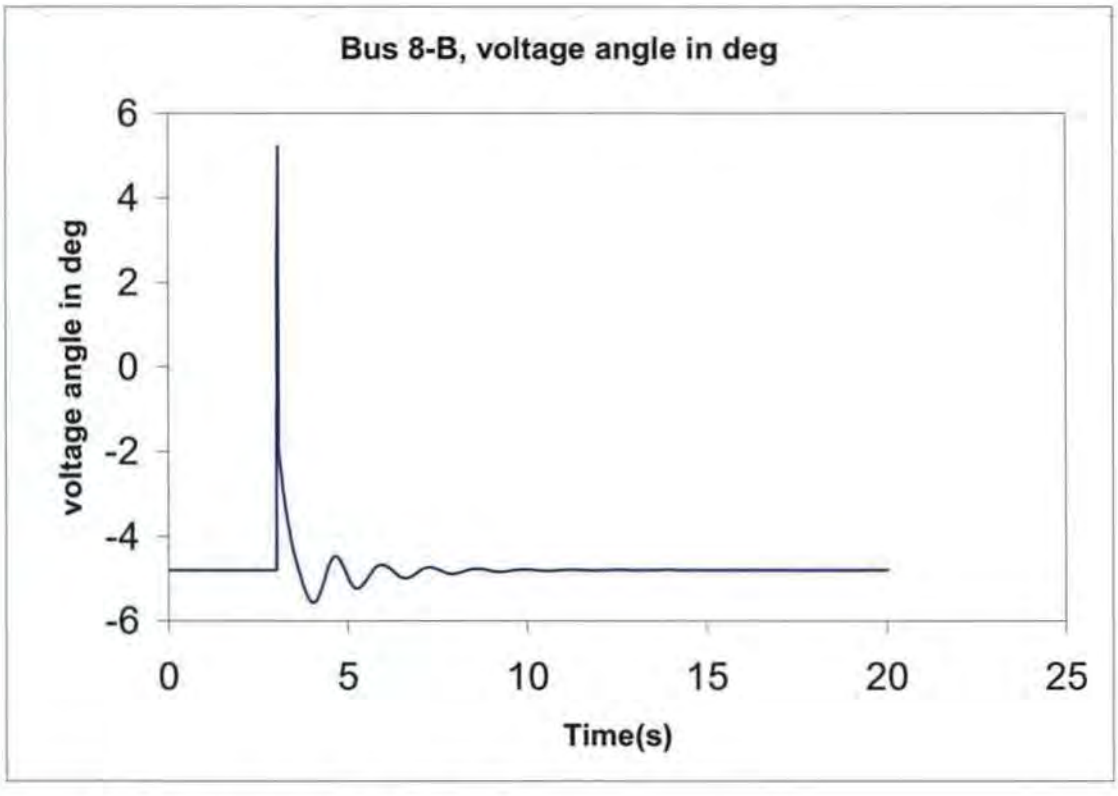

Figure 8.26 Voltage angle in rad for bus 8

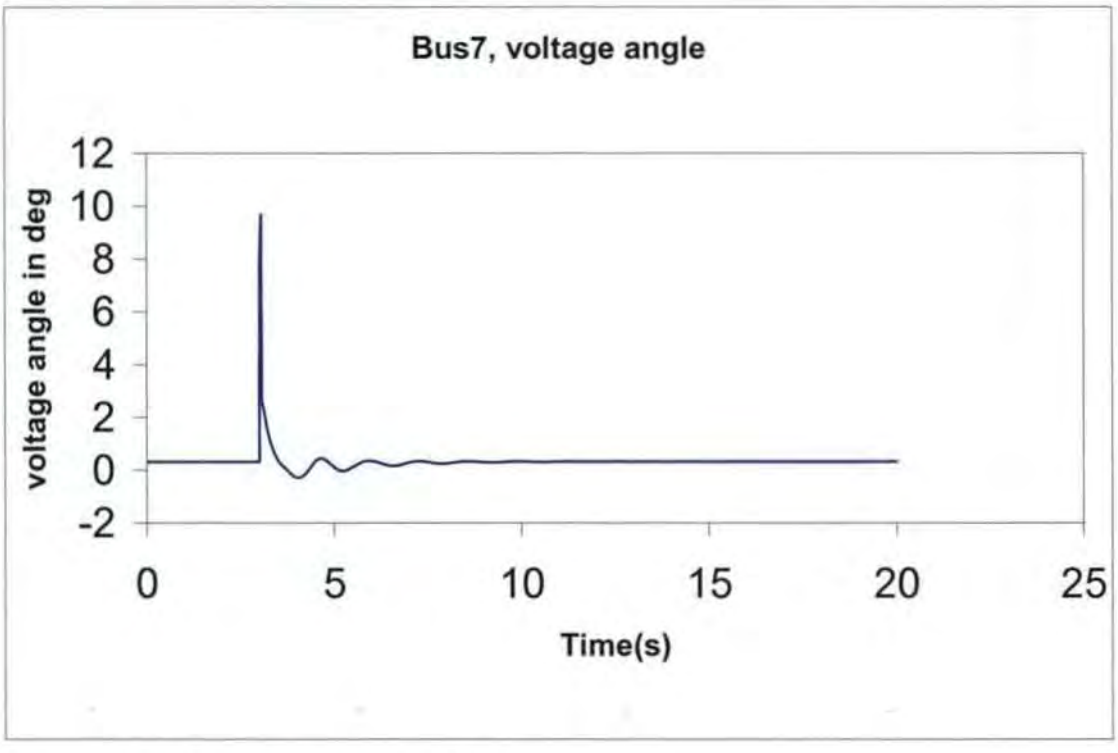

Figure 8.27 Voltage angle in rad for bus 7

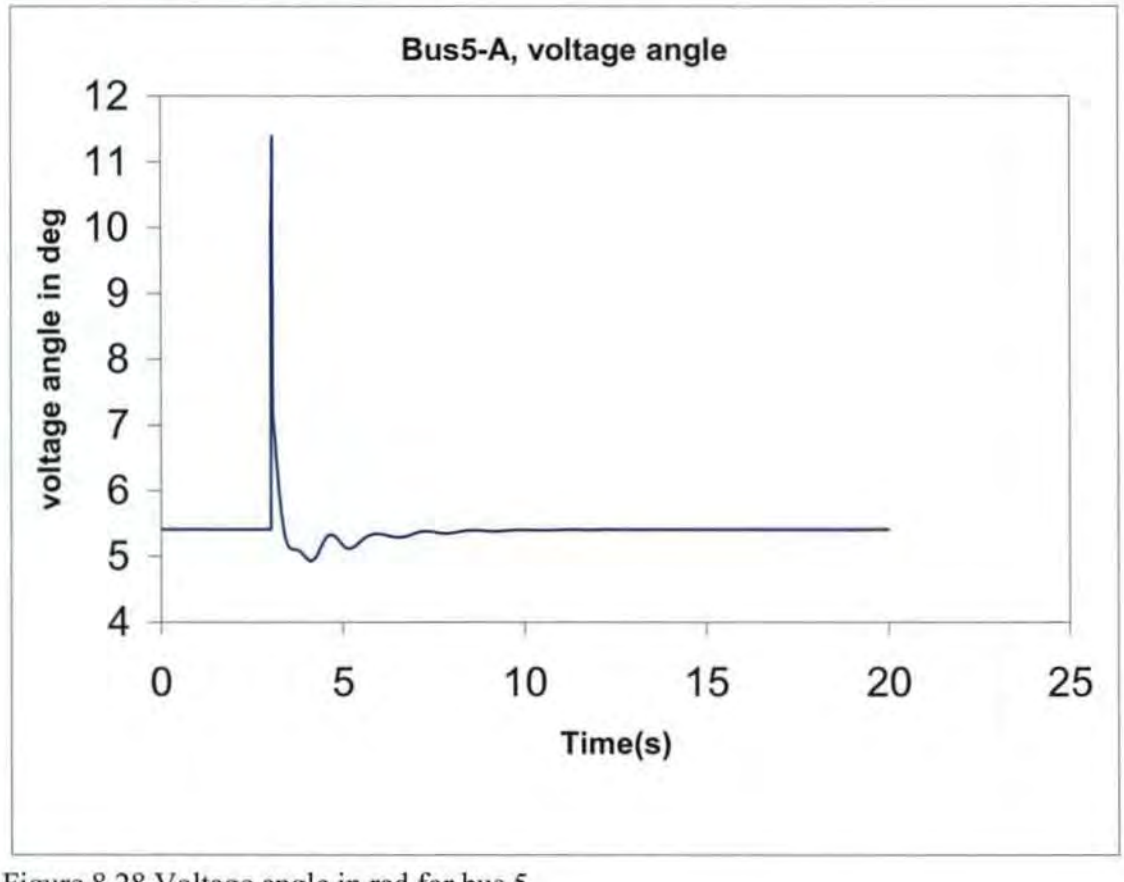

Figure 8.28 Voltage angle in rad for bus 5

8.3.4 VP curve and QV curve for voltage stability of VSC-HVDC

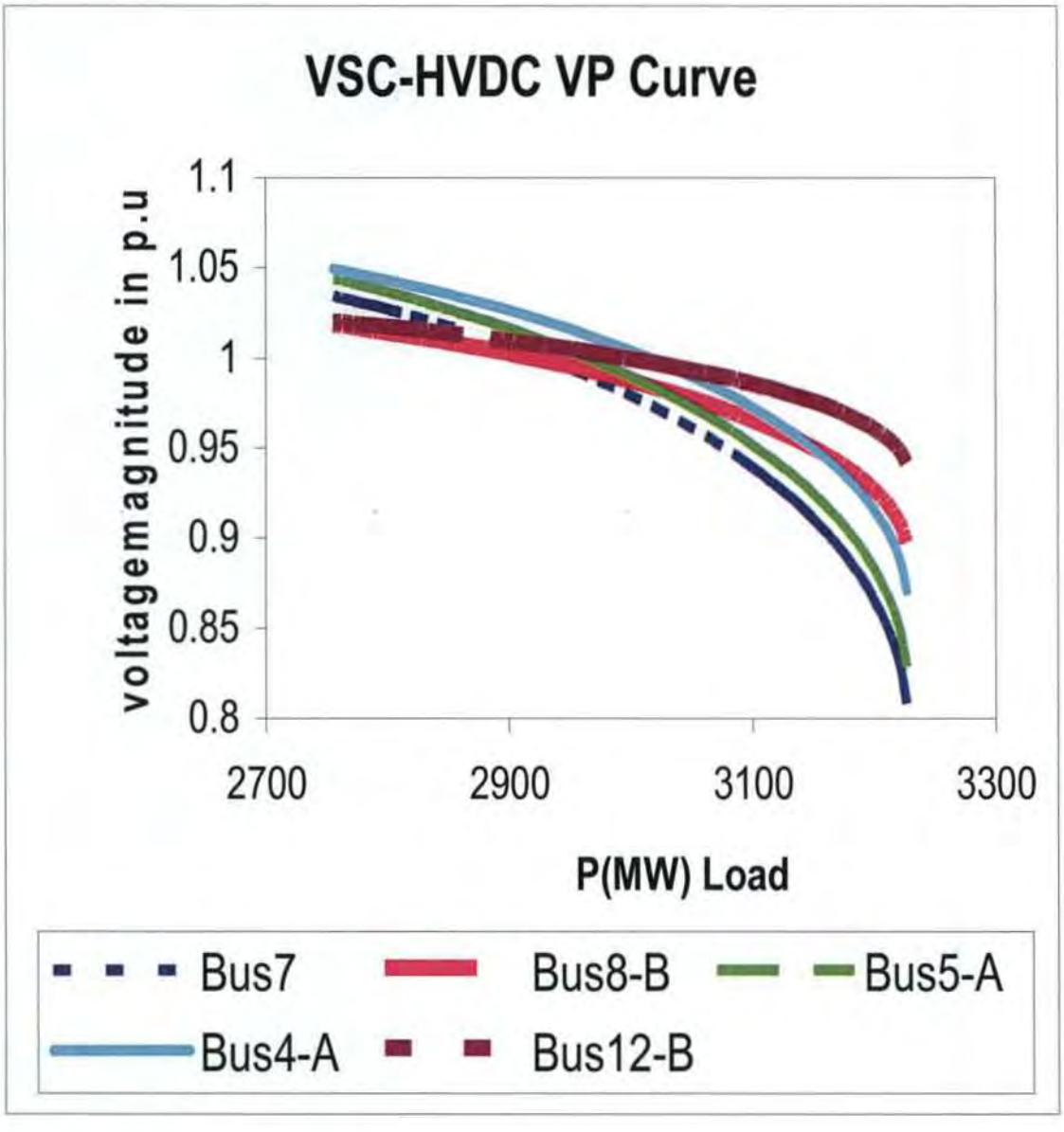

Figure 8.29 PV Curve under VSC-HVDC Interaction

Figure 8.29 above shows the MLP under the VSC-HVDC network transmission and it was found to be 3226.11MW.

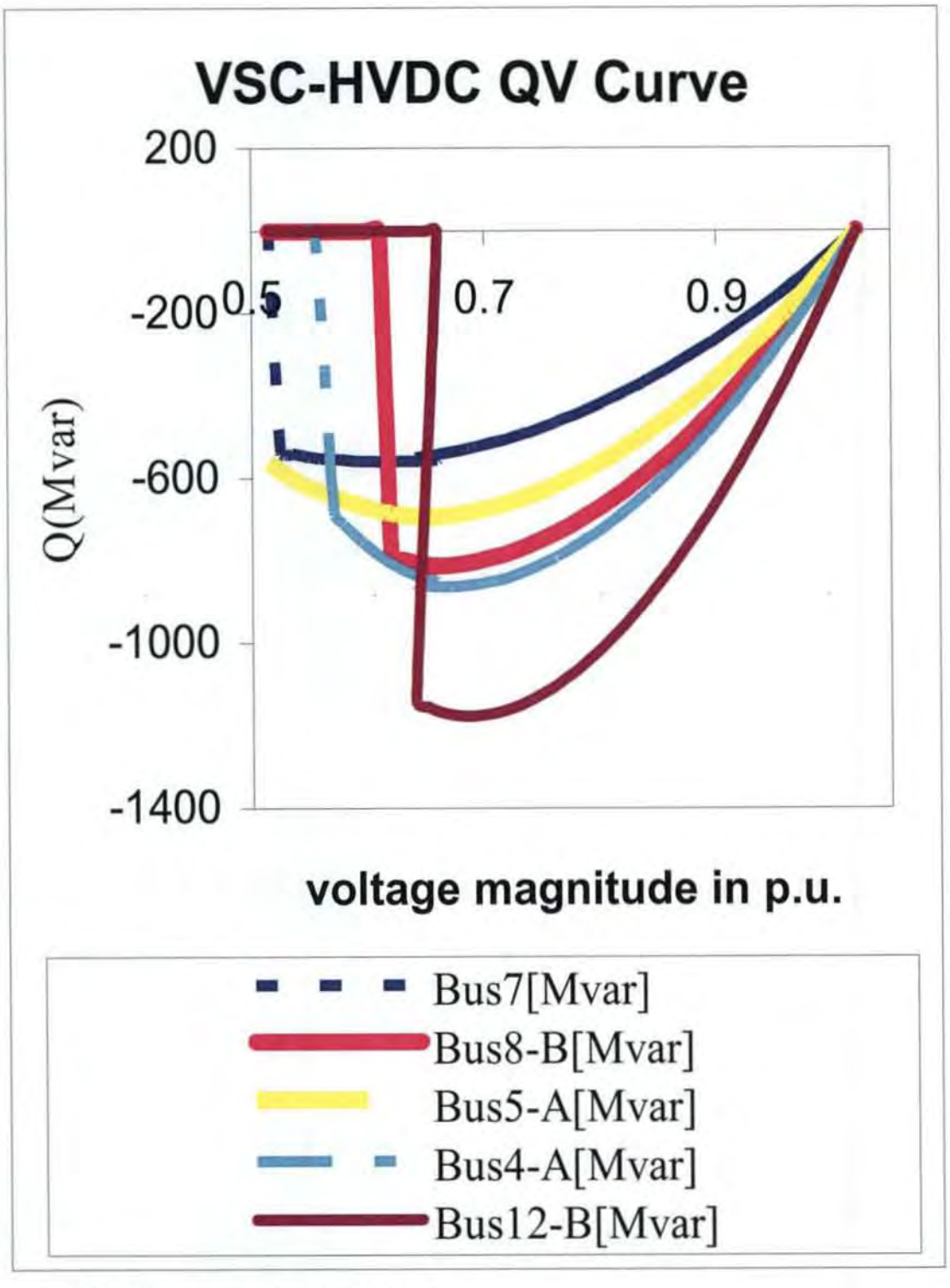

Figure 8.30 VQ Curve under VSC-HVDC

In figure 8.30 the ability of the VSC-HVDC to overcome the disabilities of interconnections with a HVAC system is shown here, when compared with the hybrid HVAC-HVDC (see figure 8.18). Buses 7 and 8 were able to overcome the voltage

collapse due to the fact that VSC-HVDC has independent control of the active and reactive power. Unlike the HVDC it does not absorb reactive power it generates it instead. The voltages in all the buses in the system did not collapse as a result of the step increase in the load level.

8.4 Comparison of results of the voltage studies of the three transmission schemes

8.4.1 Voltage angles of the three transmission schemes

Figure 8.31 below shows the responses of bus 7 on voltage angle under the three transmission schemes namely, HVAC, HVAC-HVDC and VSC/HVDC-HVAC networks.

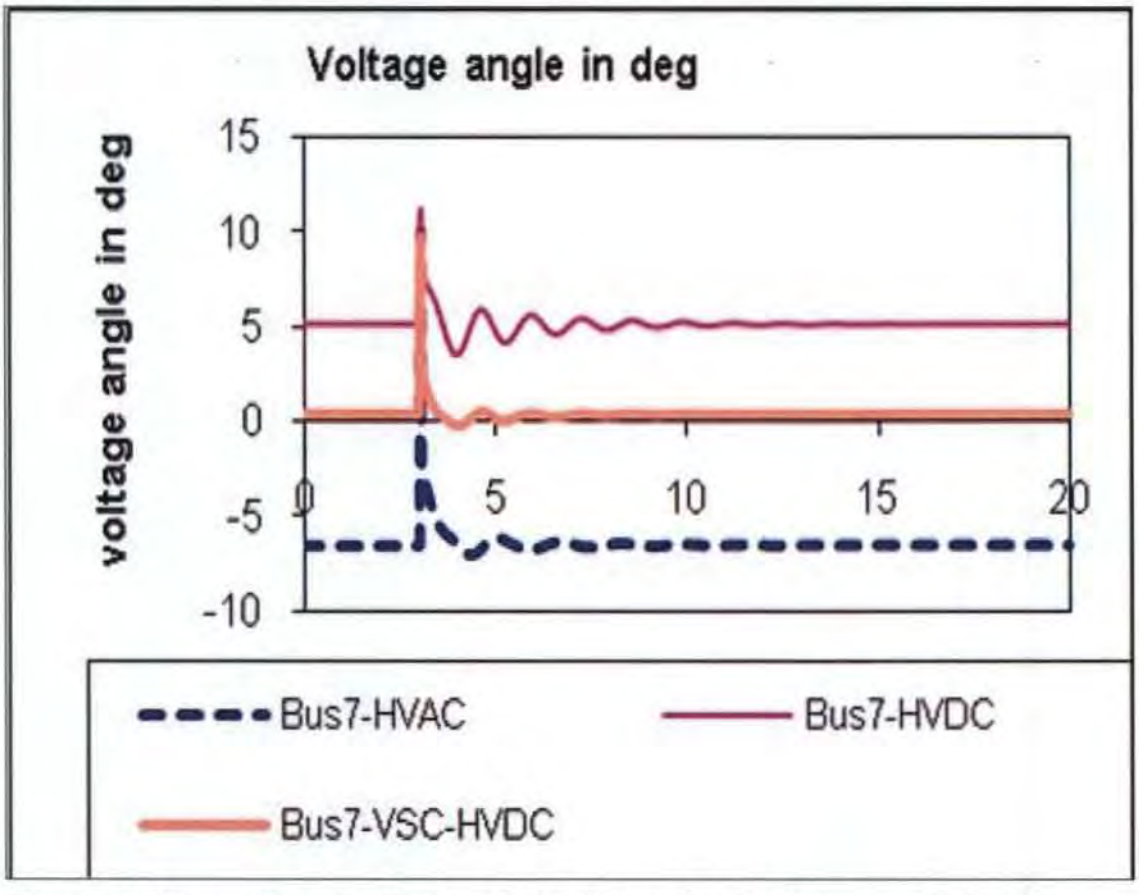

Figure 8.31 Comparison of voltage angle for Bus7 under the three transmission schemes

8.4.2 Analysis of Voltage angles of the three transmission schemes

The VSC-HVDC has the advantage of being able to almost instantly change the active and reactive power independently [60] and [61] it behaves like an ideal generator to the grid with flexible working point and no inertia. This capability helps it in improving the Voltage stability as shown in the figures above. The voltage stability of the system was investigated using Voltage angle, Voltage magnitude, PV and QV curves for the analysis. As shown in Figure 9.19 the voltage angle of VSC-HVDC operating at about 2^0 was able to come to a steady state within 3 seconds after perturbation. On the other hand, HVDC, operating at about 6^0 with a settling time of about 7-8 seconds after the fault and the HVAC operating at about -7.50 settles at about 11 seconds after the fault. This shows the robustness of VSC-HVDC over HVDC operating at a lower voltage angle to deliver the same amount of power from Area A to Area B in comparison with the other networks.

8.4.3 Voltage magnitudes of the three transmission schemes

Figure 8.32 below shows the responses of bus 7 on voltage magnitude under the three transmission schemes namely, HVAC, HVAC-HVDC and VSC/HVDC-HVAC networks. Explanations are given below in section.

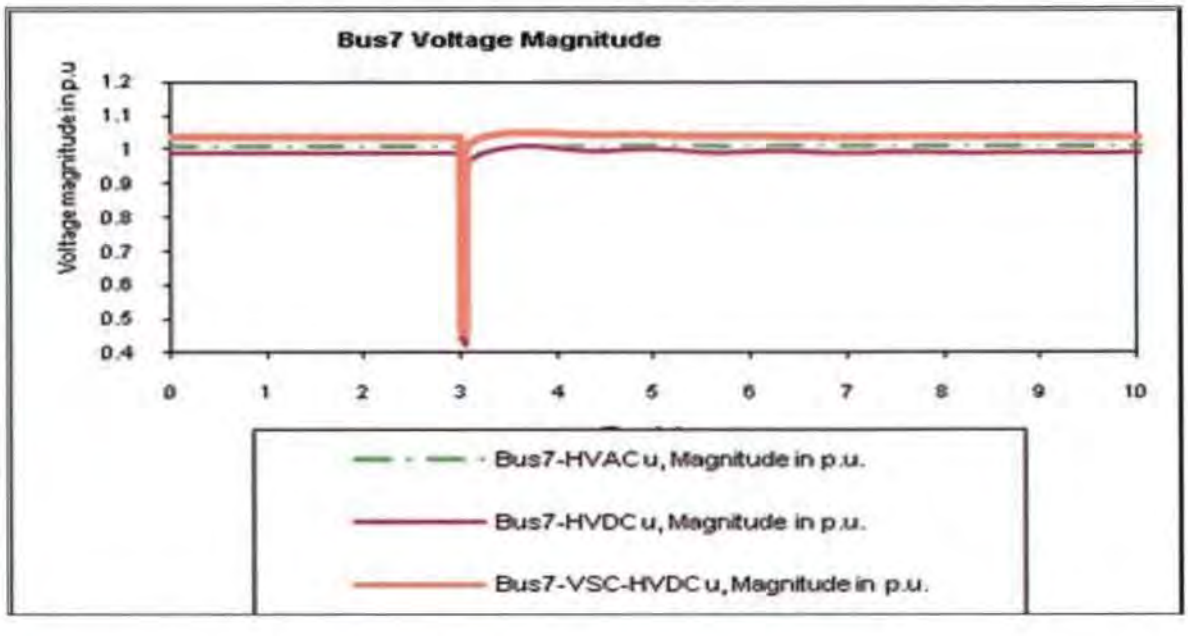

Figure 8.32 Comparison of voltage magnitude at Bus7

8.4.4 Analysis of results of voltage magnitude of the three transmission schemes

Figure 9.20 shows the voltage magnitude of VSC-HVDC to be about 1.05 p.u at steady state and dipped to about 0.45 p.u during the fault, it came to steady state after the fault in about 2 seconds, the HVAC voltage magnitude was 1.0 p.u and came to a steady state after 4 seconds of perturbation, also the HVDC voltage magnitude was about 0.98 p.u the difference is as a result of reactive power consumption by the converter stations. Although, the voltage magnitude of the HVDC system was lower here it maintains the same voltage profile from the sending end to the receiving end, under normal working condition.

8.4.5 Comparison of the results of PV and VQ curves from the three transmission schemes

8.4.5.1 Analysis of VQ curves

Figures 8.10 (HVAC), 8.219 (HVDC) and 8.29 (VSC-HVDC) PV Curves and Figures 8.9 (HVAC), 8.18 (HVDC) and 8.30 (VSC-HVDC shows the VQ Curves for the voltage stability study, they were used to investigate the sensitivity to voltage collapse and the maximum loading points (MLP) respectively on buses 4,5,7,8 and 12 and the result are as follows: Figure 8.18 shows HVDC VQ Curve, in this bus7 has the highest sensitivity to voltage instability with a critical point of 0.8353p.u (voltage magnitude), -456.13 Mvar (reactive power). The voltage collapsed at this point due to insufficient reactive power, (this bus is often recommended for the location of compensators like Static var compensators (SVC) and synchronous condensers,) the second critical bus is bus 8 (0.7453p.u, -464.6246Mvar) and the third critical bus is bus12 (0.7653p.u, -515.8819Mvar) in that order, buses 4 & 5 collapse due to the fact that reactive power flowed from Area B to Area A in the network, after the collapse of bus 7 no reactive power flowed in buses 4 and 5 Also, these two buses are located close to converter station on the AC side that consumes reactive power, the control action of the converter station affects the voltages and power transmitted by the buses close to the converter station, couple with the fact that HVDC converter stations absorbs reactive power. In a weak

system with low effective short circuit ratio (ESCR) changes in HVAC network or in HVDC transmission power could lead to voltage collapse necessitating the need for special control strategies i.e. dynamic reactive power control at the sensitive ac bus or near the HVDC substations [62] Figure 8.30 shows QV Curve under VSC-HVDC the curve shows the sensitivity of the buses to voltage collapse, like in the previous cases the sensitivity of bus 7 to voltage collapse was the highest with 0.6595 p.u and -534.02 Mvar and bus12 has the lowest with 0.700197 p.u, -1174.403 Mvar followed by bus 4 with 0.680197 p.u, -862.8795 Mvar. Figure 8.9: Shows the VQ Curve for HVAC system, bus 12 had the lowest sensitivity with 0.77102 p.u, -642.1245 Mvar and the highest was bus 7 with 0.7510 p.u, -359 Mvar followed by bus 4 with 0.7610p.u, -642.12Mvar.

8.4.5.2 Analysis of PV curves

The PV curve depicted in figure 8.19 shows the maximum loading points (MLP) on the buses. The MLP achieved with HVDC-HVAC network was 3234.37MW for all the buses (active power load) and bus 12 had the highest voltage magnitude at 0.9532p.u, followed by bus 8 (0.9142p.u), bus4 (0.9028p.u), bus5 (0.8679p.u) and bus 7 with (0.8572) this also shows that bus 7 at the centre has the lowest voltage profile and therefore, more prone to voltage instability. The VSC-HVDC -HVAC PV Curve in Figure 8.29 shows the MLP under VSC-HVDC, the MLP achieved here for all the buses was 3226.11MW (active load power), bus 12 have the highest voltage profile at 0.9415 p.u (voltage magnitude) and the lowest was bus7 at 0.8069 p.u. Figure 8.10: Shows PV Curve for HVAC system, the MLP achieved with HVAC was 3168.25 MW, and bus12 achieved this at 0.9431p.u and buses 7 & 5 achieved this with lowest voltage magnitude of 0.8028 p.u this makes them more susceptible to voltage instability during perturbation, because at this critical operating point their voltage profile is lower than the rest of the buses in the system, before getting to the (MLP) of the system.

Chapter 9

Study of the transient Stability of the power system

This chapter covers further studies on transient stability of the three transmission schemes same system as in chapter 8. At the end of the study, a comparison of results obtained from the three networks were made in order to understand the impact of the three transmission schemes, namely, HVAC, HVAC-HVDC and VSC-HVDC/HVAC on transient stability of power systems. The transient investigation was conducted by applying a three phase short circuit fault midway on line 9 (the upper link connecting bus 7 and bus 8) of the HVAC network, the fault was applied 3 seconds and cleared after 0.05 seconds as in previous cases (see figures 7.14, 7.7 and 8.1) for the network model used for the three transmission schemes.. The study shows that transient stability is enhanced with VSC-HVDC and HVDC links

9.1 Transient stability analysis of the HVDC network

In order to understand the impact of the three transmission schemes on the transient stability of the power systems network, further investigations were carried out using the three networks. The responses of the generators speed, active and reactive power, and rotor angle results obtained were compared and analyzed as shown below.

9.1.1 Active and reactive power generators G1 and G4 for HVAC system

Generators G1 in area A and generator G4 in area B of the network were chosen for this analysis, in order to understand the effects of the large fault on the two areas.

From the result below in figure 9.2 generator G4 which is closer to the fault during the disturbance was affected most during the transient disturbance judging by the impact on the active and reactive power as shown below, the first swing of the active power due to the fault was downwards from 700 MW to about 300 MW and settles after 3 seconds, the reactive power had a surge from 200 Mvar to 850 Mvar and settles after 2 seconds following the fault, the effect of the fault on the reactive power was more severe. In figure 9.1 generator G1 dipped from 700 MW to 400 MW and the reactive had little surge

from 10 Mvar to about 250 Mvar both the reactive and active power settled in less than 3 seconds. Therefore the power flow was stable following the fault.

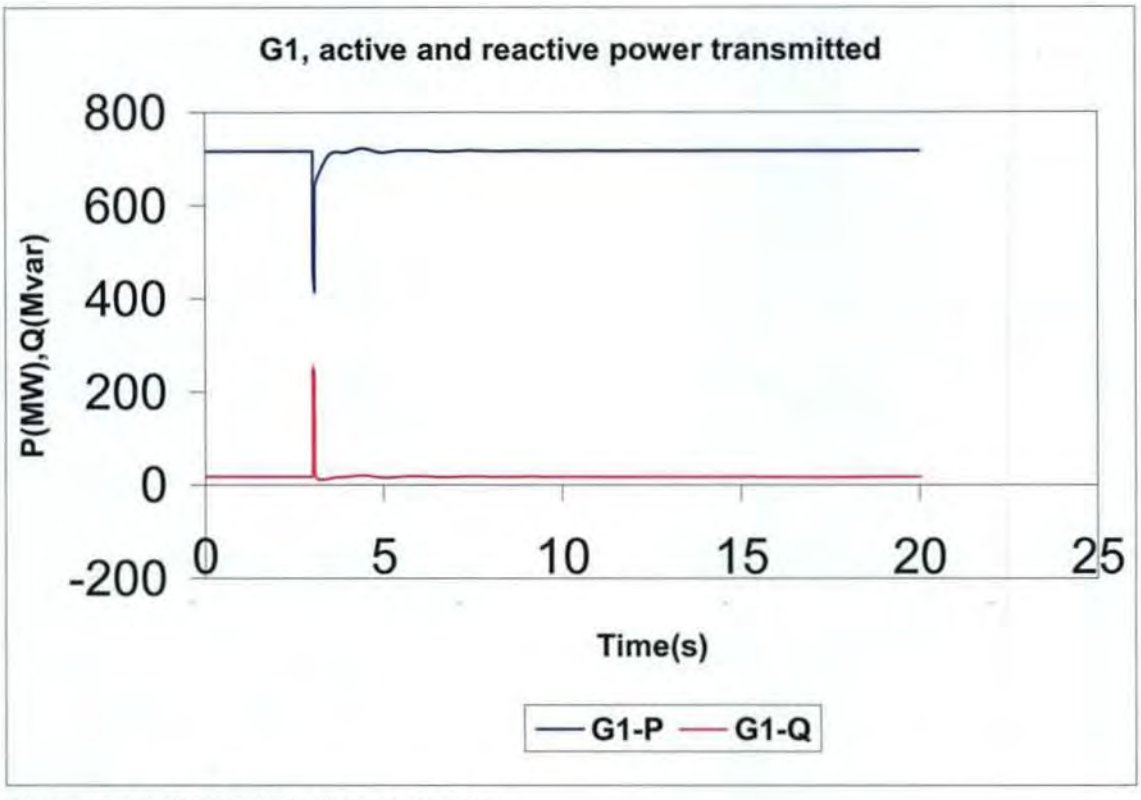

Figure 9.1 P (MW) & Q (Mvar) for G1

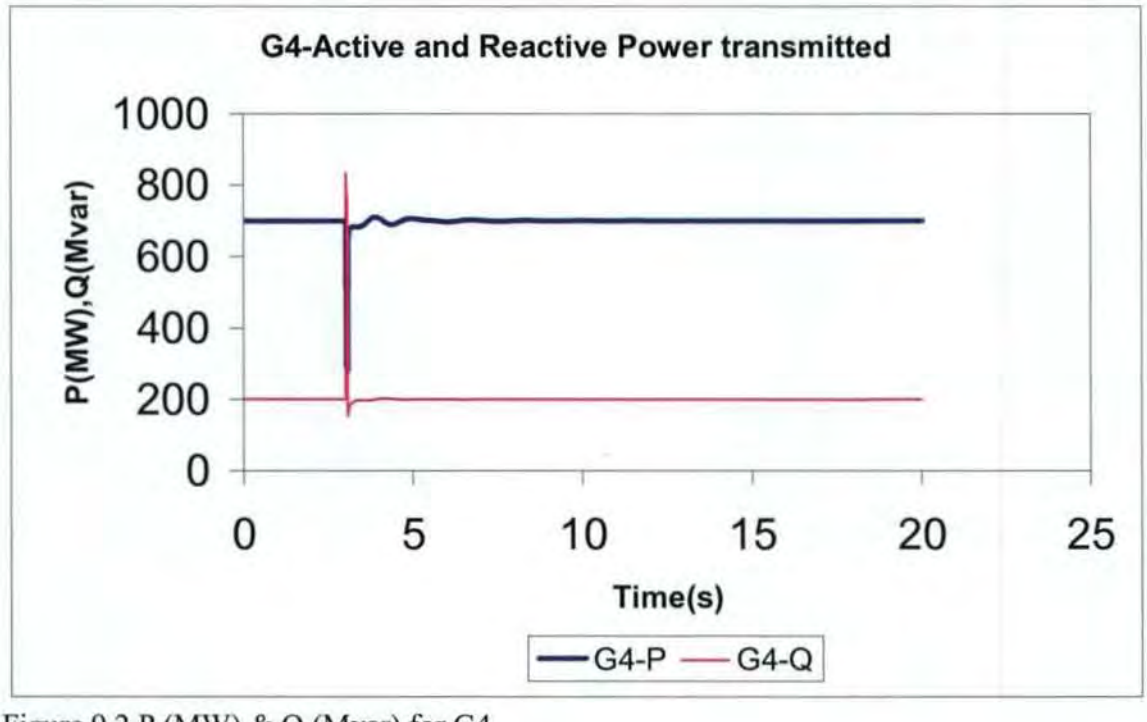

Figure 9.2 P (MW) & Q (Mvar) for G4

9.1.2 Speed of the Generators for HVAC system

In analyzing the speed responses results generators G1 & G4 on both sides of the network were again chosen, since it shows what happened on both sides of the network.

The speed of generator G1 as shown in figure 9.3 was less disturbed by the fault it returned to a steady state of operation in less than 7 seconds after the fault, operating at a steady speed of 1.0 p.u before the fault and suddenly rose to almost 1.00156 p.u during the first swing as a result of the fault. In figure 9.4 generator G4 came to a state of equilibrium after 10 seconds also it was operating at a steady state speed of 1.0 p.u and then rose to 1.00158 as a result of the fault. The result shows that the systems' speed was stable following the transient perturbation. The generator G4 took a longer to settle but the speed was stable after the perturbation

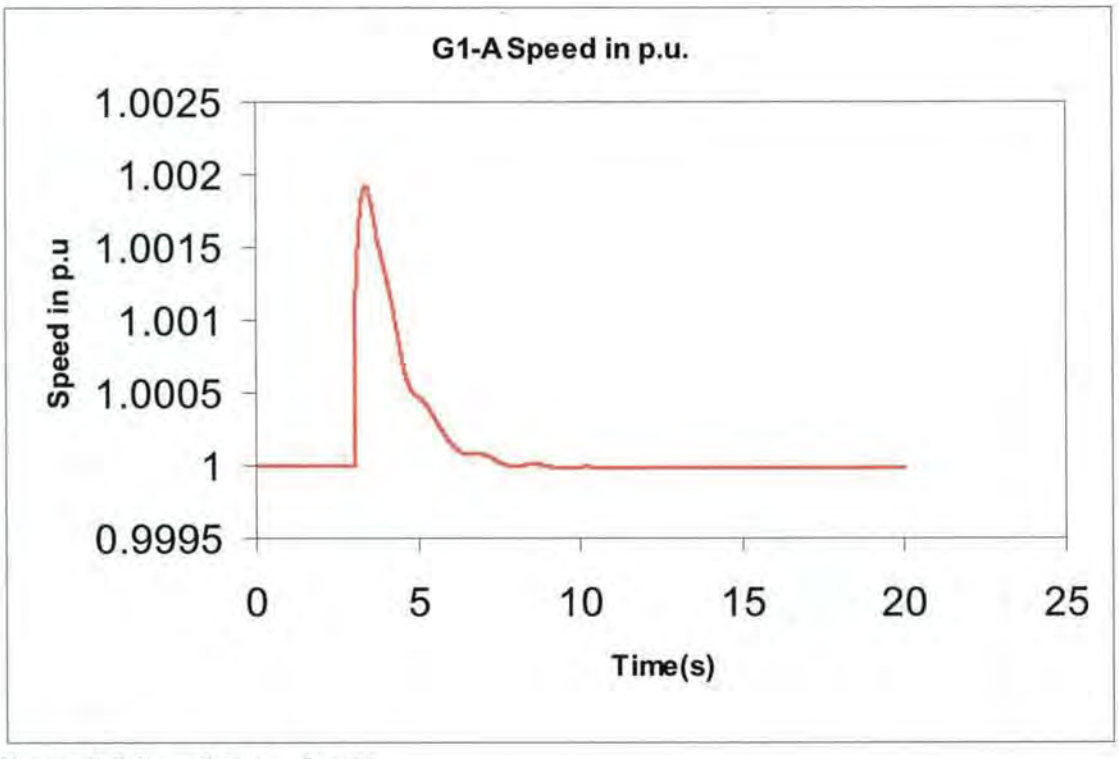

Figure 9.3 Speed in p.u for G1

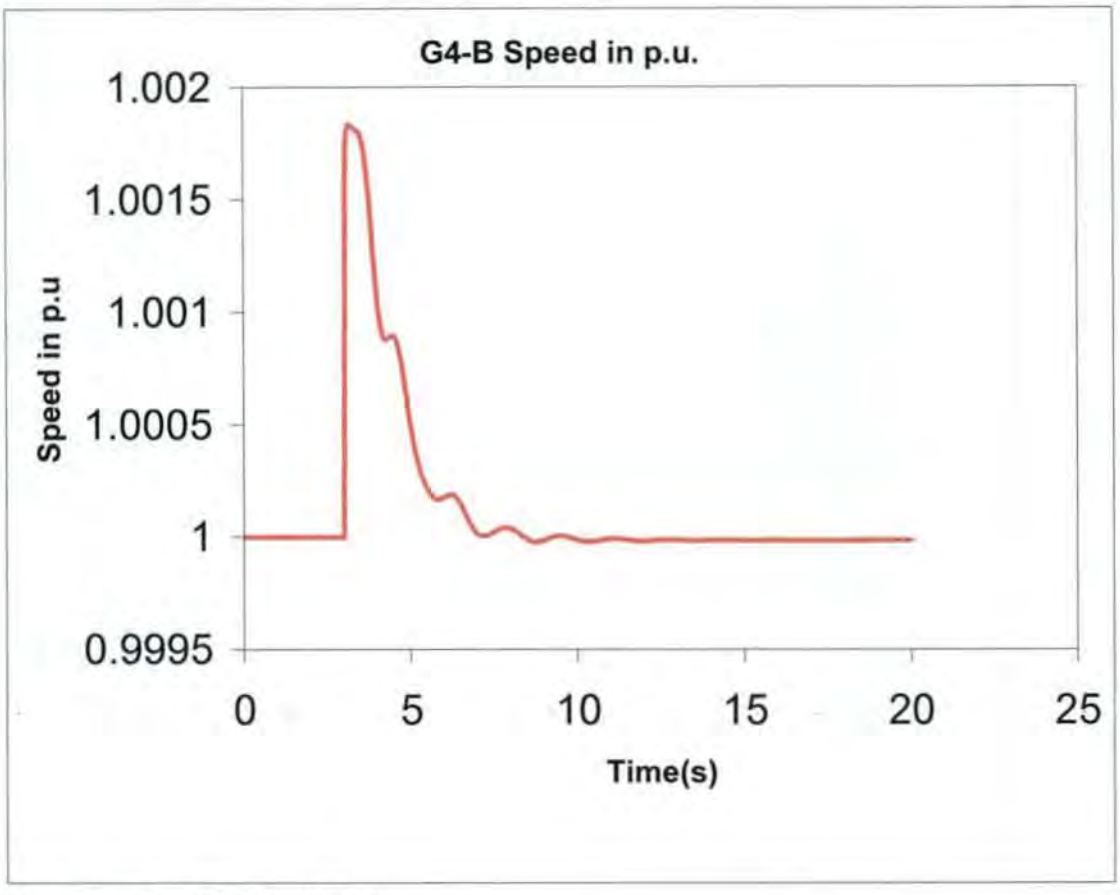

Figure 9.4 Speed in p.u for G4

9.1.3 Rotor angle for HVAC system

Generators G3 in figure 9.5 and generator G4 in figure 9.6 were used here for the purpose of this analysis since they are both on different sides of the network.. G3 in area B close to the fault (see figure 7.14) is more perturbed during the disturbance as shown below, operating from -0.63 rad at steady state and rose to -0.595 rad during the first swing after the fault and further went down to -0.648 rad, it oscillated with decreasing amplitude to equilibrium in about 17 seconds. G2 in area A at steady state was -0.638 rad before the fault, following the fault the first swing oscillation rose to -0.627 rad and then dropped to -0.6455 rad before decaying to a steady state of operation in about 8 seconds after the fault. The result shows that the rotor angle was stable following the transient disturbance.

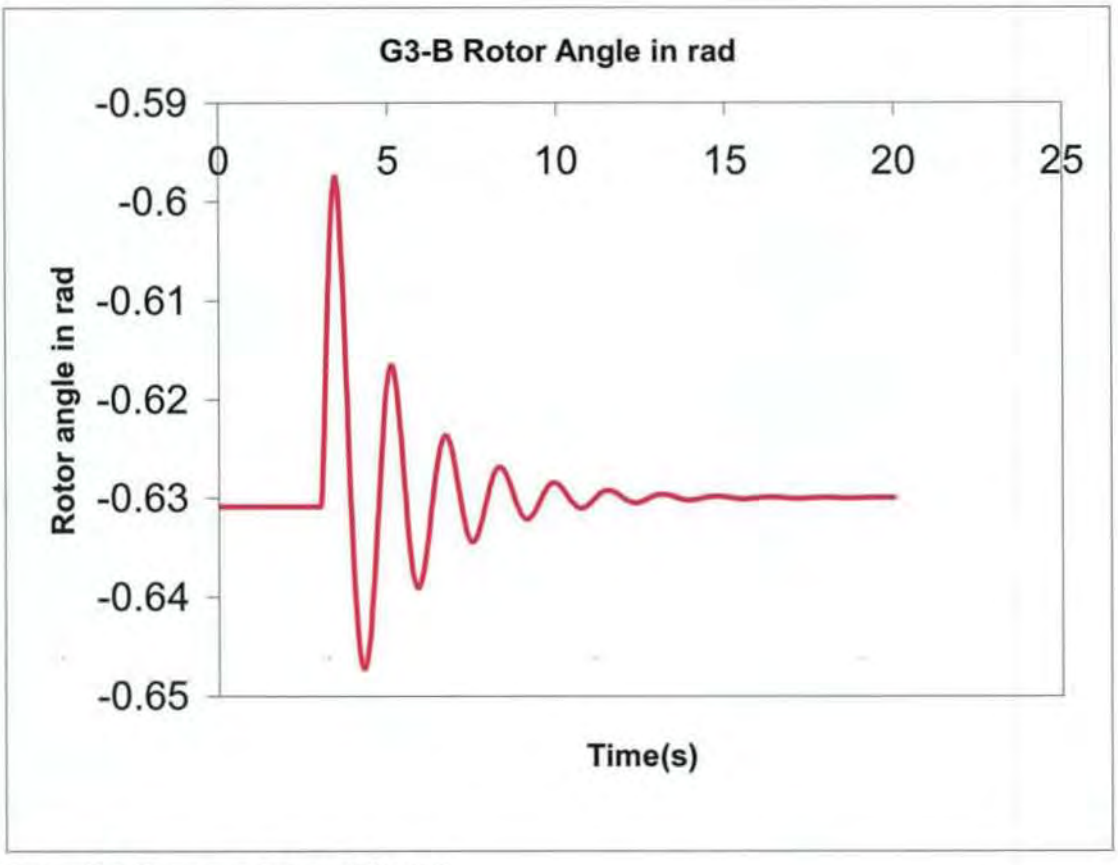

Figure 9.5 Rotor angle in rad for G3

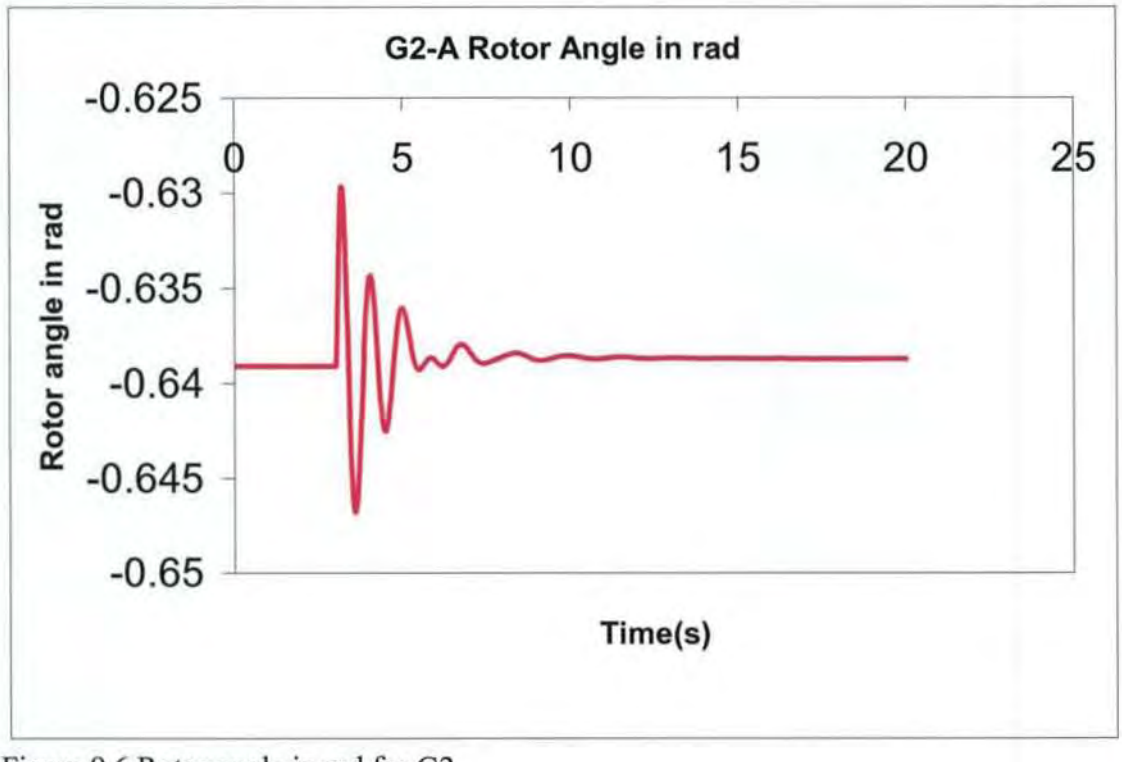

Figure 9.6 Rotor angle in rad for G2

9.2 Transient stability analysis of the HVAC-HVDC network

9.2.1 Active and reactive power of HVAC-HVDC network

Generators G4 and G1 in figures 9.7 and 9.8 in different areas of the network were used for the analysis, because both areas of the network are affected differently by the effect of the fault. G4 have the highest first swing during the fault. From figure 9.8 the active power dipped from 700 MW to about 250 MW and decayed to a steady state with decreasing amplitude in about 6 seconds after fault, the reactive power moved upward from about 200 Mvar to about 700 Mvar and settles in less than 3 seconds. In figure 9.7 area A, generator G1 active power dipped from 720 MW at rest to 600 MW during the fault. The reactive had a surge from 100 Mvar to about 300 Mvar; therefore generator G4 close to the fault is more perturbed by the effects of the fault.

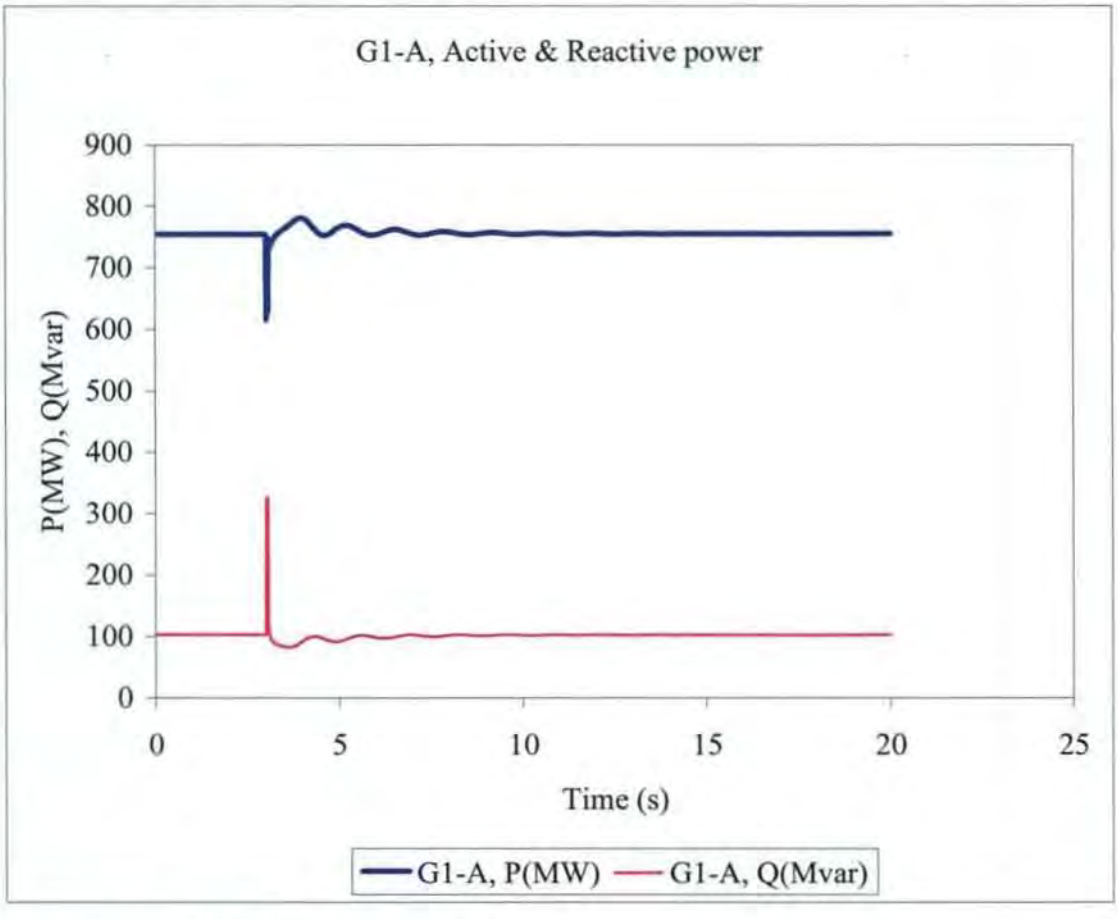

Figure 9.7 P (MW) & Q (Mvar) for G1

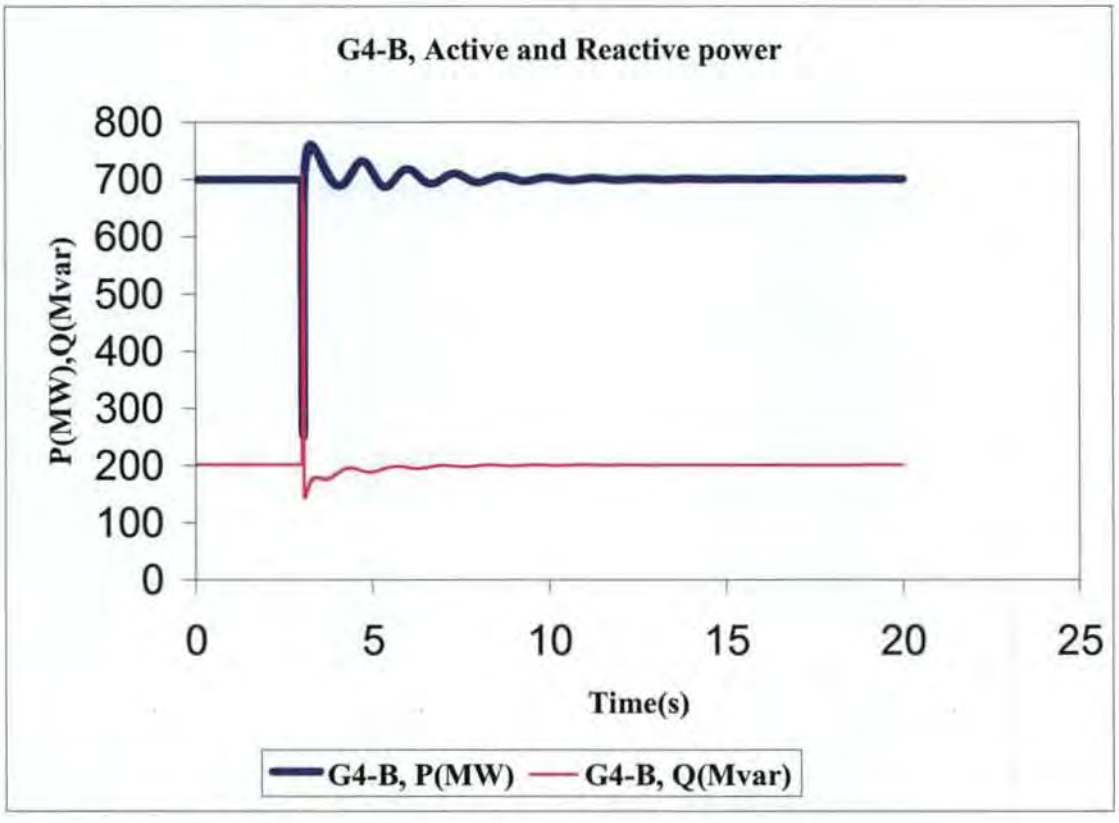

Figure 9.8 P (MW) & Q (Mvar) for G4

9.2.2 Speed of the generators under HVAC-HVDC

One generator was chosen from each area for analysis for the reasons given above. The result below shows that the speed of the generator G4 in figure 9.10 area B was affected most by the fault more than generator G1 despite the damping effect of the HVDC system. G4 at rest was 1.0 p.u, during the fault it oscillates to about 1.00158 p.u in the first swing oscillation; it dropped to 0.9995 p.u but was further dropped by the action of the HVDC control system to 0.99857 p.u and then oscillates upward with low amplitude to a steady state in about 15 seconds after perturbation. In figure 9.9 G1 also at rest was 1.0 p.u during the fault the first swing oscillation moved it up to 1.0053 p.u and the dropped to about 0.99955 p.u and oscillates at low amplitude (due to HVDC control action) to steady state in about 11 seconds. The system did not lose stability as a result of the fault.

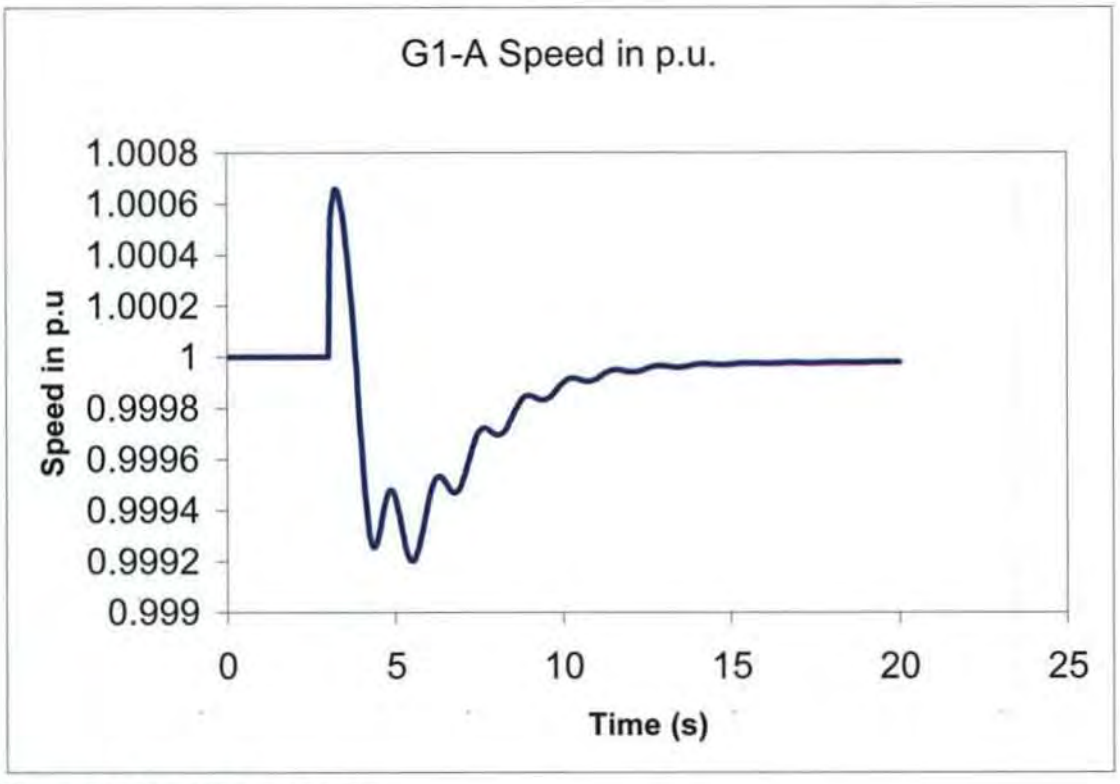

Figure 9.9 Speed in p.u for G1

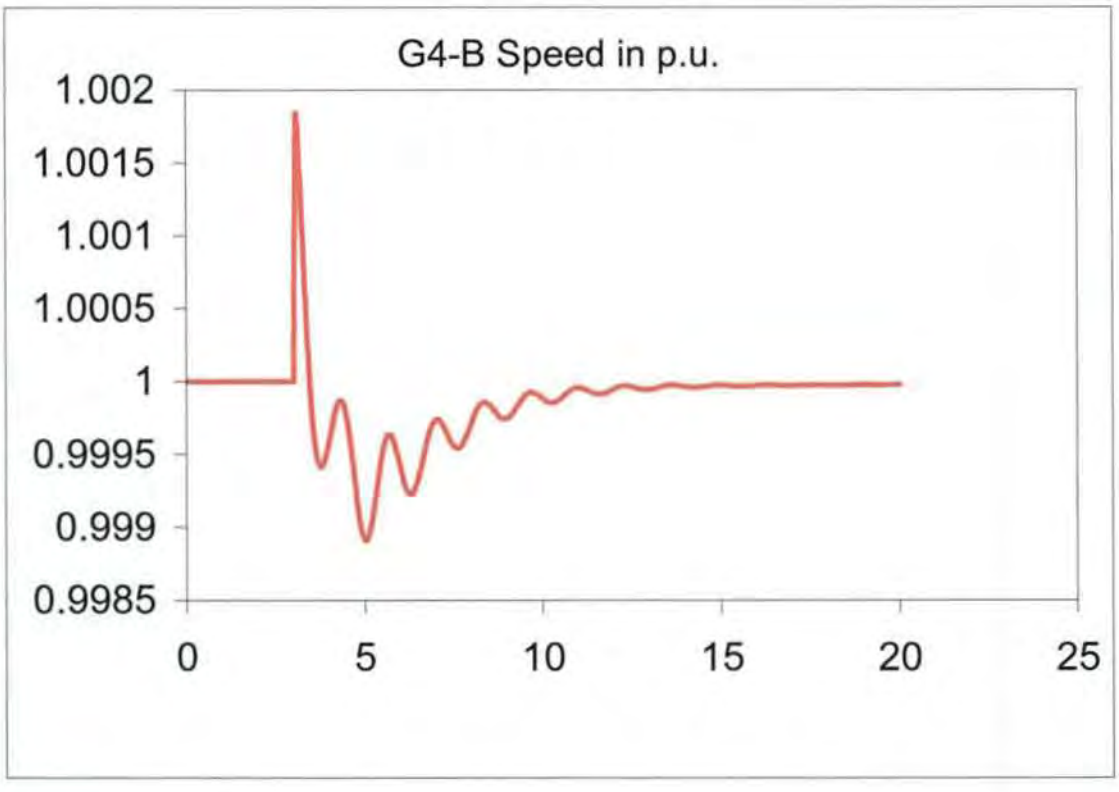

Figure 9.10 Speed in p.u for G4

9.2.3 Rotor angle under HVAC-HVDC network

Generators G3 and G2 were used for this investigation. The results of generator G2 in figure 9.12 and generator G3 in figure 9.11 were used here for the purpose of this analysis, since they are both on different sides of the network. G3 in area B close to the fault is more perturbed during the disturbance as shown below, operating from -0.63 rad at steady state and rose to -0.595 rad during the first swing after the fault and further went down to -0.648 rad, it oscillated with decreasing amplitude to equilibrium in about 17 seconds. G2 in area A at steady state was -0.638 rad before the fault, following the fault the first swing oscillation rose to -0.627 rad and then dropped to -0.6455 rad before decaying to a steady state of operation in about 8 seconds after the fault. The result shows that the rotor angle was stable following the transient disturbance as shown below.

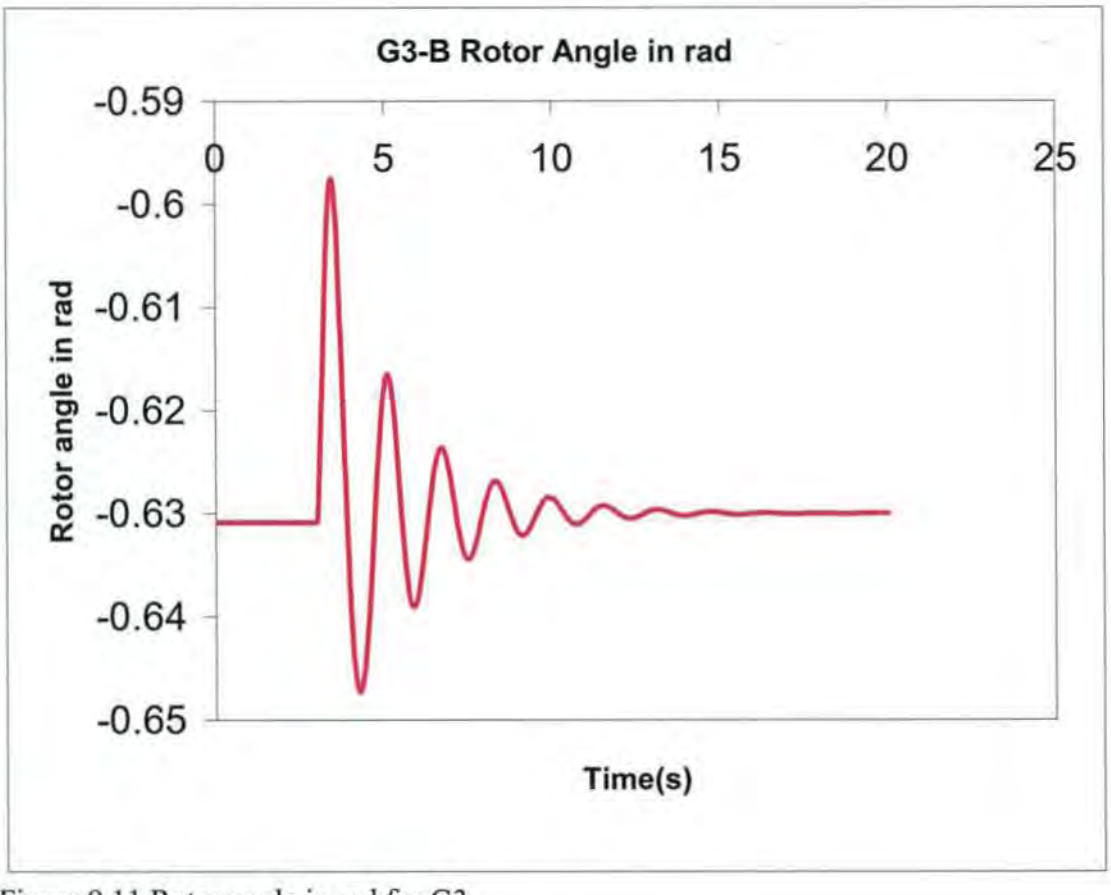

Figure 9.11 Rotor angle in rad for G3

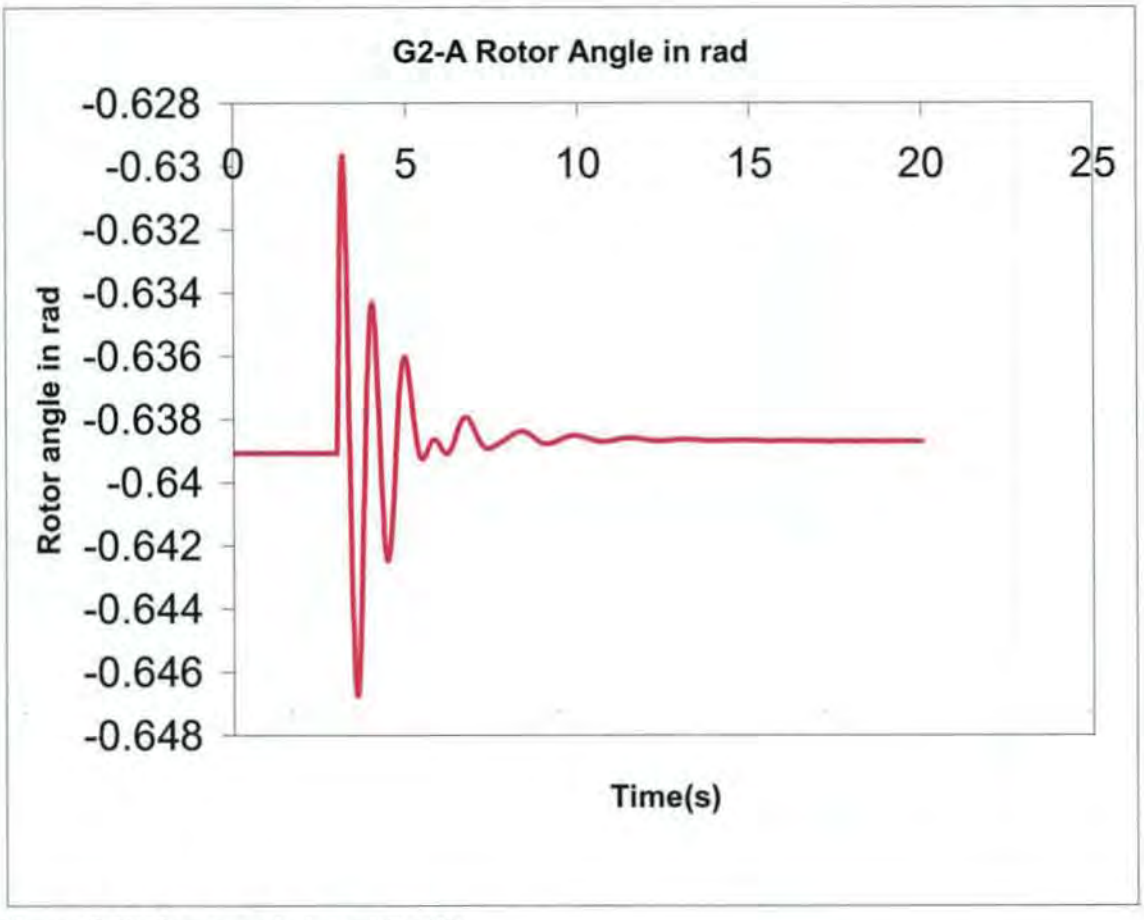

Figure 9.12 Rotor angle in rad for G2

9.3 Transient stability analysis of the HVAC-VSC-HVDC network

9.3.1 Active and reactive power of VSC-HVDC network

This investigation was conducted using the power network model shown in figure 8.1. The results of the responses of the active and reactive power, generator speed and rotor angle as a result of the three-phase fault are shown and analyzed in this section. The results obtained are discussed below.

The results from the figures 9.13-9.14 below shows that generator G4 in figure 9.14 again was the most affected by the fault, given the response of the active and reactive power to the perturbation, the penetration of the dip in power was higher than the rest.. Generator G1 in figure 9.13 in area A was not affected as those generators in area B, G1 active power at rest was 700 MW but dipped to 550 MW during the fault, the reactive power at

rest was operating at –j100 Mvar and then rose to about 100 Mvar during the fault they both returned to steady state in less than 3 seconds after perturbation. In figure 9.14 G4 active power was 700MW at steady state it dipped to 350 MW (representing a drop of 50%) during the fault but came back to steady state in about 3 seconds after the fault. The reactive power was 200 Mvar at rest but surged to 750 Mvar following the fault, this shows a surge of 220% it settles in less than 2 seconds. The result shows that generators in area A are less perturbed than the generators in area B which were closer to the fault.

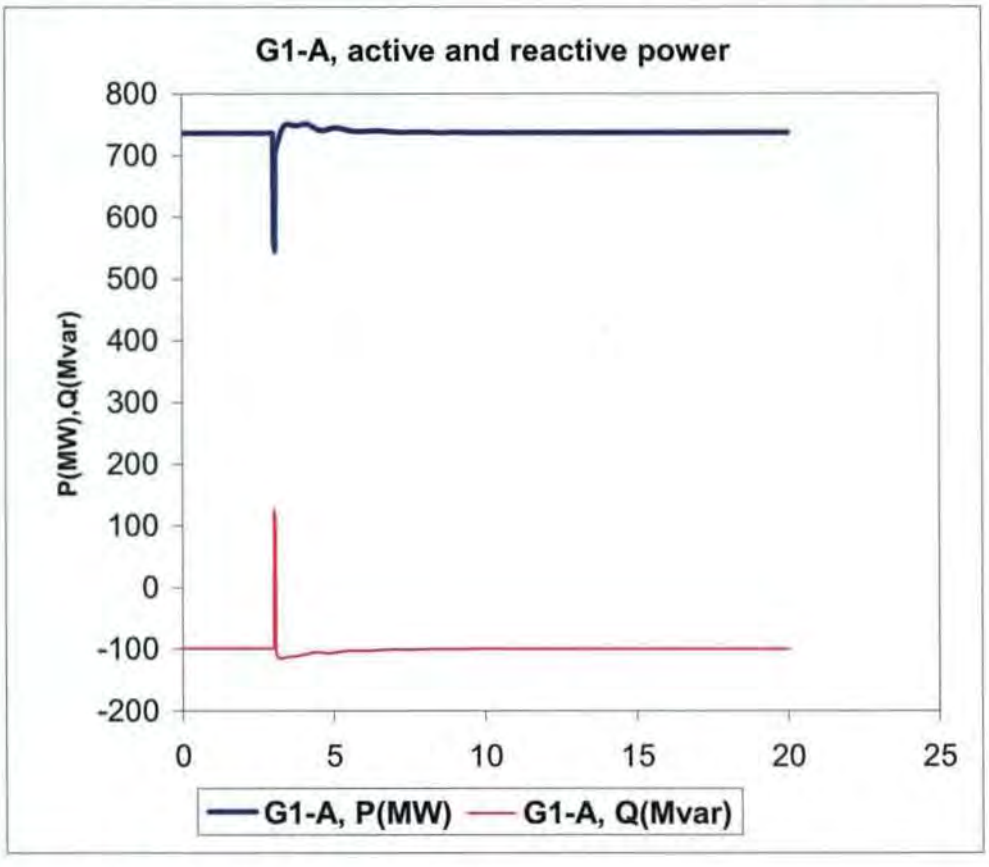

Figure 9.13 P (MW) & Q (Mvar) for G1

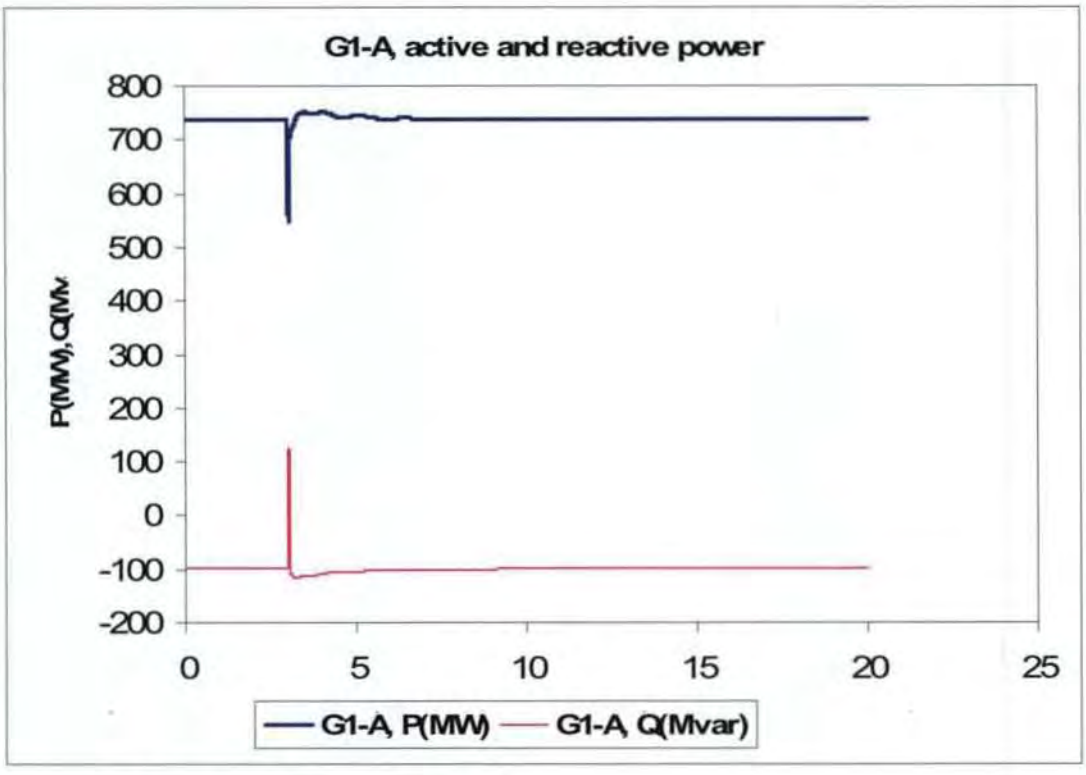

Figure 9.14 P (MW) & Q (Mvar) for G4

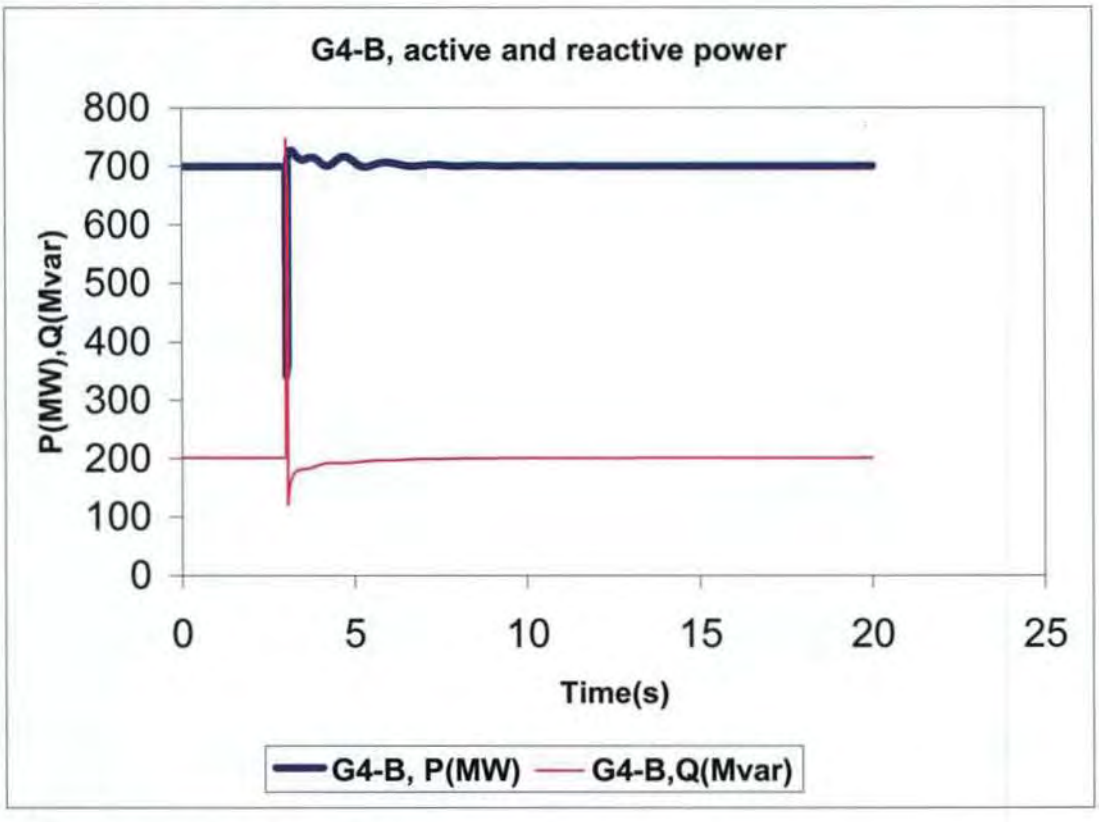

Figure 9.15 P (MW) & Q (Mvar) for G4

9.3.2 Rotor angle under HVDC-VSC/HVDC network

The rotor angle of generator G3 again was most disturbed, despite the mitigation by VSC-HVDC system as shown bellow, in figure 9.16 at steady state before the fault generator G3 operated from a rotor angle of -0.475 rad, and oscillates to -0.44 rad and dropped to -0.49 rad during the fault before reducing with low amplitude to a steady state in less 6 seconds. From figure 9.15 generator G2 operated from -0.6625 rad at steady state before fault, the first swing oscillation during the fault caused the rotor angle to rise to -0.655 rad and the dipped to -0.672 rad before oscillating to steady state with low amplitude in less than 6 seconds. The effect of the control action of the VSC-HVDC is again noticeable here in figure 9.15:

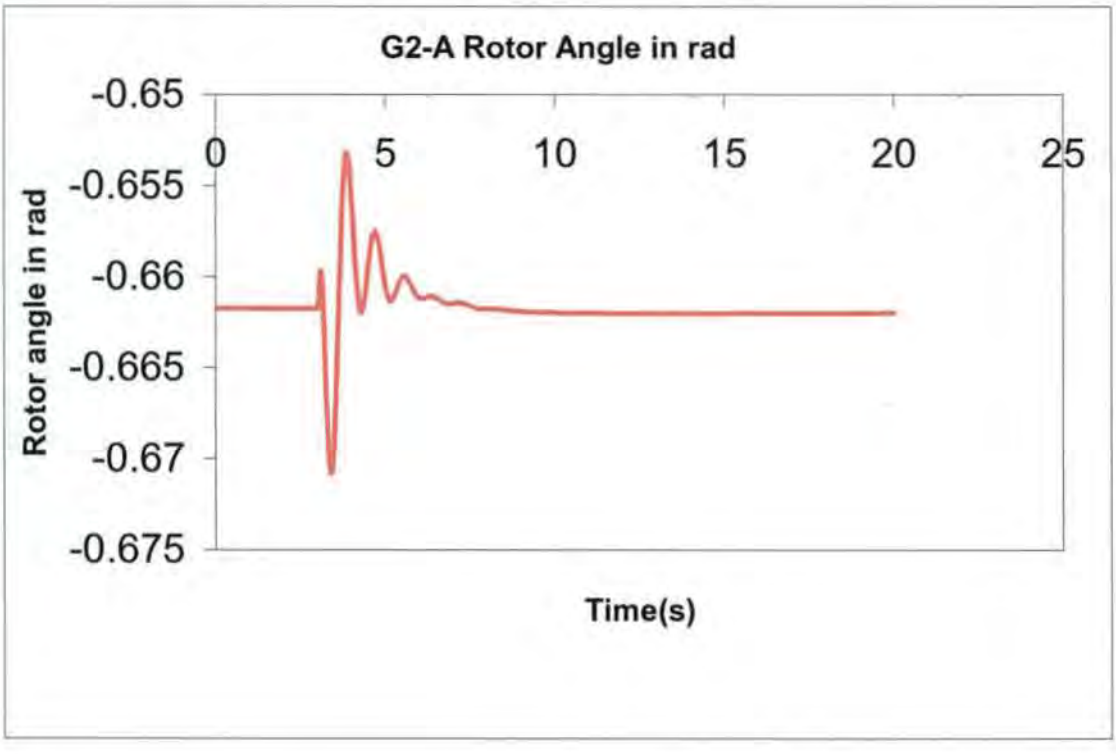

Figure 9.16 Generator 2 rotor angle in rad

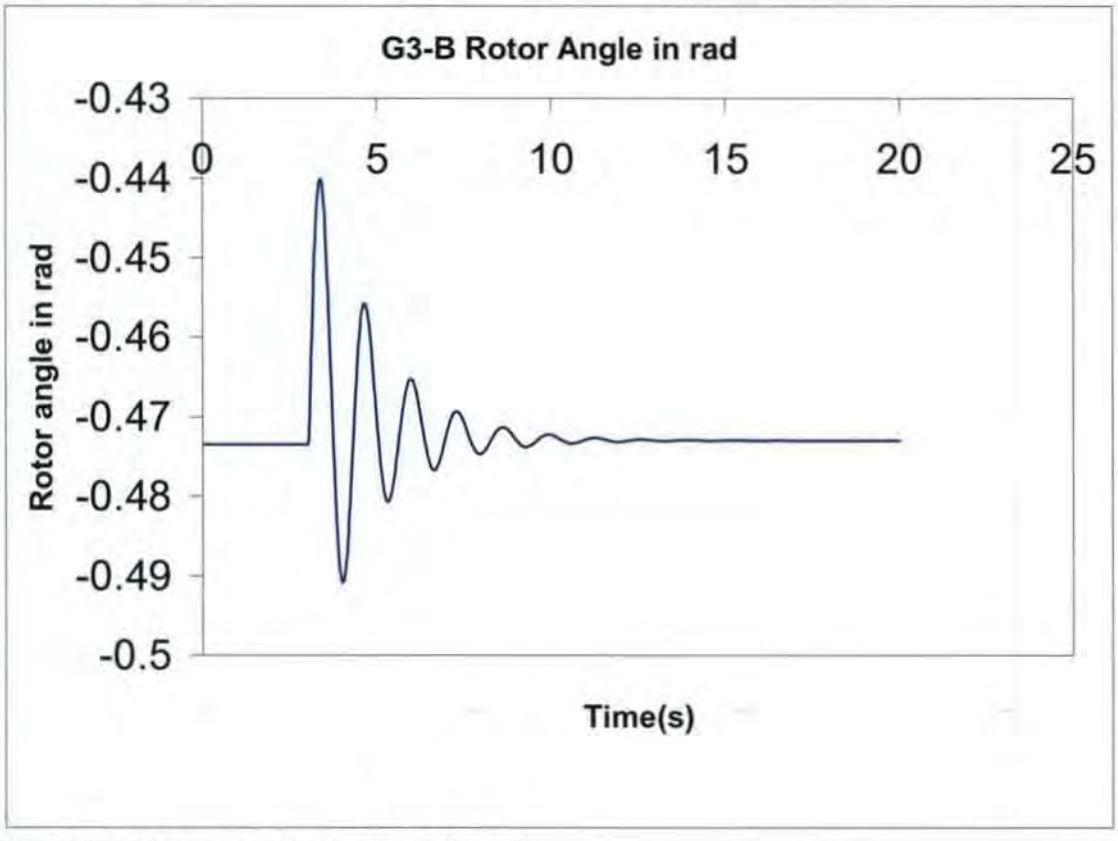

Figure 9.17 Generator 3 rotor angle in rad

9.3.3 Speed of the generators under VSC-HVDC-HVDC network

The result of the generators speed as shown in figures 9.17 and 9.18 below shows that generator G1 operated from 1.0 p.u at steady state before the fault, but rose to 1.0008 p.u and dropped to 0.9995 p.u during the fault and settles to a to the steady in about 6 seconds without further oscillations as shown in figure 9.17. Also, figure 9.18 shows that G4 operated from 1.0 p.u at rest before the perturbation, but rose to about1.0015 p.u and dropped to 0.9996 p.u during the fault before settling to steady state in about 9 seconds without further oscillation. The result shows that generator G4 was more disturbed by the fault but the system did not lose stability.

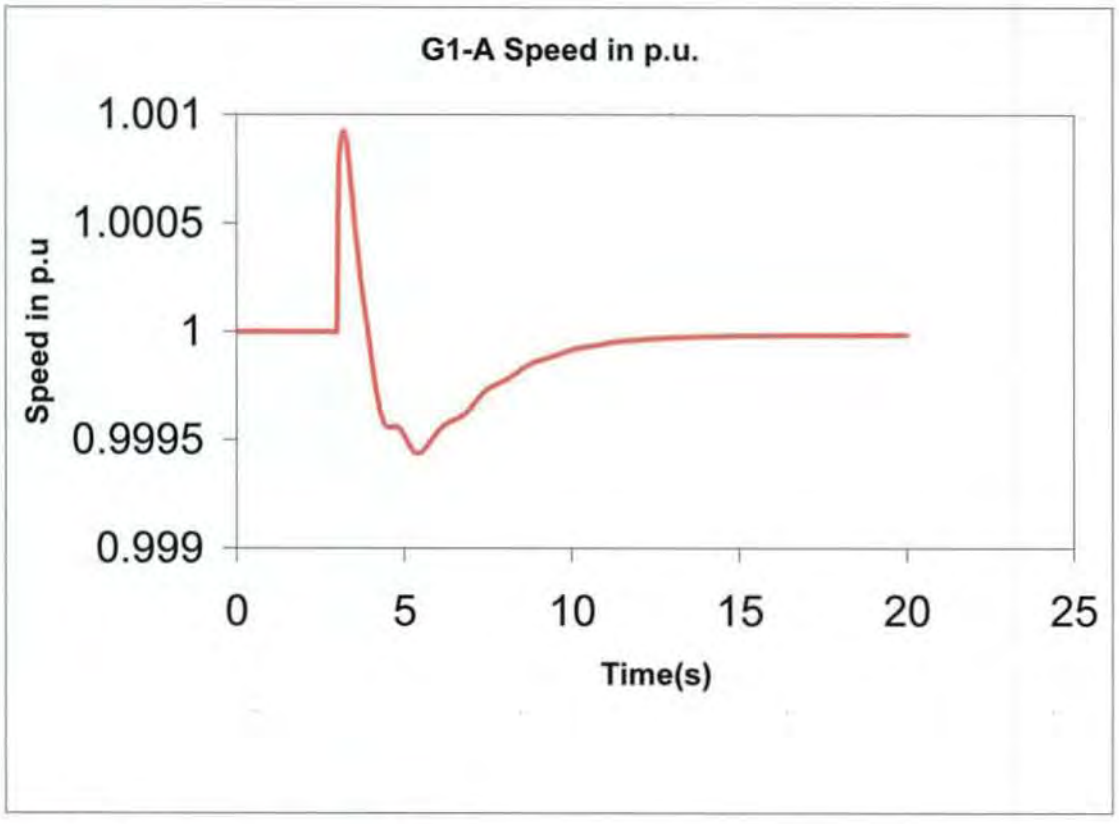

Figure 9.18 Generator 1 speed in p.u

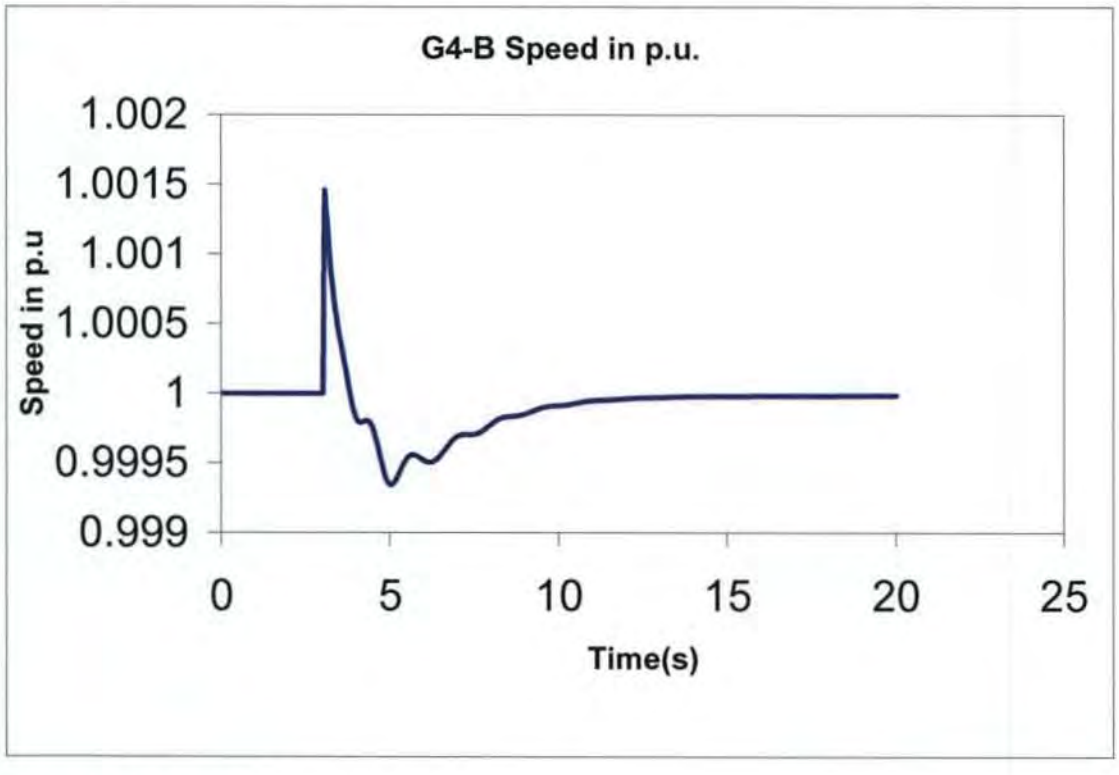

Figure 9.19 Generator 4 speed in p.u

9.4 Comparison of results transient stability studies from the three transmission schemes

The results of the rotor angle and the generator speed were used for the comparison of the three transmission schemes. For proper understanding of how the HVAC, HVDC and VSC-HVDC systems affects the power systems network, with respect to transient stability of power systems. Bus 7 which was affected most by both the transient and voltage disturbance was chosen for this analysis as shown in figures 9.19-9.20

9.4.1 Transient stability case study

This section shows comparison of the different results obtained from the three transmission schemes (as depicted in figures 9.19-9.20), under the transient stability investigation.

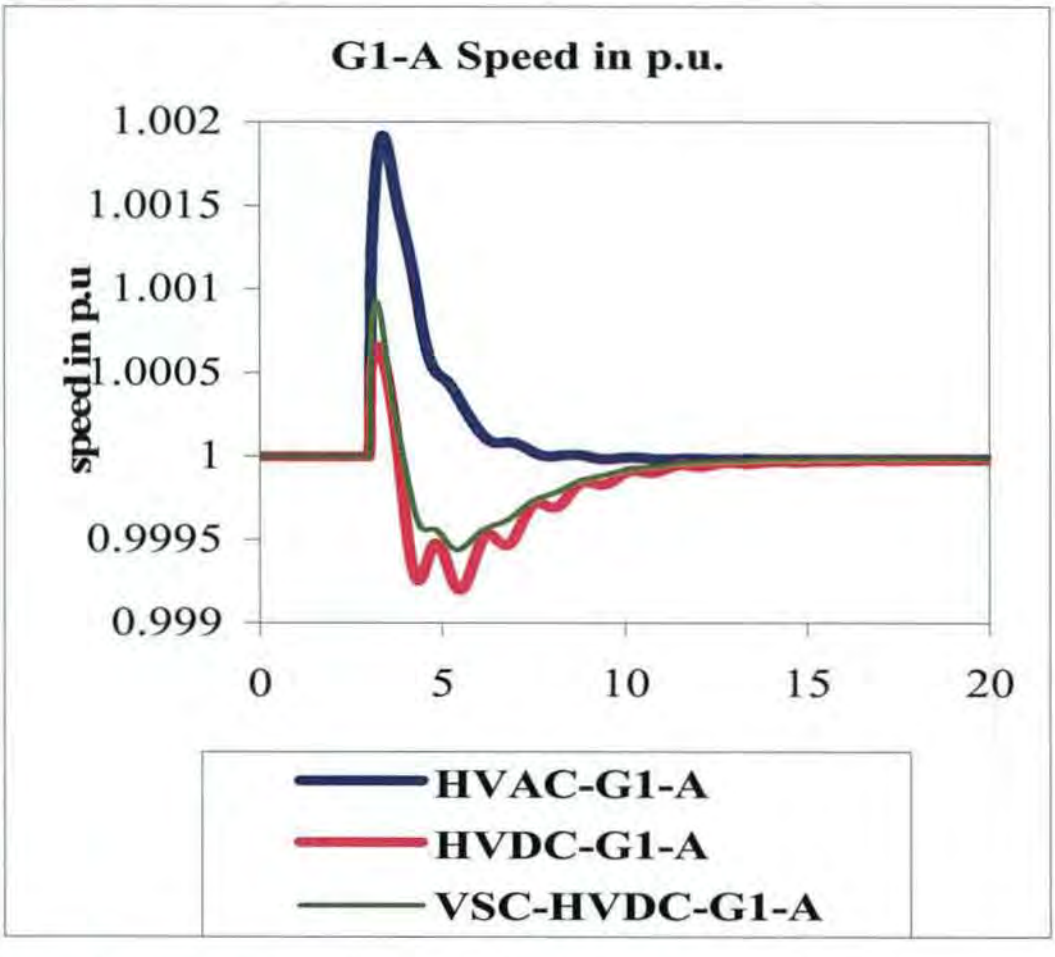

Figure 9.20 Comparison of G1 Speed of the three transmission schemes

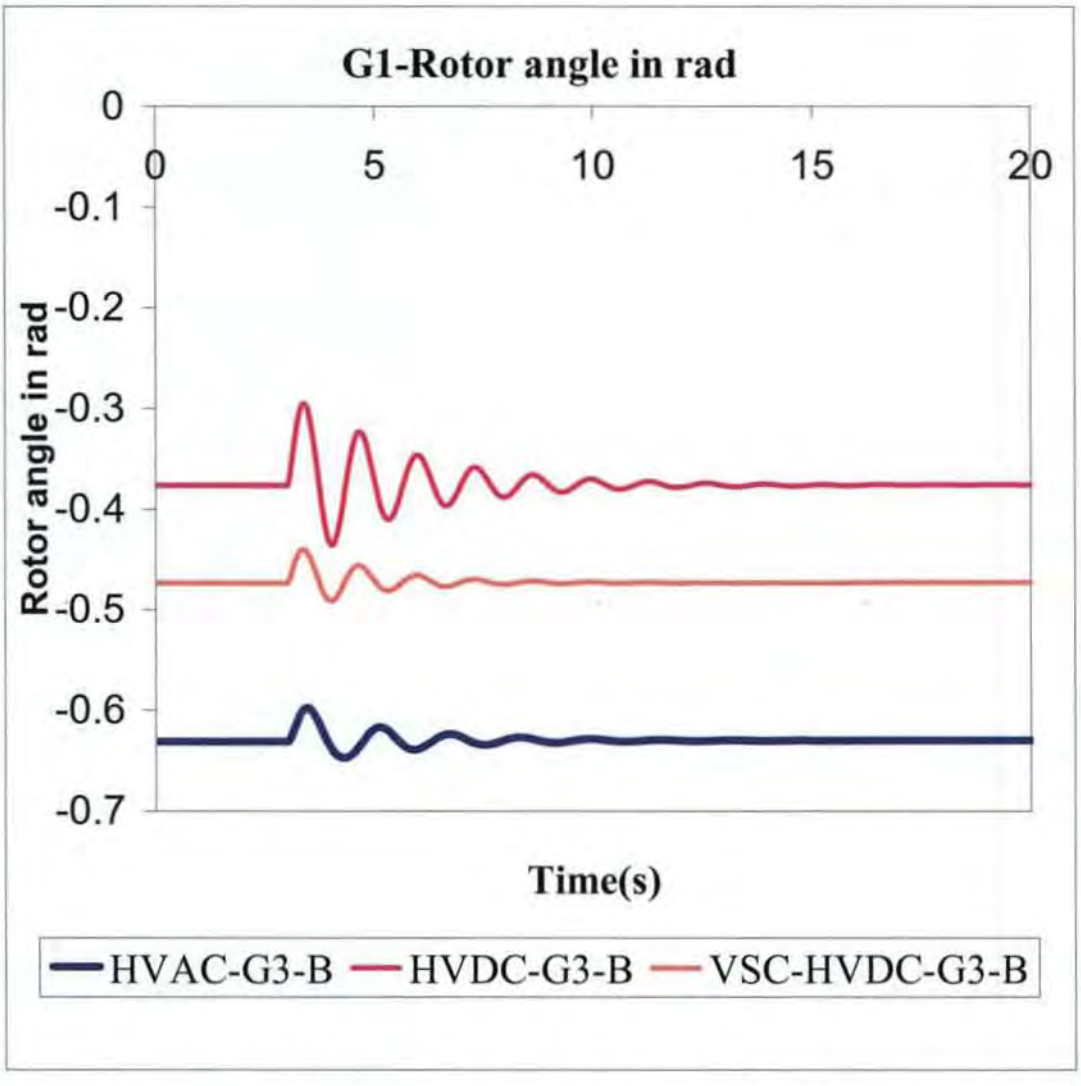

Figure 9.21 Comparison of Generator1 Rotor angle under the three transmission schemes

9.4.2 Analysis of Generator speed

The generator 1 in area-A (Slack bus) G1 was used to investigate the responses of the speed and rotor angle of the network under transient (three phase short circuit) fault situation as shown in figure 9.19 and 9.20. From figure 9.19 (G1 speed) it is evident that the VSC-HVDC reduced the systems oscillation better than the rest, with a speed of (1.001p.u) and came to a steady state of operation 7 seconds after perturbation. The HVDC also reduced the first swing oscillation from 1.001p.u to 0.9997 before coming to a steady state of operation at about 8 seconds after perturbation, the HVAC system was

less damped of the three cases, at rest the speed was 1.0 p.u but raised to1.002 p.u more than the rest before settling in about 10 seconds.

9.4.3 Analysis of rotor angle

Figure 9.20 shows generator1 (G1) rotor angle, from the result HVAC rotor angle was -0.65 rad at steady state of operation, it was raised to -0.59 rad during the fault but late settle at about 15 seconds after the perturbation. HVDC rotor angle was -0.35 rad and rose to about -0.30 rad during the fault, it reached a steady state of operation after about 10 seconds and VSC-HVDC rotor angle was -0.47 rad at steady state of operation before rising to -0.45 rad during the fault, it came to a steady state of operation 5 seconds after perturbation. The result shows that the VSC-HVDC system improves the transient stability of the power system. The fast power run back capability of VSC-HVDC is very useful in helping the system to overcome transient instability after a system fault [2] Also, the instant power reversibility of VSC makes it possible for it to change up to 2 times the power of its rated value.

Chapter 10

Conclusions and Recommendations

10.1 Conclusions

From the analysis of the above simulation results the following conclusions can be deduced:

- The power flow analysis in a HVAC power system network indicates that the reactive power requirement for transmission of power increases as the length of the network increases. Therefore, long distance transmission is limited by reactive power requirement, hence the system becomes unstable beyond a distance of about 550 km, in practice the best power quality is within the maximum range of 500 km-600 km; also It requires large voltage gradient for the power to be transmitted over a long distance. Power transmission is limited by distance in a HVAC network. Integration of HVDC link in the network, improved the power transmission distance of the HVAC link on the hybrid network by 18%. With HVDC link, more power is transmitted over a longer distance. Also, transmission of power using the HVAC transmission scheme brings about more power loss than the hybrid HVDC-HVAC transmission scheme.
- The HVDC system, the power systems stabilizer (PSS) in conjunction with AVR and VSC-HVDC have the ability to improve transient stability under large disturbance , like three-phase short circuit fault in power systems as demonstrated in this study. The transient stability study also shows that generators in the areas of the network with close proximity to a source of disturbance are more affected by the effects of the fault, the knowledge of this will guide network planner on where to locate damping devices in the network.
- The analysis of the small signal stability shows that even when the parent networks (HVDC, HVAC) are stable; their hybrid network (HVDC-HVAC) could be problematic if the tie-line between the two networks is weak (low short circuit ratio).
- Several interesting features of HVDC, VSC-HVDC and HVAC have been shown in this investigation. It is shown that the VSC-HVDC is able to improve voltage

stability and transient stability of the hybrid HVAC-VSC-HVDC system. Also in a weak ac link interaction it overcomes the problems of low short circuit ratio, which was not achievable using the standard current source converter or line commuted HVDC system.

- The HVAC-HVDC system in hybrid with HVAC link, also, improved the transient stability but was problematic with the voltage stability due to the weak link in the network. The HVDC system was able to extend the maximum loading point of the network beyond the capability of the VSC-HVDC. Therefore, for bulk power transmission it is advisable to use the HVDC link.
- Analysis of the whole results under transient stability study shows that, power system regains stability quicker with VSC-HVDC transmission scheme, followed by the HVDC scheme.

10.2 Recommendations

Based on the results obtained from this study the following recommendations can be given.

- This study has clearly demonstrated that when a fault occurs in transmission lines the system responds according to the nature of fault and the strength of the system. The knowledge of this will assist network planners to design for contingencies.
- With the arrays of advantages that the VSC-HVDC systems have over the HVDC and HVAC systems, further research is recommended to find a way of improving the power transfer capability of VSC-HVDC system. Since bulk power transfer is one its greatest limitation at the moment. The power transfer capability is still limited to the ratings of the converter stations.
- Furthermore, a power network should not be loaded close to the percentage loadability limit of the transmission line, since this will ultimately lead to collapse of the network.
- From the result of the study it is further recommended that, interconnections with weak HVAC system i.e., systems with weak short circuit ratio (SCR) should be done with VSC-HVDC transmission scheme, because, it has been able to overcome the problems of power stability, which is normally associated with such

interconnections. This is a far departure from the classical HVDC system, which could be unstable with such connections, due to the control actions of it's converter stations and the fact that the converter stations absorbs reactive power

- For verification and validation of these results, further investigation with other power simulation software should be carried out these studies.
- This research has clearly demonstrated the problems of power systems stability, and also proffered some solutions to these problems, as well as pointing out the grey areas with the hope that it will spur further research in this study.

Reference

1. Prabha Kundur: "*Power system stability and control* "1994 Edition by McGraw-Hill
2. Lidong Zhang, Lennart Harnefors Pablo Rey: "*Power System reliability and transfer capability improvement by VSC-HVDC (HVDC Light© "Security and reliability of electric power systems*" CIGRE Regional meeting, June 18-20, 2007, Tallinn, Estonia
3. Nang Sabai, Hnin Nandar Maung and Thida win, "*voltage control and dynamic performance of power transmission system using static var compensator*" Proceedings of world academy of science, engineering and technology volume 32 August 2008 ISSN 2070-3740
4. K. Pandiaraj, G. Hodgkirson, B. Fox, "*use of embedded generators for voltage support in rural distribution networks*" UPEC 2002 35th universities power engineering conference 2000
5. Prabha Kundur, John Paserba, Venkat Ajjarapu, Goran Anderson, Anjan Bose, Claudio Canizares, Niko Hatziargyriou, David Hill, Alex Stankovic, Carson Taylor, Thierry Van Cutsen and Vijay Vittal," *Definition and Classification of Power System Stability*" IEEE Transaction on power systems, Vol. 19. 2. May 2004
6. K. Padiyar, "*HVDC Power transmission systems: technology and system interaction*", New Delhi: Wiley Eastern, 1990
7. J. Arrillaga, "*High Voltage Direct Current transmission*" London: The institute of Electrical Engineers, 1998
8. Karen George, "*DC power production, delivery and utilization*" Electric power research institute (EPRI) white paper, June 2006
9. D.M Larruskain, I. Zamora, A.J Mazon, O. Abarrategui, J. Monasterio, "*Transmission and distribution Networks: AC versus DC*" Dept. of Electrical Engineering, University of the Basque Country-Bilbao Spain, 20 August, 2009
10. R. Rudervall, J. P Charpentier, and R. Sharma, "*High voltage direct current (HVDC) transmission systems technology review paper,* "Energy week 2000, Washington, D.C, USA, March 2000
11. Owen Pearke, "*The history of High Voltage Direct Transmission*" 3rd Australian Engineering Heritage Conference 2009.
12. Gunar Asplund, "*Application of HVDC light to power system enhancement*" ABB power systems, IEEE winter meeting, January 2000 Singapore
13. A. Praca, H. Arakaki, S. R. Alves, K. Eriksson, J. Graham, G. Biledt, "*Itaipu HVDC Transmission system 10 years operational experience*" V SEPOPE, Recife, Brazil 19 May, 1996
14. Stijn Cole, Ronnie Belmans, "*Transmission of bulk power-The history and application of Voltage Source Converter High Voltage Direct Current Systems*" IEEE Industrial Electronics Magazine 19, September 2009
15. Narendra Bawane, Anil G. Kothari, and Dwarkadas P. Kothari. "*ANFIS base HVDC control and fault Identification of HVDC converter*" HAIT Journal of Science and

Engineering B, Volume 2, Issues 5-6, pp. 673-689 Copyright © Holon Academic Institute of Technology, June 2005

16. J. Partanen," *DC Power transmission*" Lappeenranta University of Technology, November 2008 www.ee.lut.fi/fi/lab/sahkomarkkna
17. W. Breuer, D. Povh, D. Retzmann, E. Teltsch,"*Trends for future HVDC applications*" The 16th conference of the electric power industry (CEPSI 2006) Mumbai, India 6-10 November 2006
18. Lazaros P. Lazaridis, "*Economic comparison of HVAC and HVDC solutions for large offshore wind farms under special considerations of reliability*" Master's thesis Royale Institute of Technologies, Stolkhom 2005
19. N. Mohan, T. M. Undeland, and W. P. Robbins, "*Power Electronics: Converters, Applications and design*", 2nd ed. New York, NY. John Willey and Sons, 1995
20. Juan Miguel Perez de Andres, Miguel Muhlenkamp, Dietmar Retzmann, Roland Waltz, "*Prospect for HVDC-Getting more power out of the grid*" Jornadas Technicas Sobre LA 'Session Plenaria CIGRE 2006' Madrid, 29-30 November 2006
21. L. Carlsson, A. Nyman, L. Willburg, G. Hjaimrsson," *The Fenno-Skan HVDC submarine cable transmission system and design aspects. Commissioning and initial operating experience*", ABB Tech. Rep. by L Carlsson 1991
22. Paulo Fischer de Toledo,"*Feasibility of HVDC for City Infeed*", PhD Thesis, royal Institute of Technology Hogskolan, Stockholm, September 2003
23. Hui Pang, Guang Fu and Zhiyuan He, "*Evaluation of losses in VSC-HVDC Transmission system*" National basic research program of China (973 program) 2007
24. N. Mohan, T.M Undeland, and W. P. Robbins, "Power Electronics: Converters applications and design,", 2nd ed. New York, NY. John Willey and Sons, 1995
25. D. A. Paice, "Power Electronics Converter Harmonics (multiple methods for clen power" New York, NY IEEE press 1996
26. J. Reeve, G. Fahmy, and B. Stott, "*Versatile load flow method for Multi-terminal HVDC Systems*" IEEE Trans., Vol. PA-96, pp. 925-933, May/June 1977
27. M. M. El Marsafawy and R. M. Mathur,"*A new, fast Technique for load flow solution of integrated multi-terminal DC/AC Systems,*" IEEE Trans., Vol. PAS-99. 246-255, January/February 1980
28. Roberto Rudervall, J. P. Charpenter and Raghuuveer Sharma, "*High Voltage Direct Current (HVDC) Transmission systems*", ABB Technology review paper, 7-8 March, 2000
29. J. D Glover, *"Power system analysis and design*", Glover, M. Sarma, 2nd Ed, PWS publishing Company, 1994
30. C. V. Thio, J. B. Davies, K. l. Kent," Commutation failures in HVDC transmission systems" IEEE transactions on power delivery, Vol. 11. No. 2, April 1996

31. J. Robson, G. Joos, "*VSC HVDC transmission and offshore grid design for a linear generator based wave farm*" IEEE 978-1-4244-3508-1© 2009 IEEE
32. K. Erikson, "*Operational experience of HVDC Light*" *International conference on AC-DC Power transmission*", London, U.K., November 2001
33. B. Jacobson, Y. Jiang-Hafner et al, "*HVDC with voltage source converters and extruded cables for up to* ± *300KV and 1000 MW*," CIGRE conference, Paris, France, August 2006
34. DIgSILENT Technical Documentation, "*Synchronous Generators, and VSC-HVDC technical reference*" DIgSILENT GmbH, Germany, 2007
35. D.U Cuiqing, "*VSC-HVDC for industrial Power Systems*", PhD thesis department of energy and environment Chalmers University of Technology, Goteborg, Sweden 2007
36. Stijn Cole, Ronnie Belmans, "*The history and applications of voltage-source converter High-voltage direct current systems*", IEEE Industrial electronics magazine 19, September 2009
37. L. Weimers, "*New markets need new technology*," proceedings of International conference on power system technology, vol. 2, perth, Australia, December 2000, pp. 873-877
38. R. Grunbaum, B. Halvarssion, and Wilk-Wilczynski, "*Facts and HVDC Light for power system interconnections*", Power delivery conference, Madrid, Spain, September 1999
39. G. Daelemans, K. Srivastava, M. Reza, S. Cole, "*Minimization of steady-state losses in meshed network using VSC-HVDC*" , IEEE transactions on power delivery, 978-1-4244-4241-6, © 2009 IEEE
40. B. Van Eeckhout, D. Van Hertem, K. Srivastava and R. Belmans, " Economic comparison of VSC-HVDC and HVAC as transmission system for a 300 MW offshore wind farm", European transaction on electrical power, 10 June 2009
41. C. P Steinmetz, "Power control and stability of electric generating stations", AIEE trans., Vol. XXX1X, Part 11. pp. 1215-1287, July 1920
42. G. S. Vassell, "*Northeast blackout of 1965*," IEEE power Engineering Review, pp. 4-8, Jan. 1991
43. Peter Ang, " *Transmission planning criteria*" Western power system planning branch, transmission division, report No. TDWP 79-97, January 2006
44. PTI-Network consulting, Siemens " Dynamic performance of transmission systems," http://w3.energy.siemens.com/cms//00000011/en/reused/Documents/ff_dynamics_transmission_1451451.pdf
45. CIGRE Task force 38.01.07on power system oscillations, "*Analysis and control of power system oscillations,*" CIGRE Technical Brochure, no. 111. Dec. 1996

46. J. Thapar, V. Vittal, "*Interarea oscillations in power systems*" IEEE/PES Power and Energy Systems Working Group on Systems Oscillations, IEEE Special Publication 95-TP-101, 1995
47. R. G Ramey, AC, Sismour, and G.C Kung, "*Important parameters in considering transient torques on turbine-generator shaft systems*"; IEEE Trans, vol. PAS-99, PP.311-317, January/ February 3rd 1978
48. Rusejla Sadikovic, "*Single machine infinite system*" Internal Report, Zurich, July 2003
49. J. Thapar, V. Vittal, "*Interarea oscillations in power systems*" IEEE/PES Power and Energy Systems Working Group on Systems Oscillations, IEEE Special Publication 95-TP-101, 1995
50. J.G.F Francis, "*The QR transformation*", parts 1 and 2 the computer journal, vol. 4, PP. 265-271, 1961, PP 332-345, 1962
51. J. D. Ainsworth, A. Gavrilovic, and H. L. Thanawala, "*Static and synchronous compensators for HVDC transmission converters connected in a weak AC systems*," 28th session CIGRE. 1998, paper 31-01
52. Hanif Livani, Mohsen Bandarabadi, Yosef Alinejad, Saeed Lesan, Hossein Karimi Darijani,"*Improvement of fault ride through capability in wind farms using VSC-HVDC*" European journal of scientific research © Eurojournal publishing, Inc. 2009
53. Jennifer Chiu, Philip Pidgeon, "*Wellington Voltage stability study during HVDC south transfer*" 21 September 2006
54. H.K Clark, "*New challenge: Voltage stability*", IEEE power engineering review, Vol.10, pp 33-37, April 1990
55. L.S Vargas, E. Huber, R. Palma-Behnke, "*Impact of Industry Restructuring on the Chilean Central Interconnected System Security and dynamic performance*" Electrical Engineering Dept University of Chile ISBN 1-4244-0493-2/06 © 2006 IEEE
56. Horia S. Campeanu, Eric L Helguen, Yasmine Asset, Nicolas Vidal and Savu C. Savlescu, "*Real-time stability monitoring at transelectrica*," IEEE power systems conference and exposition 2006 (IEEE PSCE'04), Atlanta, GA, October 29-November 2, 2006
57. N. Barberis Negra, J. Todorovic and T. Ackermann, "*Loss evaluation of HVAC and HVDC transmission solutions for large offshore wind farms*" Electric Power Systems Research Vol. 76, issue 11, July 2006, pages 916-927
58. Leonard L. Grigsby, Richard E. Brown, "*Power Systems Reliability*" © 2007 Taylor and Francis Group, TK1001. P65 2007
59. Graham Rogers: "*Power system oscillations*", The Kluwer international series in Engineering and Computer science, series editor: M. A Pai, 2000 Edition

60. G. Asplund, K. Erikson, H. Jiang, J, Linberg, R. Palsson, and K, Svensson, "*DC Transmission based on Voltage Source Converters*," CIGRE Conference in Paris France, 14-302, 1998
61. S. Johannsson, G. Asplund, E. Jansson, and R. Rudervall, "*Power System Stability Benefits with VSC-HVDC-Transmission Systems*," CIGRE Conference in Paris, France, B4-204, 2004
62. Dennis A. Woodford," *HVDC Transmission*" Manitoba HVDC Research Centre, 400-1619 Pembina Highway, Winnipeg, Manitoba, R3T 3Y6, Canada, 18 March 1998

Appendix

Appendix A: Table A: 1. Cables' parameters and main characteristics CIGRE Parameter

Cable	**132 kV**	**220 kV**	**400 kV**
Resistance (Ω/m)	48×10^{-6}	48×10^{-6}	45.5×10^{-6}
Inductance (mH/km)	0.34	0.37	0.39
Capacitance (mF/km)	0.23×10^{-3}	0.18×10^{-3}	0.18×10^{-3}
Nominal current (A)	1055	1055	1323
Cable section (mm^2)	1000	1000	1200

Appendix A: Table A: 2. Impedance definition in the equivalent circuit

Parameter	Description	Unit
r_s	Stator resistance	p.u.
x_l	Leakage reactance	p.u
x_{rl}	Rotor leakage reactance	p.u
x_{hd}	Mutual reactance between stator and rotor	p.u.
x_d	Mutual reactance between stator and rotor	p.u.
$x\sigma$	Leakage reactance of the damper winding	p.u.
rD, rQ, rX	Resistance of the damper winding	p.u.
$\psi d, \psi q$	Flux leakage	p.u.

Appendix B: Table B: 1. Standard parameters of the synchronous machine

Parameter	Description	Unit
x_d, x_q	Synchronous reactance	p.u.
x'_d, x'_q	Transient reactance	p.u
x''_d, x''_q	Sub-transient reactance	p.u
T'_d, T'_q	Transient time constant	p.u
T''_d, T''_q	Sub-transient time constant	p.u
T'_{d0}, T'_{q0}	Transient time constant	p.u
T''_{d0}, T''_{q0}	Sub-transient time constant	p.u

Power system Parameters

The four generators were rated as follows 900 MVA and20KV and the parameter as follows:

Appendix B: Table B: 2. shows the Configuration and parameters of the four generators

Parameters	values
X_d	1.8
X_q	1.7
X_l	0.2
X'_d	0.3
X_q	0.55
X''_d	0.25
X''_q	0.25
R_a	0.0025
T'_{do}	8.0 s
T'_{qo}	0.4 s
T''_{do}	0.03 s
T''_{qo}	0.05 s

Impedance of 0+j0.15 per unit on 900 MVA and 20/230 KV base, and off-nominal ratio of 1.0

Transmission system nominal voltage is 230 KV.

Line parameters of the lines in per unit on 100 MVA, 230 KV base

r = 0.0001 pu/km, X_l =0.001 pu/km, b_c = 0.00175 pu/km

G1: P = 700 MW, Q = 185 Mvar

G2: P = 700 MW, Q = 235 Mvar

G3: P = 719 MW, Q = 176 Mvar

G4: P = 700 MW, Q = 202 MVar

Appendix C: Table C: 1. the table shows power flow in the hybrid system

		Active Power (MW)	Reactive Power (Mvar)
GL1-A	BUS 5	967.506	100.052
GL2-B	BUS 7	1783.008	350.002
C1-A	BUS 5	0	-197.54
C2-B	BUS 7	0	-301.09
G1-A	BUS 1	729.57	□2.94
G2-A	BUS 4	700.11	234.91
G3-B	BUS 11	719.121	270.53
G4-B	BUS 9	700.12	201.78
L2-A	BUS3 BUS5	1417.08 -1397.31	153.90 9.19
L3-A	BUS5 BUS6	214.90 -207.49	44.15 -0.75
L4-A	BUS5 BUS6	214.90 -207.49	44.15 -0.75
L5-B	BUS6 BUS7	207.49 -200.07	0.75 43.94
L6-B	BUS6 BUS7	-207.49 -200.07	0.75 43.94
L7-B	BUS7 BUS8	-1382.87 1405.31	-136.79 322.29
L8-8	BUS8 BUS10	-705.19 719.12	-139.35 251.98
L1-A	BUS2 BUS3	729.57 -716.96	37.82 63.58
T1	BUS2 BUS1	-729.57 729.57	-37.82 52.94
T2	BUS1 BUS3	-700.11 700.11	-217.47 234.91
T3	BUS10 BUS11	-719.12 719.12	-251.98 270.53
T4	BUS8 BUS9	-700.12 700.12	182.941 201.78

Appendix D: Table D: 1 Eigenvalues result for HVAC/HVDC network

Eigenvalues	Real Part	Imaginary part	Damped Frequency	Damping Ratio
1	0	0	0	0
2	-28.1826	0	0	1
3	-32.0859	0	0	1
4	-31.3876	0	0	1
5	-30.3150	0	0	1
6	-9.9288	0.0355	0.0056	0.9999
7	-9.9288	-0.0355	0.0056	0.9999
8	-1.1919	6.9331	1.1034	0.1694
9	-1.1919	-6.9331	1.1034	0.1694
10	-1.2157	6.7780	1.0788	0.1765
11	-1.2157	-6.7780	1.0788	0.1765
12	-0.3038	3.1662	0.5039	0.0955
13	-0.3038	-3.1662	0.5039	0.0955
14	-4.1803	0	0	1
15	-3.6676	0	0	1
16	-0.9929	0	0	1
17	0.0102	0	0	**-1**
18	-0.0414	0	0	1
19	-0.0363	0	0	1
20	-0.0363	0	0	1

Appendix D: Table D: 2 Eigenvalues result for HVDC system

Eigenvalues	Real Part	Imaginary Part	Damped Frequency	Damping Ratio
1	0	0	0	0
2	-31.1888	0	0	1
3	-28.3979	0	0	1
4	-31.4161	0	0	1
5	-27.9120	0	0	1
6	-10.0043	0	0	1
7	-1.2483	6.8623	1.0922	0.1790
8	-1.2483	-6.8623	1.0922	0.1790
9	-9.1161	0	0	1
10	-4.0000	0	0	1
11	-1.7562	6.3687	1.0136	0.2658
12	-1.7562	-6.3687	1.0136	0.2658
13	-2.8637	0	0	1
14	-1.0680	0	0	1
15	-0.9447	0	0	1
16	-0.0514	0	0	1

Eigenvalues	Real Part	Imaginary Part	Damped Frequency	Damping Ratio
17	-0.0000	0	0	1
18	-0.0244	0	0	1
19	-0.0335	0.0068	0.0011	0.9799
20	-0.0335	-0.0068	0.0011	0.9799

Appendix D: Table D: 3 Eigenvalues result for HVAC link

Mode	Real part	Imaginary part	Damped Frequency	Damping Ratio
1	0	0	0	0
2	-31.2941	0	0	1
3	-31.3799	0	0	1
4	-28.7799	0	0	1
5	-28.1394	0	0	1
6	-9.9626	0	0	1
7	-9.8757	0	0	1
8	-1.2129	7.0157	1.1166	0.1704
9	-1.2127	-7.0157	1.1166	0.1704
10	-1.2222	6.890	1.0966	0.1747
11	-1.2222	-6.890	1.0966	0.1747
12	-0.4244	3.6371	0.5789	0.1159
13	-0.4244	-3.6371	0.5789	0.1159
14	-5.5045	0	0	1
15	-3.7751	0	0	1
16	-0.9892	0	0	1
17	-0.0015	0	0	1
18	-0.0390	0	0	1
19	-0.0333	0	0	1
20	-0.0293	0	0	1

Appendix D: Figure D: 1. Generator (G3) Speed with AVR and PSS

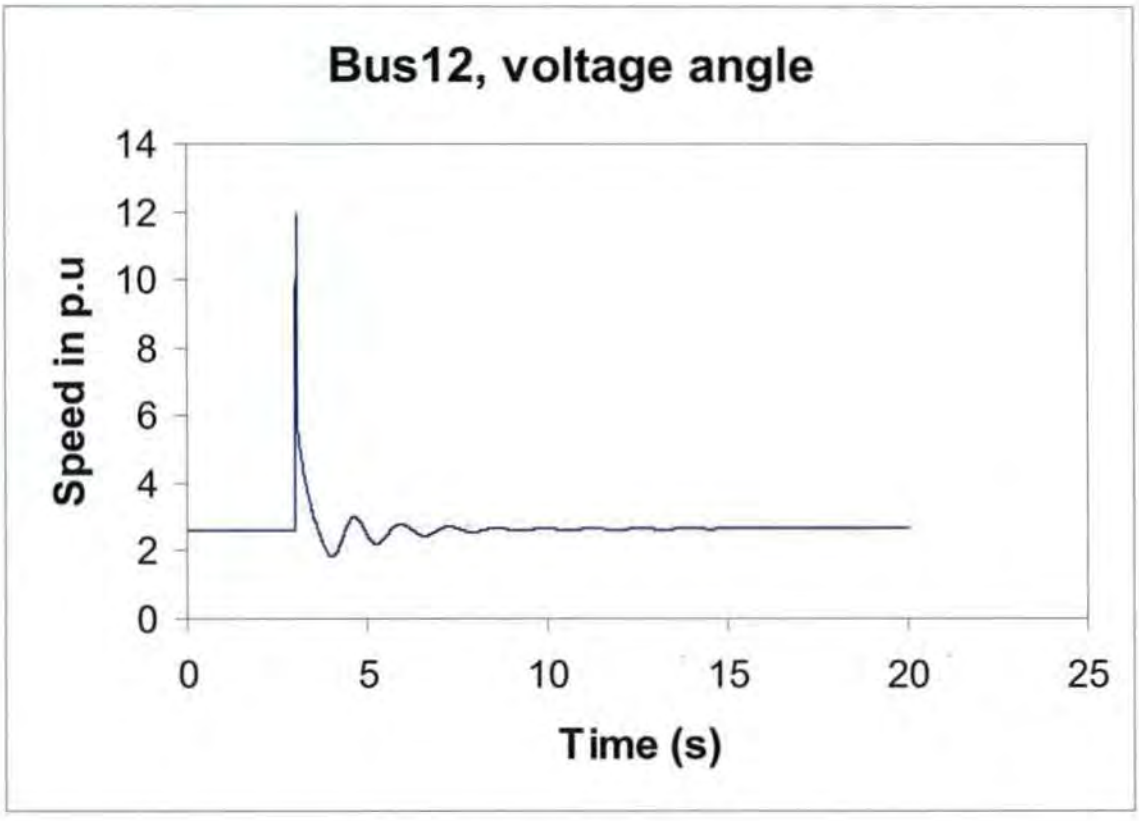

Appendix E: Figure E: 1: Voltage angle in rad for bus 12

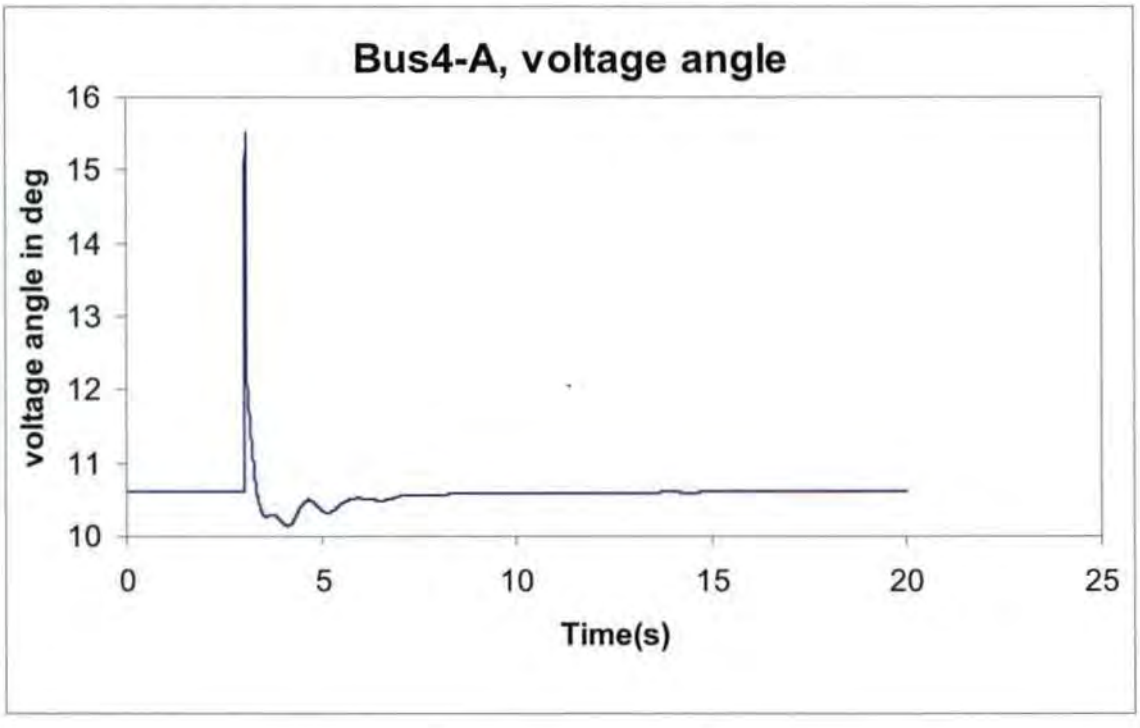

Appendix E: Figure E : 2: Voltage angle in rad for bus 4

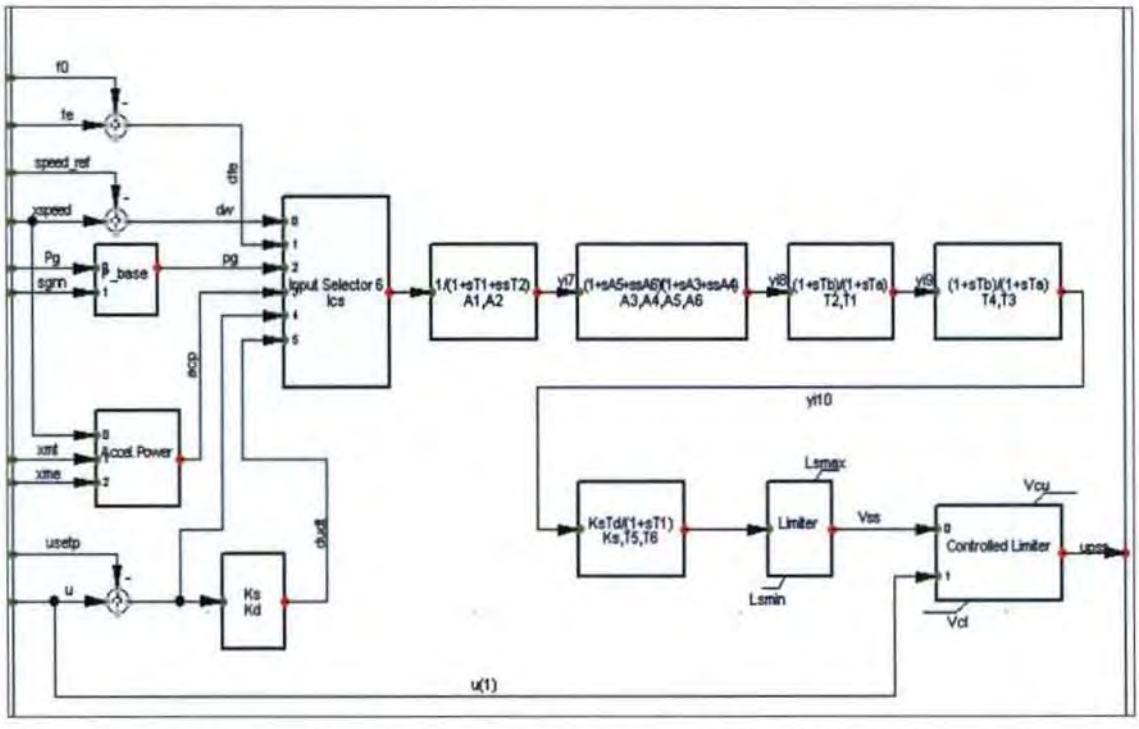

Appendix F: Figure F: 1: Schematic diagram of the PSS used for the study (PSS_IEEEST)

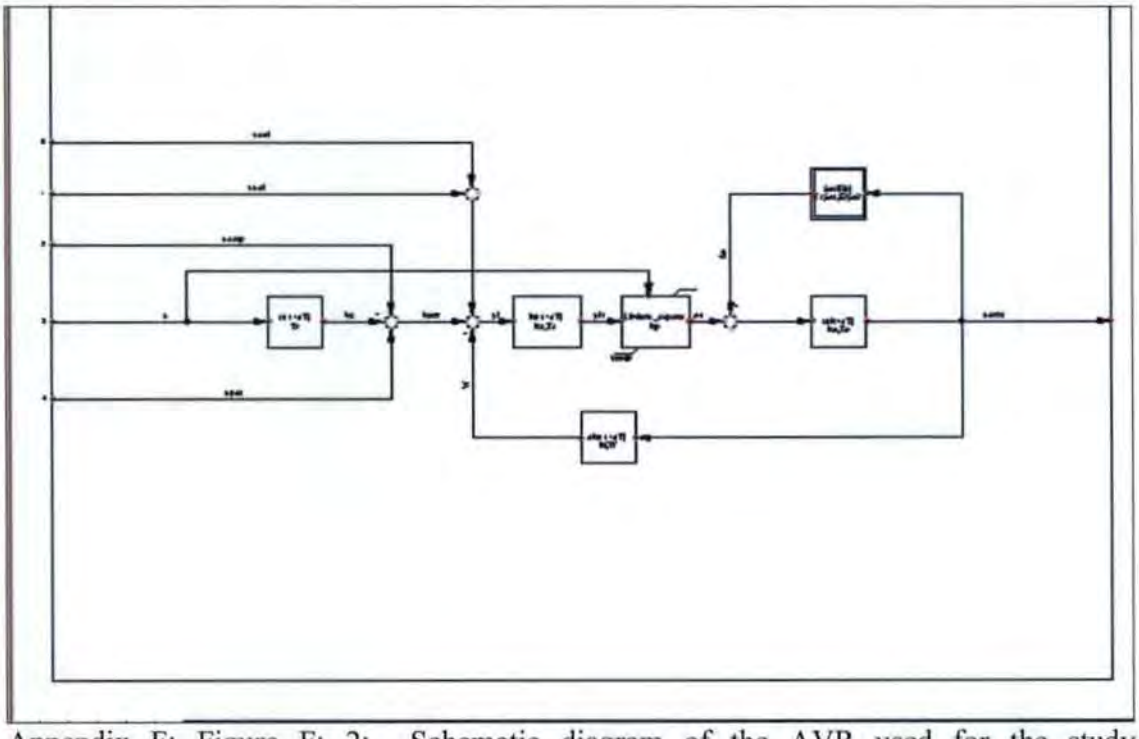

Appendix F: Figure F: 2: Schematic diagram of the AVR used for the study (Avr_IEEES1T)

Appendix G: Table G: 1: PSS Parameters

Controls	Description	Parameter
Ics	Input selector	2
T2	Delay time constant	0.3
T1	Derivate time constant	0.05
T4	Delay time constant 4^{th}	1
T3	Derivate time constant 3^{rd}	1.2
T5		1
T6		1
Ks	Stabilizer gain	50
Ls min	Controller	-0.1
Vcl	Controller	0.8

Appendix G: Table G: 2: Avr Parameters

Control	Parameter
Tr	0.02
Ka	0.5
Ta	0.03
Ke	0.5
Te	0.2
Kf	0.05
Tf	1.5
Se1	0.1
Se2	0.5
Vmin	-10
Vmax	10

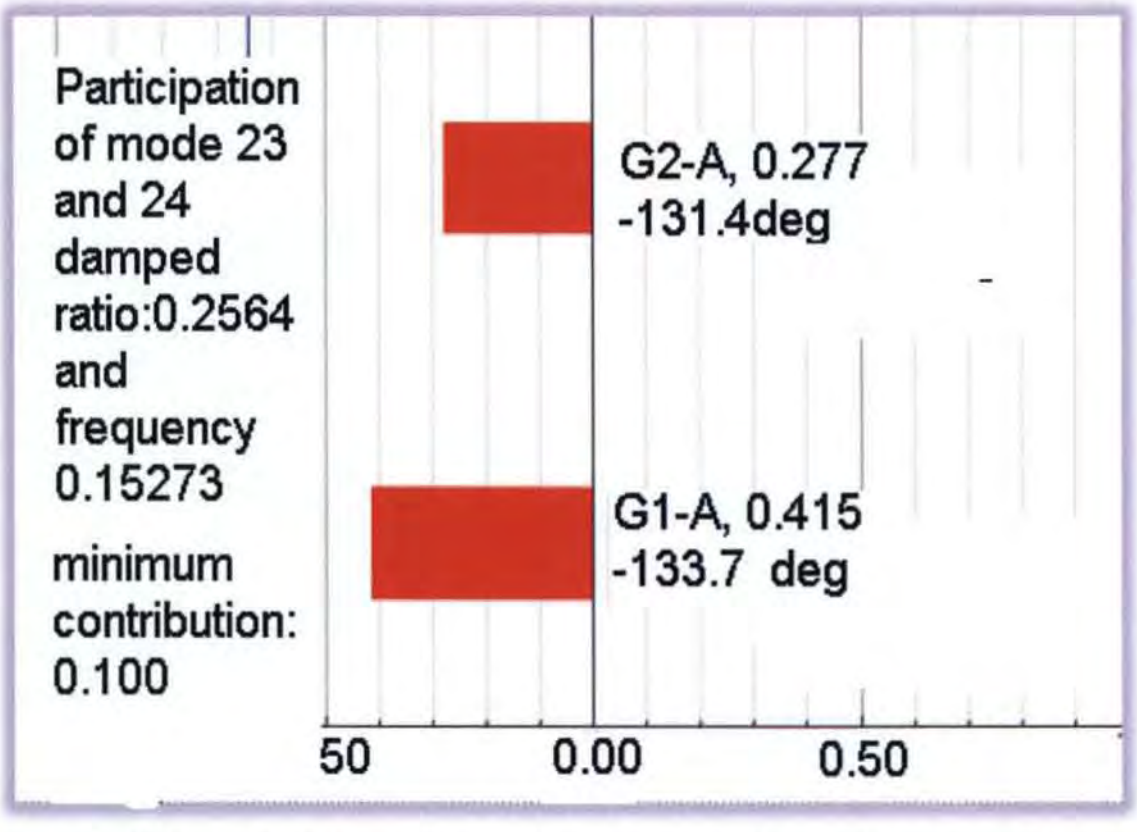

Appendix H: Figure H: 1 Participation factor for generators G1 and G2 in modes 23 and 24.